



POLITECNICO DI TORINO

Facoltà di Ingegneria

Department of Chemical and Materials Engineering

MASTER COURSE THESIS

**Thermal Gradient Assisted Growth of
Morphologically Controlled Crystals from a
Mixture of Small-Molecule Organic Semiconductor
and Polymer**

Toward Organic Field-Effect Transistor Application

Supervisors:

Prof. Takeshi Yamao

Prof. Yuhi Inada

Co-supervisor:

Prof. Marco Sangermano

Author:

Matteo Turani

A.Y. 2019/2020

“Knowledge is knowing that a tomato is a fruit; wisdom is not putting it in a fruit salad”

Miles Kington

POLITECNICO DI TORINO

Abstract

Master Course in Materials Engineering

Thermal Gradient Assisted Growth of Morphologically Controlled Crystals from a Mixture of Small-Molecule Organic Semiconductor and Polymer

Toward Organic Field-Effect Transistor Application

by Matteo Turani

Organic semiconductors have been widely studied in recent years because of their light-weight, flexibility, and low-end. Soluble materials have been developed to further minimize process costs; among these 6,13-bis(triisopropylsilylethynyl) pentacene (TIPS-pentacene) combines printability, air-stability, and high electrical performances. TIPS-pentacene crystals yielded by simple drop-casting are affected by random orientation, lack of areal coverage, and non-homogeneous film thickness, which lead to poor electrical performances and high device-to-device variability.

To reduce morphological issues and therefore increase Organic Field-Effect Transistors (OFETs) performances, in this research organic films have been yielded by applying two methods; a thermal gradient and blending TIPS-pentacene with a polymeric material (polystyrene). The former method enhances areal coverage and crystal orientation, while the latter one is mainly effective on charge mobility and its consistency.

Finally, the thermal gradient has been applied through a mixture of TIPS-pentacene and polystyrene to combine advantages given by the two single methods. Crystal orientation is optimized; however, despite electrical properties attained with pristine TIPS-pentacene have been confirmed, further performance enhancements are prevented by an unexpected lack in crystallinity and a non-homogeneous vertical phase separation between semiconductor and polymer across the whole substrate.

Contents

Abstract	v
Contents	vii
List of Figures	ix
List of Tables	xiii
Riassunto	xv
1 Introduction	1
1.1 Overview of Organic Electronics	1
1.2 Organic Semiconductors	2
1.2.1 Hybrid Orbitals	2
1.2.2 Conductivity Mechanism	4
1.2.3 Molecular Stacking	5
1.2.4 Pentacene and TIPS-pentacene	6
1.3 Organic Field-Effect Transistors	9
1.3.1 Structure	10
1.3.2 Operation Principle	11
1.3.3 Output Data Analysis	13
1.4 Research Outline	15
2 State of Art of Crystal Fabrication	17
2.1 External Methods	18
2.1.1 Spin-Coating	18
2.1.2 Droplet-Pinned Crystallization	19
2.1.3 Gas-Flow Assisted	21
2.1.4 Thermal Gradient Assisted	22
2.2 Additive Methods	23
2.2.1 Dual Solvent	23
2.2.2 Small-Molecule Blends	24
2.2.3 Polymer Blends	24

3	Materials and Methods	29
3.1	Crystal Fabrication	29
3.1.1	Materials Preparation	29
3.1.2	Thermal Gradient Assisted Growth of Crystals from a Pristine TIPS-pentacene Solution	30
3.1.3	Crystals Growth from Drop-Casting of TIPS-pentacene/Polystyrene Blend Solution	31
3.1.4	Thermal Gradient Assisted Growth of Crystals from a TIPS-pentacene/Polystyrene Blend Solution	31
3.2	Characterization	32
3.2.1	Morphology	32
3.2.2	Microstructure	35
3.2.3	Crystallinity	36
3.2.4	OFET Characterzation	37
4	Results and Discussion	39
4.1	Thermal Gradient Assisted Growth of Crystals from a Pristine TIPS-pentacene Solution	39
4.1.1	Morphology	39
4.1.2	Crystallinity	43
4.1.3	OFET Characterization	45
4.2	Crystals Growth from Drop-Casting of TIPS-pentacene/PS Blend Solution	49
4.2.1	Morphology	49
4.2.2	Microstructure	51
4.2.3	Crystallinity	52
4.2.4	OFET Characterization	54
4.3	Thermal Gradient Assisted Growth of Crystals from a TIPS-pentacene/ PS Blend Solution	56
4.3.1	Morphology	56
4.3.2	Microstructure	60
4.3.3	Crystallinity	62
4.3.4	OFET Characterization	63
5	Conclusions	65
	Bibliography	69

List of Figures

1	Comuni modelli di impacchettamento per piccole molecole semiconduttrici	xvii
2	Formule chimiche dei materiali utilizzati	xviii
3	Apparecchiature sperimentali utilizzate per la crescita dei cristalli.	xix
4	Bottom-gate/top-contact OFET rappresentato in condizioni di funzionamento.	xxi
5	Andamento di (a) copertura superficiale e (b) dimensione dei cristalli per diversi valori di gradiente termico.	xxii
6	Coerenza della mobilità al variare del rapporto volumetrico di blend.	xxiii
7	Confronto tra i valori medi e massimi di mobilità ottenuti dall'analisi degli OFET prodotti secondo i diversi metodi studiati.	xxiv
1.1	Energy diagram of sp^2 hybridization.	3
1.2	Spacial orbitals arrangement before and after hybridization.	3
1.3	Formation of σ and π bonds between two sp^2 hybrid carbon atoms.	4
1.4	Commons conjugate small-molecules stacking motives	6
1.5	Pentacene structural formula.	7
1.6	TIPS-pentacene structural formula.	8
1.7	TIPS-pentacene 3-dimensional molecular stacking	9
1.8	Organic field-effect transistors configurations.	10
1.9	Energy band diagram at the contact electrode-semiconductor.	11
1.10	BG-BC device working conditions.	13
1.11	Output characteristic	14
1.12	Transfer characteristics in saturation region.	14
2.1	Crystal Growth by spin-coating.	18
2.2	Droplet-pinned crystallization crystal growth.	20
2.3	Crystal growth on a tilted substrate	20
2.4	Crystal growth assisted by gas-flow.	21
2.5	Schematic theoretical diagrams showing effects of temperature on crystal growth parameters.	23
2.6	Structural formula of common polymers used in blend with small-molecules semiconductor	25

3.1	Crystal growth assisted by thermal gradient.	31
3.2	Schematic of organic crystal misalignment and Crystal size	34
3.3	Schematic representations of Bragg geometry and XRD peaks properties.	36
4.1	Optical micrographs of pristine TIPS-pentacene crystals grown assisted by thermal gradient.	40
4.2	Average misorientation angle between crystals and thermal gradient direction for different T_h	41
4.3	Crystal size for different T_h	42
4.4	Surface topology comparison for different T_h	43
4.5	Areal coverage for different T_h	43
4.6	X-Ray diffraction spectra and FWHM values for samples yielded with thermal gradient assistance	44
4.7	Typical (a) output and (b) transfer characteristic in saturation region of organic field effect transistors having a TIPS-pentacene film as active layer grown with thermal gradient assistance.	45
4.8	Average electrical properties for different T_h	47
4.9	Thermal cracks originated in pristine TIPS-pentacene films grown with thermal gradient	47
4.10	Crystals alignment influence on output characteristic shape	48
4.11	Optical micrographs of crystals made from TIPS-pentacene/polystyrene blend solution.	50
4.12	Average misorientation angle between crystals and long axis direction of a crystal chosen as a baseline for different volume mixing ratios.	51
4.13	SEM images of cross-section of samples yielded from a mixture of TIPS-pentacene and polystyrene at different blend ratios.	52
4.14	X-Ray diffraction spectra and FWHM values for samples yielded from mixture of TIPS-pentacene and polystyrene	53
4.15	Average electrical properties for different blending ratios measured both in top-contact and bottom-contact configuration.	55
4.16	Mobility consistency at different TIPS-pentacene/polystyrene blend ratios.	56
4.17	Optical images of crystals obtained by thermal assisted growth of TIPS-pentacene/PS blend at 1:1 mixing ratio at high temperature.	57
4.18	Optical micrographs of crystals made from TIPS-pentacene/polystyrene blend solution and grown with thermal gradient assistance.	58
4.19	Average misorientation angle between each crystal and thermal gradient direction at different mixing ratio values.	59
4.20	SEM images of cross section of samples yielded from a mixture of TIPS-pentacene and polystyrene with thermal gradient application ($T_h = 40^\circ\text{C}$).	61
4.21	X-Ray diffraction spectra and FWHM values for samples yielded from a mixture of TIPS-pentacene and polystyrene with Thermal Gradient Assistance	62

4.22 Average electrical properties for different blending ratios for samples produced with thermal gradient application 64

List of Tables

1.1	Properties of the most common organic solvents for TIPS-pentacene	8
3.1	Specifics of devices used to measure electrical properties of organic films.	38
4.1	FWHM values correspondent to (001) peak for different T_h	44
4.2	FWHM values correspondent to (001) plane for each volume ratio.	53
4.3	FWHM values correspondent to (001) plane for each volume ratio, samples are yielded with thermal gradient assistance ($T_h = 40^\circ\text{C}$)	62

Riassunto

Introduzione

Conducibilità Elettrica nei Materiali Organici

In passato i materiali organici sono stati quasi universalmente considerati come materiali isolanti, ma più recentemente, se sintetizzati secondo particolari strutture e se implementati in appropriati circuiti, è stato dimostrato un loro comportamento da semiconduttori.

Leggerezza, flessibilità, printability, ridotte temperature di processo, oltre che basso costo sono alcune delle proprietà peculiari che hanno permesso ai semiconduttori organici di ritagliarsi uno spazio non indifferente all'interno dell'industria dell'elettronica. Al contrario della controparte inorganica, come silicio mono o policristallino; i semiconduttori organici mostrano proprietà elettriche nettamente inferiori (mobilità delle lacune ridotta tra le 10 e 20 volte). Quindi l'obiettivo di mercato dei semiconduttori organici non è quello di competere con quelli inorganici, ma piuttosto di completare l'offerta disponibile. In particolare essi sono utilizzati per la produzione di dispositivi flessibili, indossabili o implementabili in capi d'abbigliamento (smart clothes) quali celle fotovoltaiche, sensori o displays.

La conducibilità nei materiali organici è possibile grazie all'ibridizzazione degli orbitali degli atomi di carbonio. Per questioni energetiche gli orbitali più esterni di un atomo di carbonio (un orbitale s e tre orbitali p) si possono ricombinare tra loro in varie soluzioni dando origine a orbitali ibridi sp. L'ibridizzazione di un orbitale s e due p (ibridizzazione sp²) permette ad un singolo atomo di carbonio di formare tre legami σ e un legame π con gli atomi vicini. Il legame σ è caratterizzato da elettroni strettamente localizzati vicino ai nuclei dei due atomi coinvolti nel legame, invece il legame π permette la delocalizzazione degli elettroni. Pertanto, nel caso di molecole coniugate, composte da catene aventi una serie di legami π alternati; gli elettroni possono muoversi liberamente lungo tali catene e conferire alle molecole proprietà elettriche. Un risultato simile è ottenuto anche nel caso in cui le molecole organiche siano caratterizzate da un core di anelli benzenici invece che da una serie di doppi legami alternati.

Per assicurare un'ottimale conducibilità elettrica al materiale non è importante solo la struttura di una singola molecola, ma anche la posizione reciproca di molecole adiacenti e la formazione di un reticolo cristallino. Infatti il trasporto di carica è regolato dal cosiddetto hopping, un fenomeno di tunnelling delle cariche termalmente attivato; diversamente da quanto avviene nei materiali inorganici, in questo caso, è un processo fonone-assistito e quindi facilitato ad alte temperature. Tale fenomeno è descritto matematicamente da:

- Integrale di trasferimento, legato all'accoppiamento di molecole adiacenti e quindi strettamente dipendente dallo stacking delle molecole
- Energia di reorganizzazione, differenziata in interna ed esterna. La prima dipende dal grado di libertà intermolecolare, dalla rigidità delle molecole e dalla lunghezza di coniugazione. La seconda invece dipende dai cambiamenti nel mezzo in cui è immerso il materiale durante il trasferimento di carica; tale grandezza è generalmente trascurabile.

Pertanto differenti disposizioni di molecole sono stati osservati nel caso di diverse molecole (Figura 1):

- (i) Lisca di pesce senza sovrapposizione di orbitali π
- (ii) Lisca di pesce con sovrapposizione di orbitali π
- (iii) Lamellare con sovrapposizione unidimensionale degli orbitali π
- (iv) Lamellare con sovrapposizione bidimensionale degli orbitali π

Teoreticamente parlando le migliori performances elettriche sono assicurate per elevati valori di integrale di trasferimento e bassi valori di energia di riorganizzazione, valori ottenuti per elevate sovrapposizioni e corte distanze tra orbitali π , quindi per disposizioni lamellari con sovrapposizione bidimensionale degli orbitali π . Pertanto numerosi studi sono stati condotti al fine di ottenere piccole molecole o polimeri semiconduttori che cristallizzino secondo queste caratteristiche e che quindi assicurino le migliori proprietà elettriche.

Stato dell'Arte della Produzione di Cristalli Organici

La disposizione delle molecole all'interno del reticolo cristallino è fortemente influenzata anche dal metodo di produzione dei cristalli. Nel corso degli anni varie tecnologie sono state sviluppate, esse si differenziano principalmente in tecniche in fase vapore o fase liquida. Nel primo caso sono richieste elevate temperature e complessi macchinari sperimentali per fare evaporare il materiale, e sono prodotti cristalli la cui variabilità in forma e dimensione è difficilmente controllabile. Al contrario la produzione per fase liquida, ossia sciogliendo in un solvente il materiale per poi depositarlo tramite drop-casting è possibile anche a basse temperature e non richiede alcun complesso set-up sperimentale. In questo caso però il problema principale risiede nella elevata variabilità morfologica ottenuta, quindi diversi metodi di deposizione sono stati sviluppati al fine di ottenere film organici a morfologia controllata.

Tra le tecniche da fase liquida si possono distinguere due tecnologie in base a quale sia la driving force che controlla la crescita dei cristalli: i cosiddetti "metodi esterni" o "metodi additivi". Nel primo caso una forza esterna controlla direttamente la direzione e velocità di evaporazione del solvente, di conseguenza l'orientazione dei cristalli e quindi le proprietà finali del film. I metodi additivi invece consistono nell'aggiungere un terzo elemento al binomio soluto-solvente al fine di modificare

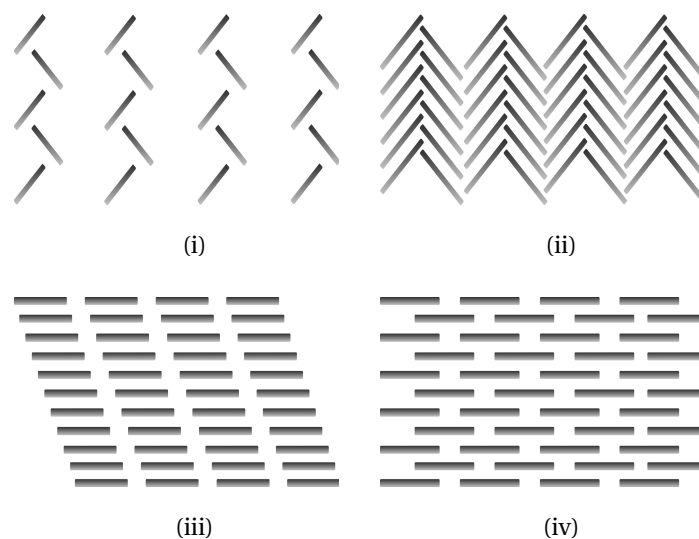


FIGURE 1: Comuni modelli di impacchettamento per piccole molecole semiconduttrici: (i) lisca di pesce senza sovrapposizione di orbitali π , (ii) lisca di pesce con sovrapposizione di orbitali π , (iii) lamellare con sovrapposizione unidimensionale degli orbitali π e (iv) lamellare con sovrapposizione bidimensionale degli orbitali π .

il processo di evaporazione del solvente e quindi migliorare copertura superficiale del film, grado di cristallinità e proprietà finali del cristallo. Gli additivi aggiunti possono essere un secondo solvente, delle piccole molecole oppure un polimero isolante.

Scopo della Ricerca

In questa ricerca sono stati studiati due metodi di crescita di cristalli organici in fase liquida, uno esterno ed uno additivo. Nel primo caso la driving force è data da un gradiente termico applicato al substrato su cui poi è stata depositata la soluzione, invece nel secondo, un polimero isolante è stato aggiunto alla soluzione originaria. Successivamente questi due metodi sono stati combinati tra loro al fine di ottenere una tecnologia che assicurasse al film ottenuto le migliori proprietà morfologiche ed elettriche.

Materiali e Metodi

Materiali

Il materiale utilizzato come semiconduttore durante la ricerca è il 6,13-bis (triisopropylsilylethynyl) pentacene (TIPS-pentacene o TP, Figura 2.a), un composto derivato dalla famiglia degli aceni aggiungendo due voluminosi gruppi laterali al terzo dei cinque anelli benzenici. In questo modo la scarsa solubilità del pentacene, i cui cristalli sono solitamente sintetizzati per via vapore, è notevolmente migliorata rendendo possibile la produzione di cristalli a partire da soluzioni con i più comuni solventi organici (clorobenzene, cloroformio o toluene). Inoltre la funzionalizzazione del pentacene ne

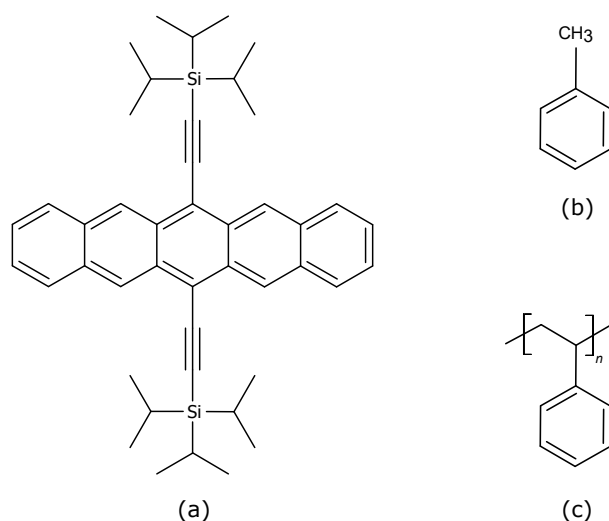


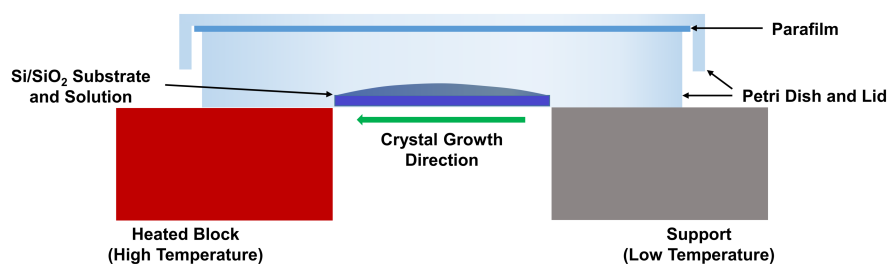
FIGURE 2: Formule chimiche dei materiali utilizzati nel corso della ricerca: (a) TIPS-pentacene, (b) polistirene (PS) e (c) toluene.

migliora la stabilità ambientale del pentacene senza intaccarne le proprietà elettriche, anche perchè invece di una disposizione a lisca di pesce senza sovrapposizione degli orbitali π tipica del pentacene, il TIPS-pentacene assume una disposizione spaziale lamellare 2D con elevata sovrapposizione degli orbitali.

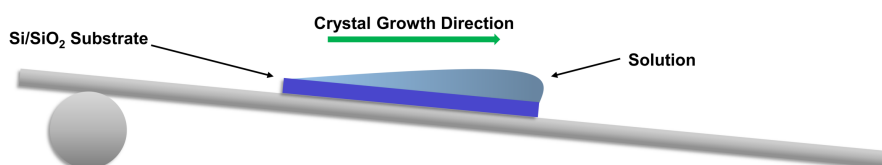
Il toluene (Figura 2.b) è stato utilizzato come solvente organico per disciogliere il TIPS-pentacene, garantendo un buon compromesso tra limite di solubilità, volatilità e viscosità. Il polistirene (PS, average M.W. 280 000, Figura 2.c) è stato usato come polimero in blend con TIPS-pentacene e toluene nel metodo additivo.

Soluzioni a differente concentrazione sono state preparate per i diversi metodi. Nel caso in cui solo il TIPS-pentacene è stato disciolto in toluene, si è usata una concentrazione di 8.5 mg/ml. Nell'altro caso, semiconduttore e polimero sono stati disciolti in toluene separatamente a 5.0 mg/ml e successivamente miscelati a diversi rapporti in volume (TP/PS): 1:1, 2:1 e 3:1.

Le soluzioni sono state depositate su substrati di silicio su cui in precedenza è stato termicamente cresciuto uno strato di diossido di silicio (SiO_2). I wafer sono stati tagliati manualmente in forme rettangolari di 10 mm per 15 mm, successivamente lavati in solventi organici (acetone, 2-isopropanolo, etanolo e acqua) tramite un bagno a ultrasuoni per 10 minuti. Dopo di che sono stati asciugati con flusso di azoto (N_2) e in forno per 15 minuti a 120 °C. Infine i substrati sono stati trattati con UV/ O_3 per rendere la superficie idrofila e pertanto facilitare lo spargimento uniforme della goccia di soluzione in seguito al drop-casting.



(a)



(b)

FIGURE 3: Apparecchiature sperimentali utilizzate per la crescita dei cristalli secondo (a) metodo esterno e (b) metodo additivo.

Metodi

Apparecchiatura Sperimentale L'apparato sperimentale utilizzato per la crescita dei cristalli con applicazione di gradiente termico è mostrato in figura 3.a. Il gradiente è garantito dall'applicazione di due differenti temperature a due blocchi di metallo tra i quali è posta una petri dish in cui è riposto il substrato. Uno dei due blocchi, che funge da supporto, è posto a bassa temperatura (T_l), idealmente a temperatura ambiente; mentre l'altro è riscaldato a temperatura fissa (T_h). Le temperature del blocco impostate per stabilire il gradiente di temperatura sono tra 40 °C e 60 °C, incrementate di 5 °C. Dopo aver atteso che il gradiente termico risulti omogeneo all'interno della petri dish e del substrato, si procede con la deposizione di 70 μ l di soluzione di TIPS-pentacene e toluene. Al fine di garantire una ridotta velocità di evaporazione del solvente, una certa quantità dello stesso è stata lasciata all'interno della petri dish (solvent annealing), la quale è stata inoltre sigillata con film di paraffina.

Come mostrato in figura 3.b, la soluzione blend di semiconduttore e polimero è stata depositata su un substrato posto all'interno di una petri dish a sua volta posizionata su un piano inclinato ($\sim 5^\circ$) al fine di conferire una direzione preferenziale di crescita ai cristalli. Anche in questo caso 70 μ l

di soluzione sono stati depositati sul substrato e la petri dish è stata sigillata con qualche strato di parafilm.

Infine la deposizione secondo il metodo combinato è avvenuta in maniera del tutto analoga a quella del caso della soluzione di TIPS-pentacene puro utilizzando solamente 40 °C come temperatura del blocco riscaldato. A differenza del caso con puro TIPS-pentacene in soluzione, in questo caso in una singola petri dish sono stati posti tre substrati su cui sono stati depositati 70 μl di soluzione a tre differenti rapporti volumetrici, in modo tale che le condizioni di crescita siano analoghe per i tre campioni. Anche in questo caso è stata sfruttata la tecnica del solvent annealing e del sigillare la petri dish con parafilm al fine di ridurre la velocità di evaporazione del solvente.

Caratterizzazione Analisi morfologiche, micrografiche, cristallografiche ed elettriche sono state condotte al fine di valutare le proprietà dei film prodotti.

Un microscopio ottico a luce polarizzata è stato utilizzato per misurare orientazione e taglia dei cristalli. La prima è definita come l'angolo tra l'asse longitudinale di un cristallo ed una baseline scelta come riferimento, la taglia invece è la lunghezza dell'asse trasversale, ossia la larghezza del cristallo. Per valutare spessore e rugosità dei cristalli è stato usato un profilometro superficiale; lo stesso strumento è stato usato per valutare il grado di copertura superficiale.

Il microscopio elettronico a scansione (SEM) è stato usato per investigare la microstruttura dei film. In particolare gli elettroni secondari sono stati analizzati per avere informazioni sulla morfologia delle cross-sections ottenute tagliando i substrati in direzione perpendicolare agli elettrodi depositati, ossia lungo l'asse corto dei cristalli. Inoltre la spettroscopia EDS (Energy Dispersive X-ray Spectrometry) è stata effettuata per distinguere i diversi strati che si sono formati durante la cristallizzazione del materiale (TIPS-pentacene, polistirene e substrato).

Spettroscopia ai raggi X (XRD) è stata invece utilizzata per valutare il grado di cristallinità del film, inoltre dall'analisi dei dati raccolti anche la spaziatura tra i piani cristallini è stata calcolata.

Infine la caratterizzazione dei transistor ad effetto di campo (OFET) è stata condotta per valutare le proprietà elettriche dei film. I dispositivi sono stati prodotti sia in configurazione top-contact (TC) che bottom-contact (BC), mentre il l'elettrodo di gate è sempre stato posizionato al di sotto del film organico in una disposizione bottom-gate (BG). In Figura 4 è raffigurato un dispositivo BG-TC in cui è mostrato come i voltaggi sono applicati agli elettrodi d'oro. In particolare il voltaggio di gate (V_{GS}) è stato applicato in step mode da 10 V a -40 V con incremento di -5 V; invece la tensione tra drain e source è stata applicata in sweep mode tra 10 V e -40 V con step di -2V.

Risultati e Discussione

Deposizione di puro TIPS-pentacene con gradiente di temperatura L'analisi morfologica condotta sui campioni prodotti a partire da una soluzione di TIPS-pentacene puro in toluene con l'applicazione

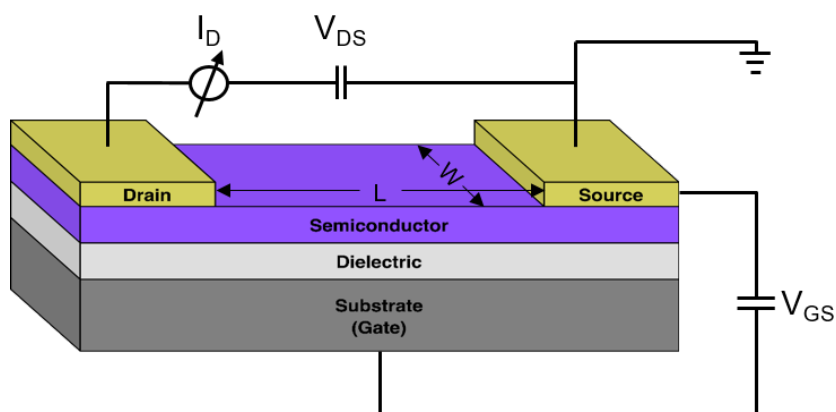


FIGURE 4: Bottom-gate/top-contact OFET rappresentato in condizioni di funzionamento.

di un gradiente termico mostra come i cristalli risultino prevalentemente allineati con la direzione del gradiente. In particolare l'allineamento è ottimizzato al centro del substrato, mentre lungo i bordi l'effetto di pinning influenza oltremodo una corretta direzione di crescita del film.

Inoltre la dimensione dei cristalli decresce incrementando il valore di T_h imposto al blocco di metallo riscaldato (Figura 5.a). Tale risultato è legato alla maggiore solubilità del TIPS-pentacene ad alta temperatura che pertanto porta ad una maggior differenza in supersaturazione tra le due estremità del substrato; ciò si riflette quindi in un crescente tasso di nucleazione di cristalli rispetto ai casi con minori T_h e pertanto si ottengono molti cristalli di piccole dimensioni.

Al contrario aumentando il valore del gradiente termico il film mostra una maggiore copertura superficiale del substrato (da 59.2% nel caso di semplice drop-cast a 96.0% per $T_h=60^\circ\text{C}$) e una rugosità più regolare ed omogenea (Figura 5.b). Tale risultato è di fondamentale importanza per assicurare proprietà elettriche uniformi tra i diversi dispositivi prodotti sui vari substrati.

Il grado di cristallinità, valutato tramite una analisi XRD, non è significativamente influenzato dall'applicazione del gradiente termico. Inoltre anche la distanza tra i piani cristallografici resta costante al variare dei valori di gradiente applicati.

L'analisi delle proprietà elettriche degli OFET mostra come le migliori performances (mobilità delle lacune e subthreshold slope su tutte) sono state ottenute per i campioni prodotti con valori intermedi di gradiente di temperatura in quanto essi rappresentano un ottimale compromesso tra le proprietà morfologiche sopra riportate. Inoltre a valori di T_h elevati spaccature e crepe dovuta all'alta temperature si possono osservare nei film e pertanto le performances dei dispositivi risultano ulteriormente ridotte.

Deposizione di blend di TIPS-pentacene e polistirene a temperatura ambiente Le osservazioni al microscopio ottico dei campioni prodotti per semplice drop-cast della soluzione blend tra TIPS-pentacene e polistirene mostrano come le proprietà morfologiche risultino scarsamente influenzate

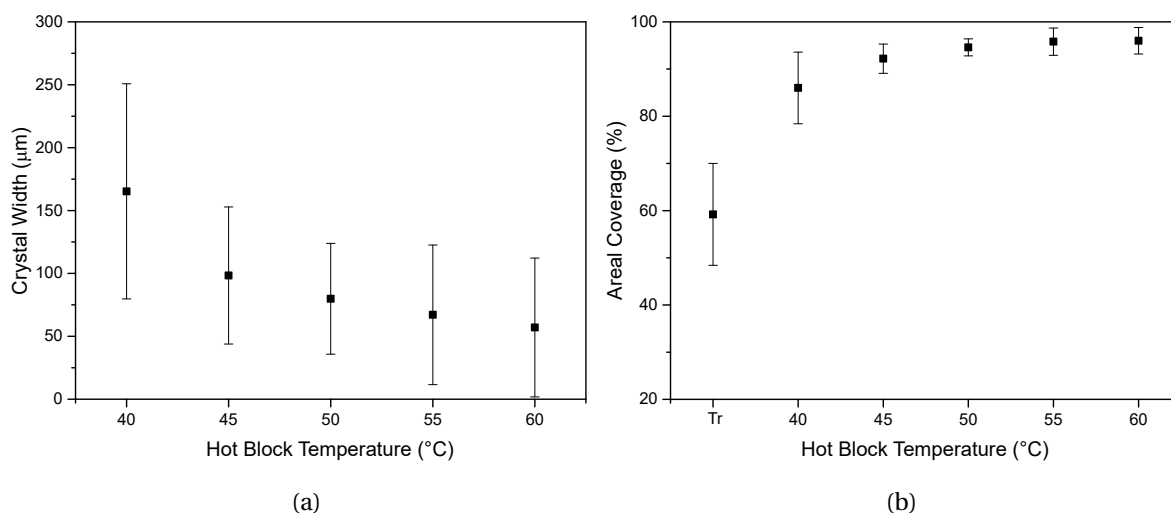


FIGURE 5: Andamento di (a) copertura superficiale e (b) dimensione dei cristalli per diversi valori di gradiente termico.

da diversi rapporti di blend. Per tutti e tre i differenti rapporti, l'allineamento tra cristalli appartenenti allo stesso dominio risulta migliorato rispetto al caso della soluzione di TIPS-pentacene puro la quale dà cristalli orientati in maniera casuale. Rispetto al caso di riferimento che mostra lacune in copertura superficiale, utilizzando soluzioni blend una completa copertura del substrato è ottenuta. Inoltre taglie medie di cristalli di $200 \pm 10 \mu\text{m}$ sono state ottenute, mentre sono stati osservati cristalli giganti di $2236 \mu\text{m}$ e $2576 \mu\text{m}$ per rapporti volumetrici di 1:1 and 2:1, rispettivamente.

I miglioramenti morfologici presentati sono frutto della separazione di fase in direzione verticale ottenuta tra TIPS-pentacene e polistirene. Come confermato dalle osservazioni al SEM, un sottile film di polimero si forma tra substrato e strato attivo; la formazione di tale strato di polistirene influenza il processo di cristallizzazione del TIPS-pentacene i cui cristalli presentano pertanto una morfologia migliorata.

Oltre a proprietà morfologiche migliori anche un più elevato grado di cristallinità è atteso a causa di una più lenta evaporazione del solvente. In questo caso però l'ipotesi teorica non è confermata poichè per tutti e tre i rapporti volumetrici l'analisi XRD mostra una leggera diminuzione della cristallinità rispetto al caso di TIPS-pentacene puro. Inoltre anche un aumento della distanza tra i piani cristallini è stato misurato, ciò potrebbe essere causato da un residuo di polistirene nello strato ricco di TIPS-pentacene il che potrebbe anche giustificare la leggera diminuzioni del grado di cristallinità del film.

Infine le proprietà elettriche sono state valutate, nel caso di dispositivi prodotti in configurazione sia top-contact che bottom-contact. In entrambi i casi sono state ottenute prestazioni simili, confermando una buona adattabilità dei cristalli prodotti nel lavorare in diverse condizioni. Inoltre l'utilizzo di soluzioni blend migliora notevolmente l'affidabilità dei dispositivi in quanto solo il 5%

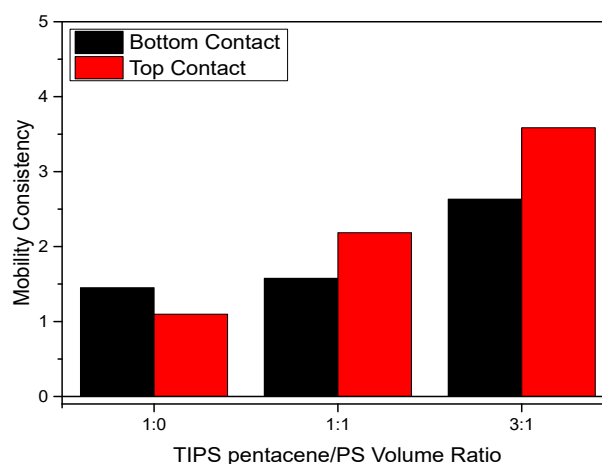


FIGURE 6: Coerenza della mobilità al variare del rapporto volumetrico di blend.

di quelli testati incorre in breakdown durante la misura, mentre nel caso di quelli prodotti con TIPS-pentacene puro, tale percentuale è dell'80%.

Le proprietà elettriche risultano migliori per il rapporto di blend 3:1 il quale mostra un miglioramento delle proprietà morfologiche dovute all'aggiunta di polimero in soluzione, e al tempo stesso la quantità di polistirene, materiale isolante, non è troppo alta da ostacolare il moto dei portatori. Infine è stata valutata anche la coerenza della mobilità, espressa come il rapporto tra mobilità e la sua deviazione standard; tale parametro permette di stimare la ripetibilità della misura. Anche in questo caso i valori migliori sono stati ottenuti per rapporto di blend 3:1 (Figura 6).

Deposizione di blend di TIPS-pentacene e polistirene con gradiente di temperatura Per la deposizione della soluzione blend è stato scelto di utilizzare solo 40 °C come temperatura per il blocco riscaldato in quanto, come è stato verificato, temperature più alte comporterebbero velocità di evaporazione troppo elevate da non formare film cristallini di adeguata qualità. Al contrario temperature minori non sarebbero in grado di impartire ai cristalli una driving force sufficiente per ottenere la morfologia desiderata.

L'applicazione di gradiente termico a soluzioni blend tra TIPS-pentacene e polistirene permette di ottenere cristalli allineati lungo la direzione di applicazione del gradiente stesso e in più, rispetto al caso di riferimento con soluzioni con TIPS-pentacene puro, sia il valore assoluto che la variabilità dell'angolo tra i cristalli e la baseline sono migliorati.

Come prevedibile invece, dimensione media e soprattutto massima dei cristalli risultano diminuite aumentando la temperatura ad un'estremità del substrato.

Dalle osservazioni microstrutturali al SEM si nota come la separazione di fase tra semiconduttore e polimero si sia raggiunta. Tuttavia, al contrario del caso in cui la deposizione è stata effettuata a temperatura ambiente, in cui una omogenea struttura a doppio strato è stata osservata su tutto il substrato, in questo caso tale microstruttura è stata osservata solamente nelle zone laterali del substrato.

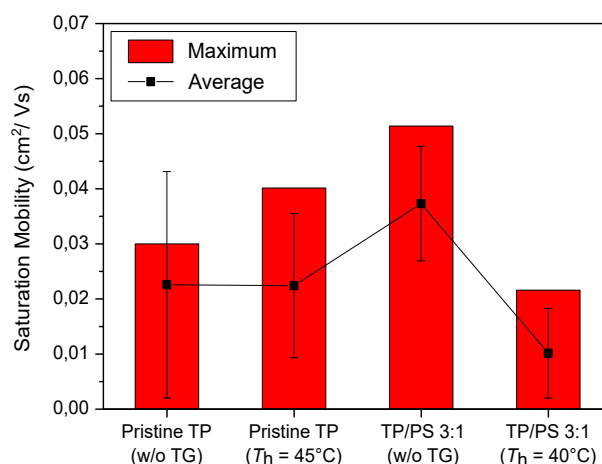


FIGURE 7: Confronto tra i valori medi e massimi di mobilità ottenuti dall'analisi degli OFET prodotti secondo i diversi metodi studiati.

Nelle aree centrali invece sono state osservate microstrutture indesiderate come un secondo strato di polimero isolante al di sopra dello strato di semiconduttore, oppure lo strato di polimero in una ottimale posizione, ma di spessore troppo elevato. Tali problematiche sono riconducibili al processo di evaporazione del solvente (più rapido ai bordi a causa della maggiore interfaccia soluzione-aria) e di come la differente solubilità di TIPS-pentacene e polistirene influenzi la loro precipitazione. Infatti depositandosi prima il soluto meno solubile (TIPS-pentacene), esso cristallizza ai bordi del substrato lasciando un eccesso di polistirene in soluzione che si deposita successivamente nella parte centrale del campione.

Le osservazioni al diffrattometro a raggi X confermano i risultati precedentemente ottenuti, ossia che l'applicazione del gradiente di temperatura durante la cristallizzazione non ha influenza su grado di cristallinità e distanza interspaziale. Tuttavia, anche in questo caso, l'aggiunta di polistirene al TIPS-pentacene provoca un leggero calo in cristallinità e un aumento di distanza interspaziale, possibilmente imputabile a qualche residuo di polimero nello strato ricco di semiconduttore.

Infine le proprietà elettriche sono state misurate testando top-contact OFET, esse mostrano un trend del tutto simile ai campioni prodotti senza l'applicazione di gradiente termico, ossia il rapporto volumetrico di 3:1 tra TIPS-pentacene e polistirene assicura le migliori prestazioni. Tuttavia le criticità osservate nella microstruttura e nella cristallinità provocano una caduta del valore delle proprietà rispetto al caso di deposizione a temperatura ambiente (Figura 7). Inoltre una elevata variabilità delle prestazioni tra devices ($\mu_{max}/\mu_{min}=27$) è causata dalle differenti microstrutture osservate tra bordo e centro di uno stesso substrato.

Conclusioni

Durante il lavoro svolto sono stati investigati due metodi di crescita per i cristalli organici, uno applicando un gradiente di temperatura come driving force esterna e l'altro aggiungendo un polimero isolante in soluzione. Nel primo caso un trade-off tra le proprietà morfologiche (allineamento dei cristalli, copertura superficiale e dimensione dei cristalli) porta a ottimizzate proprietà elettriche per medi valori di gradiente termico. Nel secondo caso invece la sola aggiunta di polistirene alla soluzione originaria permette di ottenere cristalli di forma regolare ed allineati tra loro, ma non si è in grado di controllare l'allineamento globale del dominio. Nonostante ciò e nonostante una leggera perdita in cristallinità l'affidabilità e le prestazioni dei devices prodotti con tali film come strati attivi risultano ottimali. Come ultimo step i due metodi sono stati combinati al fine di unire i vantaggi derivanti da entrambe le tecnologie; dal punto di vista morfologico sono stati ottenuti buoni risultati, ma le criticità legate alla microstruttura e alla cristallinità dei film intaccano oltremodo le prestazioni dei transistor. Pertanto un'ulteriore indagine per capire come controllare al meglio la fase di evaporazione del solvente è necessaria al fine di evitare microstrutture indesiderate.

Chapter 1

Introduction

1.1 Overview of Organic Electronics

Organic semiconductors are one kind of organic materials, hence basically composed of carbon, hydrogen, oxygen, nitrogen, and sulfur, which seem to be insulators but show a notable semiconductive behavior if charges are injected by appropriate electrodes. Organic semiconductors have attracted considerable interest since half of the last century because of their processability and unique physical properties. In particular, light-weight, low-temperature processability, flexibility, printability, and cost-effective applications make organic semiconductor an attractive class of materials suitable to be implemented in optoelectronic applications, including transistors, diodes, solar cells, sensors and light-emitting devices [1–4].

Since the 1970s, when high conductivity was discovered in doped polyacetylene [5], remarkable developments have been reached in organic semiconductors, and electrical performance properties comparable to amorphous silicon (a-Si) have been proved. Flexibility and simple fabrication methods are two unique features that assure organic semiconductors high interest among researchers [6]. According to the type of material, different fabrication technologies have been reported: vapor-phase growth [7–9], solution casting [10–12], printing [13, 14] and melt casting growth [15] among the others. Since the final properties of crystal films are strongly affected by the fabrication technology, several studies have been conducted to investigate all different organic semiconductors materials deeply.

Despite their incredible properties and future researches developments, electrical properties of organic materials are remarkably lower than inorganic counterparts, above all monocrystalline and polycrystalline silicon. Therefore organic electronics are not expected to compete with inorganic devices; rather they are intended to complement silicon technology as lower resolution and cost-effective mass production devices, such as smart cards, rollable displays and electronic paper [6].

1.2 Organic Semiconductors

According to electrical conductivity, three categories of materials could be identified: conductors, semiconductors, and insulators. Semiconductors are those materials that show an intermediate conductivity between conductors and insulators, generally a value of about 10^{-8} - 10^3 S cm⁻¹. Conductivity differences among all the materials are given by differences in their band structure, which shows different energy gaps (E_g) namely the difference in energy between the valence and the conductive bands. Semiconductors materials have an E_g intermediate between conductors (valence and conductive bands usually overlapped) and insulators ($E_g > 4$ eV) [1]. As the band gap is bigger, the transition of charges between valence and conductive band is more difficult; this is why the insulators show an almost null conductivity. On the contrary, semiconductor materials can behave both as insulators and conductors according to different external conditions, *e.g.* an excitation of charges from the valence to the conductive band makes possible the passage of current.

1.2.1 Hybrid Orbitals

Organic semiconductors are conjugated carbon-based materials; they are classified in small-molecules or polymers according to their chemical structure [16]. Both of them show an alternation of single and double bonds between carbons and a network of π -bonding orbitals. Still, small-molecules can arrange in high crystalline structure to enhance the electrical conductivity, on the other hand, polymers generally have a semicrystalline structure with amorphous regions that limit their charge transport properties [3].

The alternating sequence of single and double bonds is possible due to the hybridization (combination) of carbon atoms [16, 17]: in original condition, two of four valence electrons of C atom occupy 2s orbital and the others two occupy two of p orbitals (p_x and p_y) (Figure 1.1a). During the hybridization process, one of the electrons in 2s orbital is promoted to a higher energy level; hence also the third p-type orbital (p_z) is filled (Figure 1.1b); to minimize the total energy orbitals change their original shape forming new hybrid orbitals (Figure 1.1c). Carbon atoms can combine all four original orbitals (hybridization sp^3), three of four (hybridization sp^2 , schematically represented in Figure 1.1) or only two (hybridization sp) [18]. Conjugated molecules are composed of sp^2 hybrid carbon atoms which show three sp hybrid orbitals having a planar structure and staggered by 120° each other, while the remaining p_z orbital is orthogonal to this plane. In Figure 1.2 it is shown the disposal of orbitals before and after a sp^2 hybridization.

During the chemical bond formation process both hybrid and not hybrid orbitals are involved: the former ones originate σ bonds which show a very high energy difference between the occupied bonding orbitals and unoccupied anti-bonding orbitals [1]; this results in strong insulator bonds (> 10 eV) forming the backbone of the molecule [3]. On the other hand, p_z orbitals, perpendicular to $x - y$ plane, form a π -bond with an analogous non-hybrid p_z orbital from the other atom. In this case the smaller energy gap, reflected in a weaker bond (< 4 eV) [3], allows the electron promotion

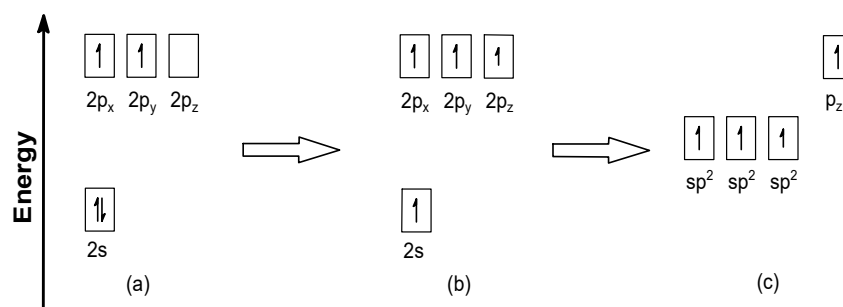


FIGURE 1.1: Energy diagram of (a) non-hybrid orbitals, (b) after promotion of one electron from 2s orbital to p_z orbital and (c) after sp² complete hybridization.

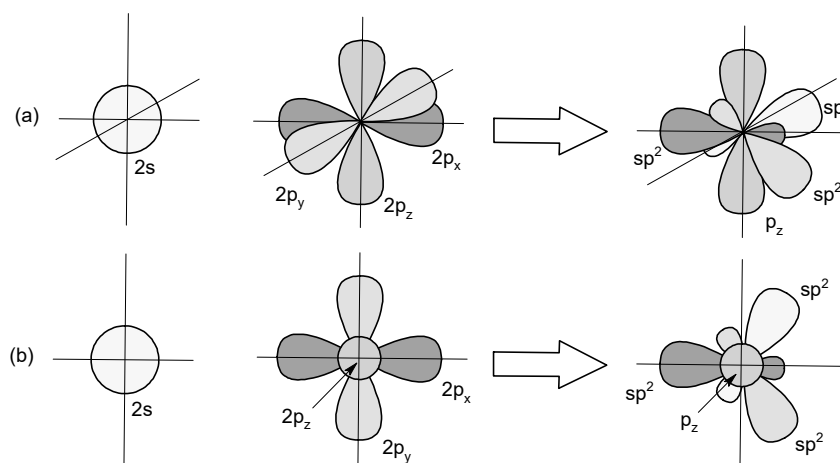


FIGURE 1.2: Spatial orbitals arrangement before and after hybridization. (a) prospective view and (b) view orthogonal to the $x - y$ plane where the hybrid orbital are lied.

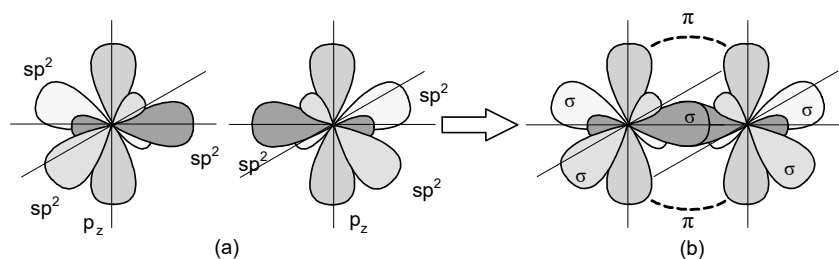


FIGURE 1.3: Formation of σ and π bonds between two sp^2 hybrid carbon atoms.

from occupied bonding orbital to anti-bonding unoccupied orbital. In Figure 1.3, the formation of σ and π bonds between two sp^2 hybrid carbon atoms, the remaining hybrid orbitals can form other σ bonds with any other atom. If the other four atoms are hydrogen ethylene molecule is formed, otherwise if sp^2 hybrid carbon atoms are connected as chain, a conjugated molecule is produced with alternating single (only σ -type) and double (both σ and π -types) bonds.

1.2.2 Conductivity Mechanism

Unlike inorganic materials which are composed of a continuous crystalline lattice, organic semiconductors lattice is made by small molecules or polymer chain bounded each other by various intermolecular interactions such as, hydrogen bonds [19], Van-der-Waals forces [20], and Coulomb interaction [2]. This different structure is reflected in a wider band-gap and in a discrete "energy level" band structure, unlike the continue structure of inorganic materials.

Moreover, an organic semiconductor lattice is affected by a large number of defects; their amount and disposition have a significant influence on electrical properties [10, 21]. It is generally accepted that at low temperature, assuming the number of defects extremely low, a band-like model can be used to describe the conductivity. In this situation, charge carriers are delocalized over several chains, and holes or electrons mobilities are determined by the total valence and conduction bandwidths that are built from interaction of the HOMO (Highest Occupied Molecular Orbital) and LUMO (Lowest Unoccupied Molecular Orbital) levels [20]. On the other hand, at higher temperatures (*e.g.* near room temperature), since the number of defects is not negligible, charges are expected to be located over a single molecule unit and their mobility is often determined by a thermally activated polaronic hopping transport process. Conjugated organic systems are generally characterized by significant static energy and/or a spatial disorder; therefore charges have to transfer from one molecule to another through a hopping process. According to semi-classical electron transfer theory and extensions theory, self-exchange rates, and thus charge carrier mobility, are determined by both transfer integral (t) and reorganization energy (λ). Transfer integral is related to the electronic couplings between adjacent molecules, and it strongly depends on the mode of molecular packing, *e.g.* degree of π orbital overlaps, $\pi-\pi$ stacking distance. Reorganization energy includes two contributions, internal and external; the former one is related to intramolecular freedom degree, molecular rigidity and conjugation length among the others. The external reorganization energy is originated from

changes in surrounding media that accompany the charge transfer; theoretically speaking, in crystals case, contribution of external reorganization energy can be neglected. To increase charge transfer, a large transfer integral (high electronic coupling) and a small reorganization energy (molecules ideally fixed in a stable position) are desirable [20].

Alkyl and aromatic molecules are applied in this field to produce conjugated compounds; they can rearrange both in large planar or long-chain systems. In general, for larger plane molecules, characterized by several aromatic rings, π orbitals are highly overlapped, it results in a larger transfer integral and so in an enhanced charge carrier mobility. On the contrary, long-chain compounds show a one-dimensional electronic system, thus a long-range order is requested to achieve efficient charge transport. Therefore small-molecules having larger planar aromatic configuration are preferred in optoelectronic applications [1].

1.2.3 Molecular Stacking

It is clear how long-range intramolecular delocalization strongly affects charge transport and how it marks a big difference between conductivity in long-chain polymer and small-molecule semiconductors. In the former case, π -orbitals overlapping along all the chain assures a great intramolecular delocalization that is impossible to achieve for small-molecule [6]. Furthermore talking about polymer semiconductors, co-presence and spacial ordering of both amorphous and crystalline phases can affect charge transport. On the other hand, in small-molecules case charge transport is largely determined by the packaging of the molecules in the crystal lattice; that is influenced by the electronic structure of the single molecule, relative position of molecules in the crystal and morphology variations generated from the static or dynamic deviations of optimal single-crystal structures [1]. Therefore assuming the common case of a crystal made of small-molecules having a chemical structure characterized by a planar conjugated backbone, the relative position of the conjugated structure belonging adjacent molecules can vary by tilting, increasing planar distance or moving along the long or short axis of the backbone [20]. Hence some common packaging motifs are [1, 20]:

- (i) Herringbone (edge to face disposal) packaging motif without $\pi - \pi$ overlap between adjacent molecules (Figure 1.4.i); *e.g.* acenes (tetracene, pentacene, *etc.*)
- (ii) Herringbone packaging motif with $\pi - \pi$ overlap between adjacent molecules (Figure 1.4.ii); *e.g.* rubrene.
- (iii) Lamellar (face to face disposal) packaging motif, one-dimensional $\pi - \pi$ stacking (co-facial stacking) (Figure 1.4.iii); *e.g.* TES pentacene (6,13-bis((triethylsilyl)ethynyl)pentacene).
- (iv) Lamellar packaging motif, two-dimensional $\pi - \pi$ stacking (bricklayer stacking) (Figure 1.4.iv); *e.g.* TIPS-pentacene (6,13-bis(triisopropylsilyl)ethynylpentacene)).

Among these different configurations, theoretically speaking, (iii) and (iv) are believed to be the most efficient disposals for the charge transport [1]: they show a better $\pi - \pi$ overlap and shorter $\pi - \pi$

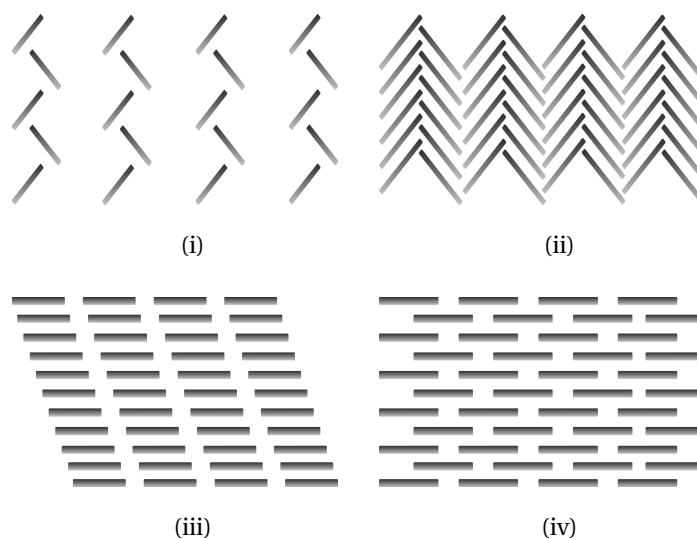


FIGURE 1.4: Common conjugated small-molecules stacking motifs: (i) herringbone edge to face without $\pi - \pi$ overlap, (ii) herringbone edge to face with $\pi - \pi$ overlap, (iii) lamellar face to face in co-facial configuration and (iv) lamellar face to face in bricklayer configuration.

distance which maximize transfer integral; therefore intensive efforts have been made to obtain this stacking motif. However, it should be noted that presently most of the organic semiconductors which exhibit high carrier mobility are still those with herringbone packing motifs, such as pentacene and rubrene [20]. This not-expected result can be explained by the fact that the large electrostatic repulsion between the adjacent co-facial conjugated backbones leads to displacement along with the short or/and long axis which, as said, affects electronic couplings and thus charge transport [22].

Both small molecule and polymer semiconductors are generally characterized by a linear conjugated backbone, that make their structures largely anisotropic. Molecular structure anisotropy is reflected on the molecular packaging anisotropy hence many crystal properties are affected by this strong direction-dependence. Among these, optical absorption, thermal expansion, exciton diffusion, and above all, charge transport. In this situation transfer integral plays an important role, it increases increasing $\pi - \pi$ overlap, so observing different molecular stackings in Figure 1.4, it is evident how in the direction perpendicular to the planar backbone $\pi - \pi$ overlap is more significant than any other direction leading to better electrical performances [4, 23, 24].

1.2.4 Pentacene and TIPS-pentacene

Linear fused acene rings are the benchmark molecule to produce an extensive class of small-molecules semiconductors. However structural modifications are required to overcome some intrinsic issues, such as poor stability and poor solubility. One possible solution has been identified in heteroatoms incorporation in acene conjugated backbone, such as sulfur or nitrogen. In this way, novel intermolecular interactions ($S \dots \pi$, $S \dots C$, or $N-H \dots \pi$, *etc*) are introduced to create more reliable

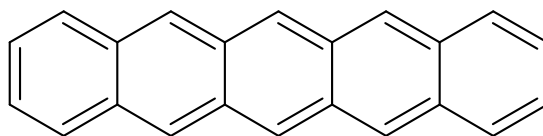


FIGURE 1.5: Pentacene structural formula.

molecule-to-molecule couplings and enhance electrical conductivity. At the same time, the aromaticity of π -systems is reduced to attain higher ambient stability [20]. Otherwise, temporary functional groups can be added to a small-molecule semiconductor to make soluble the material; however, added groups limit or destroy the electrical properties, so they have to be removed by thermal or light-induced process before devices applications [25]. Innovative and permanent side groups not heavily impacting electrical properties have been researched to avoid post-treatment processes. It is found that some side groups not only increase the solubility of the native molecule but also enhance packing motif, and sometimes even electrical properties [20, 25].

Among acenes, features such as charge carrier mobility and environmental stability are related to the increasing number of benzene rings: acenes having few rings show a too reduced charge carrier mobility; on the other hand, if the number of rings is too high, many ambient stability issues have to be faced in yielding and working conditions of the devices. Pentacene (Figure 1.5), an acene molecule having five fused aromatic rings, is commonly considered as a benchmark among this class of molecules due to an optimal trade-off between charge carrier mobility and environmental stability [20, 26]. Therefore in the last decades, it has been involved in many studies; values of maximum and average charge carrier mobilities of $35 \text{ cm}^2/\text{V s}$ and $10 \text{ cm}^2/\text{V s}$, respectively have been reported [21, 27]. Despite its good electrical properties, pentacene-based devices production is limited by stability issues, such as undesirable oxidation in 6,13-pentacenequinone at the surface [21, 27], and high-cost film fabrication, only achievable with costly vacuum evaporation method due to the non-solubility in almost all organic solvents [12, 28].

These limitations have pushed researches in developing new small-molecules semiconductors suitable to be applied in cost-effective production processes. Anthony et al. reported the effects of the functionalization of pentacene molecules on both the solid-state ordering and the electronic properties of the resulting crystals [29]. They produced a novel molecule, 6,13-bis (triisopropylsilylethynyl) pentacene (TIPS-pentacene), adding two bulky side groups at the third benzene ring of the native pentacene (Figure 1.6). Their original goals were first to increase solubility of pentacene compound to simplify purification and processing, and second induce some capability for self-assembly of the aromatic moieties into π -stacked arrays to enhance intermolecular orbital overlap. As Anthony et al. predicted, TIPS-pentacene solubility was proved in many organic solvents, including acetone, chloroform, tetrahydrofuran, hexane, toluene and chlorobenzene (Table 1.1) [30]. This achievement

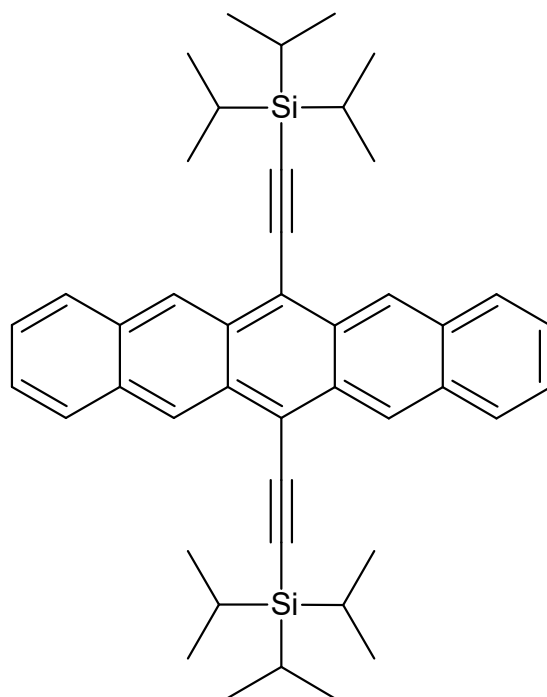


FIGURE 1.6: TIPS-pentacene structural formula.

made possible the development of several simple, cost-effective, and solution-based methods to obtain organic crystals suitable for optoelectronic applications. Due to big differences in solvent properties that affect solvent evaporation rate and residues in the resulting crystals, the choice of the most suitable solvent dramatically affects the final results [14, 31–33]. Boiling point (BP) and vapor pressure, besides TIPS-pentacene solubility in the solvent, are essential parameters for controlling solvent evaporation rate. If it occurs too fast (solvents having lower BP), smaller and less wide crystal grains are yielded. Similar results are obtained with solvents showing poor TIPS-pentacene solubility (*e.g.* hexane); therefore, toluene, having a quite high boiling point and high TIPS-pentacene solubility, is generally accepted as the best solvent for this material [30].

Besides making pentacene molecule soluble in a large number of organic solvents, the two bulky side

TABLE 1.1: Properties of the most common organic solvents for TIPS-pentacene

Solvent	Boiling Point (°C)	Vapor Pressure (KPa) (at 25 °C)	TIPS-pentacene Solubility (%)
Acetone	56.2	30.0	~ 0.1
Chloroform	61.3	26.1	~ 5
Tetrahydrofuran	65.0	17.3	~ 5
Hexane	69.0	16.94	~ 0.5
Toluene	110.6	3.79	~ 5
Chlorobenzene	131.7	1.61	> 1

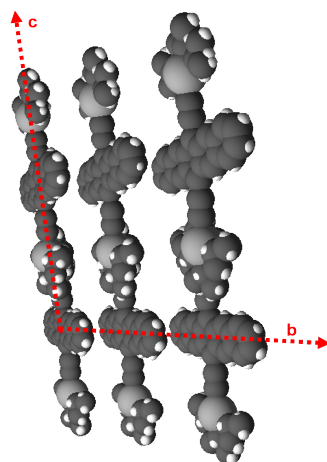


FIGURE 1.7: Schematic representation of TIPS-pentacene 3-dimensional molecular stacking. Red dotted lines point b and c direction of crystalline lattice.

groups have a great impact on the molecular stacking and thus on the charge carrier mobility [1, 2, 20, 25]. As explained in Subsection 1.2.3. After crystallization, pentacene molecules assume herringbone edge-to-face configuration namely a not optimal orbital overlapping, so a handicap can charge carrier mobility. The two bulky side groups are connected to the core of the aromatic rings through a triple bond that keeps the groups far away from the backbones and allows them to assume a face-to-face stacking [23]. This arrangement increases the lateral overlapping of aromatic rings leading to a 2D lamellar packaging motif (bricklayer disposal) that is proved to be one of the best molecules disposal to enhance the charge carrier mobility (Figure 1.7) [20].

Finally, the bulky side groups addition give TIPS-pentacene a high air and environmental stability compared to acenes molecules; for this reason, a vacuum or inert environment is not required during the crystal fabrication or the device work [3]. Thus due to these properties, TIPS-pentacene is generally used as a benchmark among *p-type* soluble small molecules semiconductors; values of hole mobility over than $10 \text{ cm}^2/\text{V s}$ have been reported for single crystals [34] and in several studies values above $1 \text{ cm}^2/\text{V s}$ have been obtained for polycrystalline structures. Although TIPS-pentacene shows one of the highest charge carrier mobility among *p-type* soluble small molecules semiconductors, film morphology has a significant influence on mobility values; hence further investigations are needed to apply this material in large-scale production.

1.3 Organic Field-Effect Transistors

Field-Effect Transistors (FET) are electronic devices that switch or amplify electrical signals; they form the basic structure of integrated circuits and displays [3, 26]. Inorganic materials, such as silicon, have been used as active layers, until when in 1987 Koezuka et al. produced the first Organic

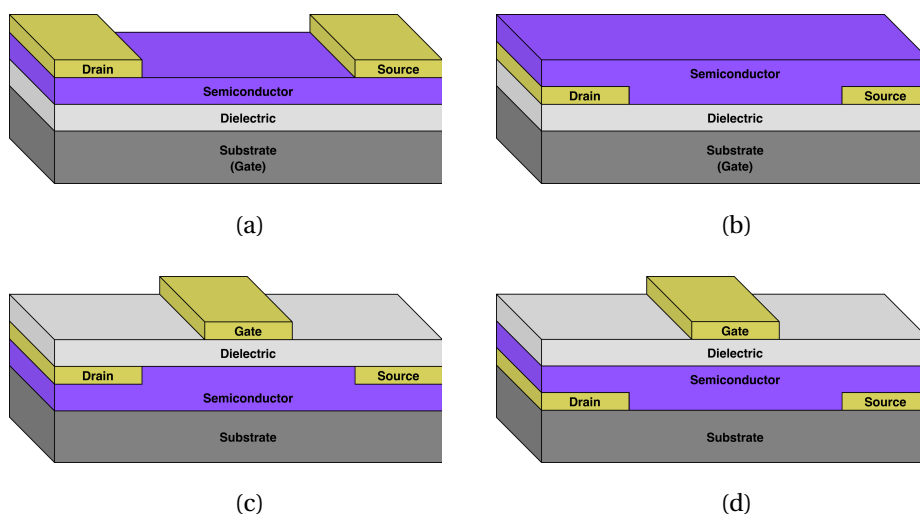


FIGURE 1.8: OFET configurations: (a) bottom-gate/top-contact, (b) bottom-gate/bottom-contact, (c) top-gate/top-contact and (d) top-gate/bottom-contact.

Field-Effect Transistor (OFET) using polythiophene as active (semiconductor) layer [35].

1.3.1 Structure

OFETs are three-contact devices consisting of two electrodes, source and drain, directly connected to the active layer, while between the third one, gate contact, and semiconductor material, a thin dielectric (insulator) layer is located forming a sort of capacitor between active layer and metal (gate). The electrodes can be located in different relative position achieving different OFET configuration as, shown in Figure 1.8: (a) bottom-gate/top-contact, (b) bottom-gate/bottom-contact, (c) top-gate/top-contact and (d) top-gate/bottom-contact.

The two bottom-gate configurations take advantage of the fact that the active layer can be directly deposited on the insulator layer, generally pre-deposited on the substrate. In this way, deposition processes of insulator layer and gate electrode above active layer are avoided, so further possible damages at semiconductor material are prevented. In bottom-contact configurations, electrodes are generally pre-patterned on the substrate or on the insulator material through photolithography before depositing the semiconductor layer; on the contrary, in the top-contact configurations, contacts are thermally evaporated through a shadow mask onto the active layer after its deposition. Top-contact OFETs result in better device performances in terms of larger drain currents and smaller contact resistances than bottom-contact ones, which generally show a larger potential drop at semiconductor/electrode interface [36]. Large metal-semiconductor contact resistance due to interface contact barrier, smaller charge injection area, irregular deposition, and poor morphology of the semiconductor film around the already patterned contacts explain the worse performances of bottom-contact OFETs [37].

Electrodes are implemented using metals or less frequently organic conductors. Still, if the choice

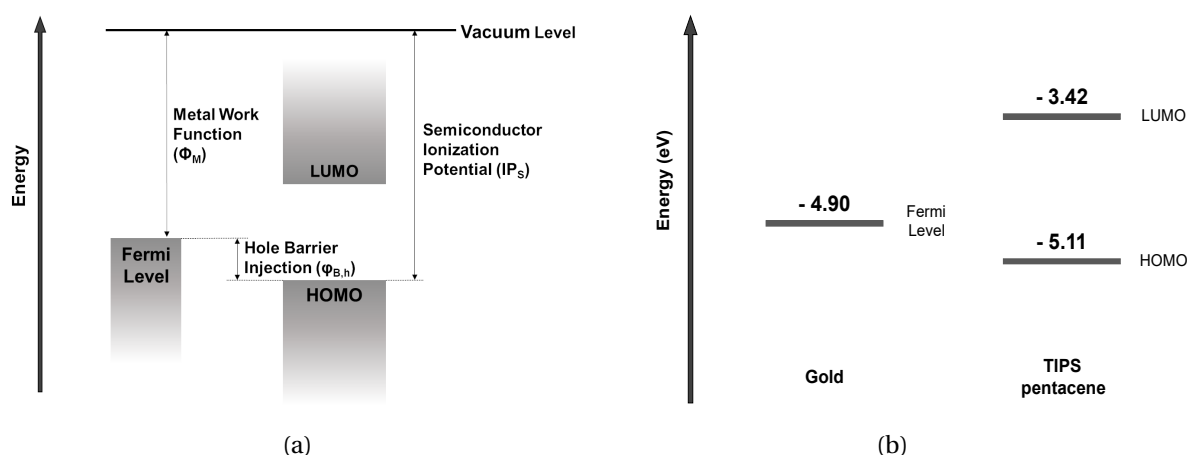


FIGURE 1.9: (a) Energy band diagram at the contact electrode-semiconductor representative metal work function (Φ_M), semiconductor ionization potential (IP_S), and hole injection barrier ($\phi_{B,h}$). (b) Energy diagram representative energy level of Gold and TIPS-pentacene.

is quite relaxed for gate electrode, for source/drain electrodes, since they are in contact with the organic semiconductor layer, it deserves a more accurate analysis. A conscientious energy matching between metal work function and semiconductor energy levels is needed to ensure a large charge injection at electrode-active layer contact. Since an ohmic contact (low contact resistance and linear I-V behavior) is preferable, metal work function has to match with HOMO semiconductor level for *p-type* materials and with LUMO level for *n-type* materials. Hence for *p-type* semiconductors, such as TIPS-pentacene, high work function metals, includes gold (Au) or platinum (Pt), are generally implied. Furthermore, oxidation at the surface is avoided thanks to their optimal environmental stability, so higher contact resistance is achieved [6].

Observing energy diagram of Gold (Au) and TIPS-pentacene it is clear the convenience of using this metal for electrodes: Au work function (-4.9 eV) is very close to TIPS-pentacene HOMO level (-5.11 eV [38]), so hole injection barrier is minimized, and an efficient charge injection at contacts is ensured [37].

1.3.2 Operation Principle

OFETs, unlike their inorganic counterparts (MOSFET) which work in inversion bias regime, work in accumulation regime; this means that an external electric field is formed applying a voltage at the gate electrode; thus a charge channel is created in the active layer at the interface between semiconductor and insulator. Different semiconductor molecules (*p-type* or *n-type*) require different voltage signs; *i.e.*, TIPS-pentacene is a *p-type* semiconductor so a negative voltage has to be applied at gate electrode to create a holes channel in the active layer.

Once holes (or electrons) channel is formed in the active layer by applying gate voltage, an independent negative (or positive) voltage applied at the drain or source electrode can attract the charges

generated in the channel. Therefore increasing the absolute value of gate voltage (V_{GS}), a larger charge density is created in the active layer, so for the same amount of drain-source voltage (V_{DS}) a higher drain-source current (I_D) is measured; it is also evident how at the equal value of gate voltage, increasing drain-source voltage drain current increases. Gate-independent voltage can be applied both at source or drain electrode, but it is generally accepted that source is grounded while the drain is used to apply tension (Figure 1.10).

In the next paragraphs, a theoretical analysis of OFET working is provided referring to a *p-type* semiconductor, for *n-type* it is enough inverts voltage and current signs. The device is turned off till the gate voltage (V_{GS}) applied between gate and source terminals is null or higher than the so-called threshold voltage (V_{Th}); in this situation, a small amount of current flows from source to drain due to the intrinsic charge carriers in the semiconductor material. Decreasing V_{GS} below the threshold value a charge channel between source and drain is formed, the device is turned on and if a non-null voltage is imposed between source and drain and a charge flow between electrodes is set.

Ohmic or Linear Region If $V_{GS} < V_{Th}$ and $V_{DS} > (V_{GS} - V_{Th})$, namely a small drain voltage is set, current starts to flow in the channel and the device operates as a linear resistor. In this situation, the intensity of drain-source current (I_D) is controlled by the gate voltage (V_{GS}) and its absolute value increases linearly with the drain voltage (V_{DS}) decreasing according to the following equation:

$$I_D = -\frac{W}{L} \mu C_i (V_{GS} - V_{Th} - \frac{V_{DS}}{2}) V_{DS} \quad (1.1)$$

Where W is the channel width, L the channel length, μ the charge carrier mobility and C_i is the dielectric capacitance per unit area.

Saturation or Active Region If $V_{GS} < V_{Th}$ and $V_{DS} \geq (V_{GS} - V_{Th})$, namely the drain voltage decreases to a value that makes the potential difference between drain and gate voltage reduces to the threshold voltage, channel pinch-off is reached. Thus current flow in the channel is independent by increasing drain-source voltage, and the so-called saturation region is attained; therefore, drain current is only gate voltage-dependent. The following equation can describe this situation:

$$I_D = -\frac{W}{2L} \mu C_i (V_{GS} - V_{Th})^2 \quad (1.2)$$

Where W is the channel width, L the channel length, μ the charge carrier mobility and C_i is the dielectric capacitance per unit area. To write both 1.1 and 1.2 equations, it is accepted that [17]:

- (i) longitudinal electric field through the channel is considered negligible compared to the transverse one.
- (ii) μ and V_{GS} are considered constants, namely, the charge carrier mobility is thought as an intrinsic material property.

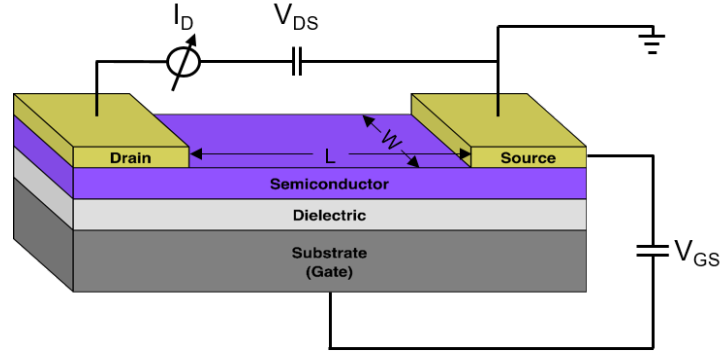


FIGURE 1.10: BG-BC device working conditions: V_{GS} is applied at gate electrode, V_{DS} at drain electrode, and source electrode is grounded. I_D is measured between drain and source. Channel width (W) and length (L) are also indicated.

1.3.3 Output Data Analysis

OFET working conditions are generally described by some parameters, such as mobility μ , threshold voltage V_{Th} , sub-threshold slope, power on voltage V_{ON} , and ratio between *on* and *off* current ($I_{on/off}$). An electrical test on the device gives as output the so-called output characteristic (I_D - V_{DS} with V_{GS} as a parameter, Figure 1.11). Rough data can also be plotted through transfer characteristics (I_D - V_{GS} and $\sqrt{I_D}$ - V_{GS} at a fixed V_{DS} , Figure 1.12) from which all parameters previously introduced can be extrapolated.

Mobility It is the relationship between charge carriers average speed and the electrical field applied across the channel; it is measured in cm^2/Vs . Observing the phenomenon at microscopic level charge carriers are constantly accelerated by the electric field, but due to the continuous scattering between carriers and lattice, their speed does not increase continuously, resulting in a quasi-constant value.

Mobility value can be extrapolated for both ohmic or saturation region; in the former case a linear fitting on characteristic in I_D - V_{GS} diagram is needed, while in the latter one $\sqrt{I_D}$ - V_{GS} curve has to be used (an example of linear fitting for saturation region is provided in Figure 1.12.b). In particular mobility can be calculated from equations 1.1 and 1.2:

$$\mu_{ohm} = \frac{L}{WC_i} \frac{-I_D}{(V_{GS} - V_{Th} - \frac{V_{DS}}{2})V_{DS}} \quad (1.3)$$

for linear region;

$$\mu_{sat} = 2 \frac{L}{WC_i} \frac{-I_D}{(V_{GS} - V_{Th})^2} \quad (1.4)$$

for saturation region; where in both cases W is the channel width, L the channel length and C_i is the dielectric capacitance per unit area.

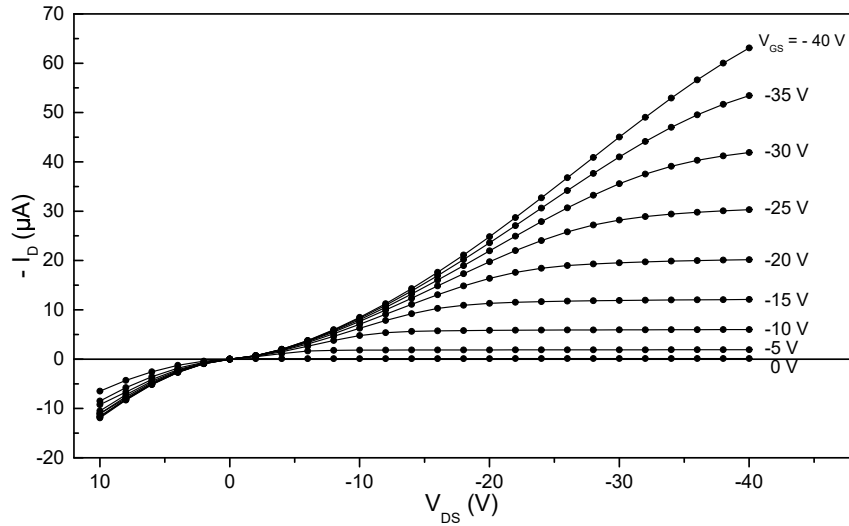


FIGURE 1.11: Output characteristic of a generic *p-type* semiconductor material.

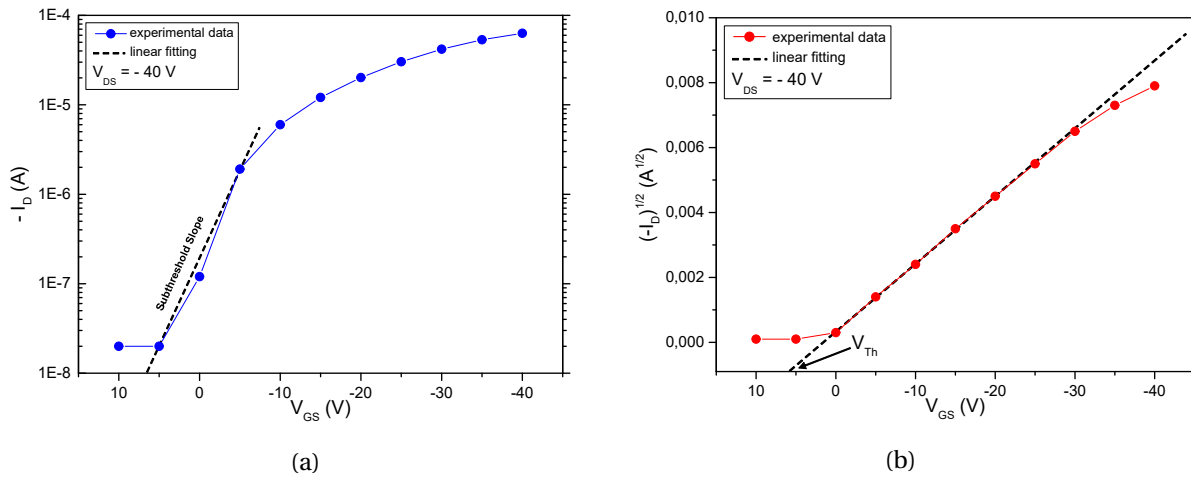


FIGURE 1.12: Transfer characteristics in saturation region showing dependence of (a) I_D and (b) $\sqrt{I_D}$ on V_{GS} at one fixed V_{DS} . In (a) is shown the linear fitting to determine subthreshold slope, while in (b) to determine saturation mobility (line slope) and threshold voltage.

Threshold Voltage It is the gate voltage value above which a rich charge density is created at the semiconductor-insulator interface, and thus, current can flow through the channel. It is calculated from the extrapolation of the interception between the fitting line and the V_{GS} axis in I_D - V_{GS} and $\sqrt{I_D}$ - V_{GS} diagrams for ohmic and saturation region, respectively (see Figure 1.12.b). Due to the gradual OFET power on the method to obtain V_{Th} is not unique and also using the same one, it depends on the range of data used to calculate the fitting line.

Sub-threshold Slope This parameter is the slope of the curve in I_D - V_{GS} (for ohmic region) and $\sqrt{I_D}$ - V_{GS} (for saturation region) diagrams with current data expressed in logarithmic scale. It is measured at the point of maximal slope and expressed in V/decade (see Figure 1.12.a). It represents how fast is the drain current increase caused by a change in gate voltage (that causes a gain in charge carrier density in the channel).

Power on Voltage and on/off current These parameters are calculated from the semi-logarithmic plots. Power on voltage (V_{ON}) is the voltage at which the drain current overcomes the noise value obtained at turned off conditions. The $I_{on/off}$ is the ratio between the maximum and minimum values of current, namely an idea of the device amplification ability.

1.4 Research Outline

TIPS-pentacene is an organic semiconductor that shows excellent intrinsic properties such as high solubility, high electrical performances, and remarkable air stability. Therefore it is considered a benchmark among small-molecule semiconductors. However, despite its notable properties, TIPS-pentacene films are affected by several critical issues caused by not optimal deposition processes. First of all, solution-processed TIPS-pentacene forms polycrystalline structures, which cause various morphological problems, including random crystal orientation and lack of substrate coverage. Large uncovered areas and grain boundaries hinder the charge carrier pathway between electrodes, resulting in very poor electrical performances. Besides bad electrical properties, low crystal ordering gives inconsistent properties, namely high device-to-device performance variation. This affects sample reproducibility and large scale device fabrication.

In recent years several studies have been carried out to identify organic crystal growth methods that allow achieving the best morphological and electrical properties and, at the same time, suitable for large scale production. Fabrication processes for soluble materials can be divided into two categories: "external method" and "additive method". In the former case crystal growth is regulated by an external driving force that influences crystal growth, controlling for example solvent evaporation direction and/or rate. The latter technology consists of producing a blend solution of semiconductor, solvent along with an additive that act as a second solvent, nanoparticles or polymer. In this

case physio-chemical interactions between blend components produce beneficial effects on morphological and electrical film properties. Specifics, advantages and disadvantages of each method, including some examples, are more deeply investigated in Chapter 2.

In this research using TIPS-pentacene as a benchmark material, organic films have been produced by both "external method" and "additive method". After that, the technologies have been mixed to evaluate the effectiveness of a hypothetical "combine method". A thermal gradient was applied to a drop-casted solution as external driving force to improve crystal alignment and film coverage; afterward, an insulator polymer (polystyrene) has been added to TIPS-pentacene solution to enhance crystal size, electrical properties and performance consistency. Finally, the last stage of the research consists of producing an organic film by depositing a blend solution of TIPS-pentacene and polystyrene onto a substrate where a thermal gradient is applied. Morphological and electrical properties are measured, along with crystallinity and microstructure, in order to provide a whole investigation of all films yielded by each type of deposition.

Chapter 2

State of Art of Crystal Fabrication

In this chapter, a summary of state of art of organic crystal fabrication techniques is provided, particularly, since TIPS-pentacene, the material used in this research, is a soluble semiconductor and generally processed through wet techniques, these methods are investigated. In following sections, the most common crystal growth methods from solution will be briefly explained; they can be divided into external (a driving force is applied on the solution) and additive (a third material is added to pristine TIPS-pentacene/solvent solution). Crystal growth methods implemented in this research will be more deeply investigate, providing some theoretical bases which will help to understand result discussion in the following chapters.

Different fabrication techniques produce different crystal morphologies that are strictly connected to microstructural features and electrical performances; hence it is important to understand the advantages and disadvantages of each growth method to obtain the most suitable crystal film. It is globally accepted that defects have deleterious effects on charge carriers mobility; hence they must be avoided [7, 39]. Charge traps, grain boundaries, thermal cracks are some of the most common defects in an organic semiconductor crystal [13, 40, 41]. Therefore the aim of researchers is obtaining large, thin, and not cracked single crystals.

The most common fabrication techniques are in vapor or liquid phase; besides the problem of the solubility of some small-molecules semiconductor [10], each one has some pros and cons. Vapor phase growth requires high temperature, vacuum or inert environment, complex and expensive equipment, but generally gives good sized crystals, although often different sizes, thicknesses and shapes are obtained, even if its application in large-area devices is difficult due to geometrical limits [8, 40]. On the other hand, solution-processed crystals require basic tools, low temperature, cost-effective and simple processes; but generally, polycrystalline structures are yielded [10]. Since it is complicated to produce large and morphologically controlled single crystals using simple-drop cast technique, some shrewdness has been studied to enhance domains size and orientation.

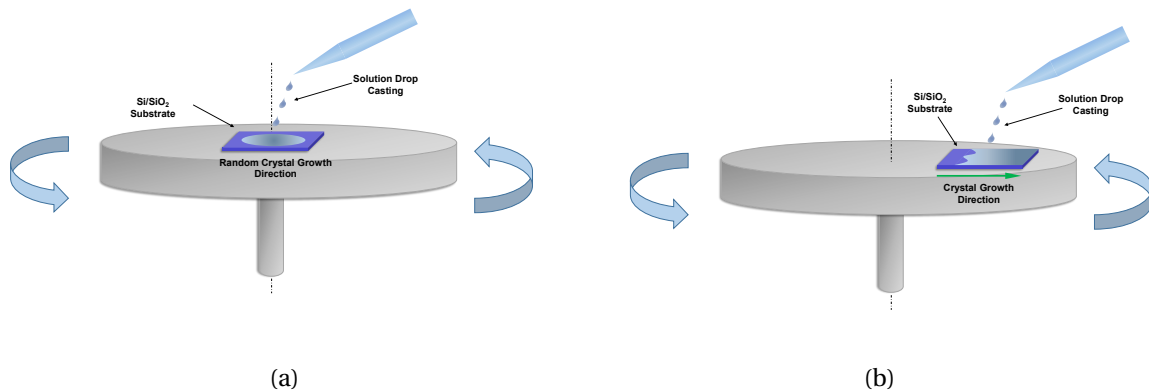


FIGURE 2.1: Schematic representation of (a) centered spin-coating technology, the substrate is placed in the middle of rotating plate (co-axial position), and (b) off-centered spin-coating, the substrate is placed closer to the boundaries of the rotating plate. In (a) a random crystal growth direction is obtained while in (b) crystals growth following a determined direction identified by the green arrow.

2.1 External Methods

During a crystallization process the solvent plays a key role: its evaporation rate and direction greatly influence the final result. Simple drop-cast technique does not provide a suitable crystal for optoelectronic applications due to the absence of external driving forces that allow controlling the morphological properties, above all crystal alignment [42]. If the droplet is simply dropped on the substrate, solvent evaporation direction is controlled only by the "pinning effect" of the droplet edge: contact lines are fixed once the droplet is deposited; thus a change of the liquid content is limited. As consequence, the volume change at the edge is smaller than in the center, but at the same time the solvent evaporation rate is faster at the contact line due to the increased available angle for solvent evaporation and thus a larger air-solution interface. The combination of these effects causes a radial flow of the solvent from the center to the edge; also the solute moves according to this flow, thus it results in a deposit of material at the contact line; which after deposition forms the so-called "coffee-ring" [43]. This particular conformation is characterized by thicker crystals along the entire original contact line and thinner needle-shaped crystals disposed of in a radial motif from the center to the edge; it means high orientation variability, large number of grain boundaries and lack of areal coverage, morphological properties reflected in bad and not consistent device performances [31].

2.1.1 Spin-Coating

One of the first and most simple methods to control the solvent evaporation is the spin-coating technique: the substrate is located on a rotating support and a droplet is deposited on it (Figure 2.1.a). Tuning rotation speed, time of rotation and amount of solution dropped it is possible to vary crystal thickness. Despite it is very simple and prevents the "coffee-ring" formation, the centrifugal force applied on the droplet causes a solvent radial flow; thus, crystals attained are aligned in multiple

directions leading to not uniform crystal orientation. Moreover, the high rotation speed requested to obtain flat and smooth surface, accelerates the solvent evaporation, therefore resulting films are characterized by small and needle-shaped crystals or even amorphous region.

An alternative method to avoid solvent radial flow is the off-centered spin-coating (Figure 2.1.b): the off-centering between the center of rotation and center of the substrate causes a unidirectional solvent flow, thus aligned crystals can be obtained [44]. Solvent evaporation rate, and therefore final crystal morphology, is controlled by a delicate trade-off between rotation rate and solution viscosity; that makes this method not so suitable to obtain good crystals for device applications [3].

Finally, high solvent waste (during the deposition a large amount of solution spreads out the substrate due to the strong centrifugal force) makes this technique not suitable for large-scale industrial processes. Indeed it is mainly employed in research field to compare different materials properties rather than as an enhancement method to improve a single material properties.

2.1.2 Droplet-Pinned Crystallization

Droplet-pinned crystallization (DPC) is one of the simplest and most effective methods to obtain well-aligned ribbon shape crystals. A simple drop-casting technique directly originates it with the difference that one edge of the droplet is forced to be pinned, while the other side is free to spread along the whole substrate. Whatever device able to induce the droplet contact line to be pinned at its edge can be used as pinner: a small piece of Si/SiO₂ wafer [45] or a glass cylinder [10] as shown in Figure 2.2. In this case, the final chemical surface treatment of the pinner is important: it has to be wettable by the solution, otherwise the desirable effect does not occur. A similar pinning effect can be obtained using an edge of the substrate where the droplet is deposited as a pinner, in this case, the substrate is tilted by a small angle (3°-5°) and the droplet, deposited by simple drop-casting, is forced to be pinned at the upper edge of the substrate, while the other side can spread to the lower side of the substrate (Figure 2.3) [28, 46, 47].

In both cases, a difference in solution volume is set between pinned and not-pinned droplet edge, hence a preferred evaporation direction is imposed to the solvent which leads to a preferred crystal growth direction. In particular, if the solution is laterally confined, generally by substrate boundaries, droplet free edge assumes a linear shape parallel to the pinned edge, and crystal growth is forced to occur in the direction perpendicular to these lines [10]. This deposition method is clearly simple and does not need any special equipment, but at the same time, since the applied driving force is not strongly applied on the solution, some undesirable growth directions can be identified. It is generally used to compare different solution compositions in research field, but it shows some critical issues in large-scale production.

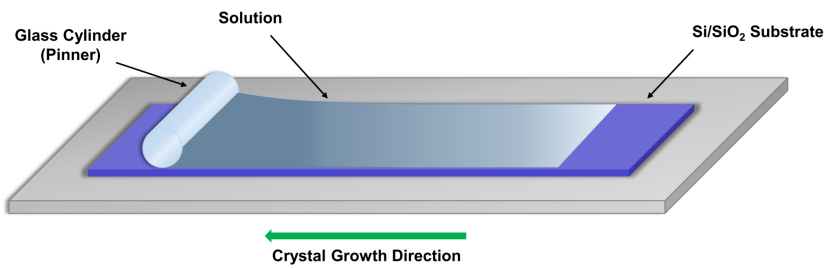


FIGURE 2.2: Schematic representation of droplet-pinned crystallization: glass cylinder (the pinner) provide a difference in droplet volume distribution causing a preferred crystal growth direction identified by the green arrow.

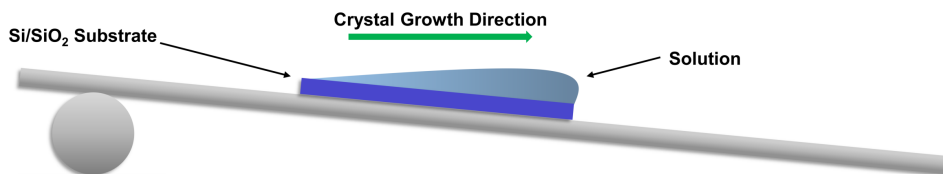


FIGURE 2.3: Schematic representation of drop casting on a tilted substrate, the profile assumed by the droplet leads to a difference in in droplet volume distribution causing a preferred crystal growth direction identified by the green arrow .

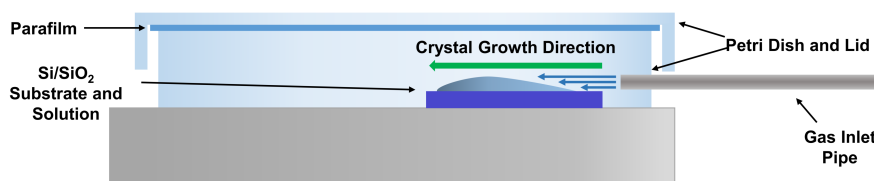


FIGURE 2.4: Schematic illustration of the experimental setup to grow crystals with gas-flow assistance. Gas is entered the chamber by a pipe on one droplet side, and it makes solvent evaporation starts from that side, leading to a preferred crystal growth direction identified by the green arrow.

2.1.3 Gas-Flow Assisted

One more method to optimize the crystal alignment consists of blowing a gas-flow from one droplet side; this method has the main goal of decreasing in misalignment angle between crystals, besides enhancing areal coverage and film thickness, leading to improvements in charge carrier mobility [31]. This technique requires quite sophisticated equipment to control the gas-flow, it should be well aligned, without any whirlpools, and with high controlled speed. In fact, if the gas-blow is too weak, it has no influence on the crystal morphology; on the other hand, if it is too strong solvent evaporation occurs extremely fast, leading to spherical-shaped crystals, thus without any advantages in charge mobility.

Due to these issues, not so many articles have been reported, and even these few papers are in contradiction: He et al. [31] used air-flow on TIPS-pentacene based solution and obtained needle-shaped crystals aligned along the air-flow direction. On the contrary, Tong et al. [48] blew nitrogen on the same type of solution, and ribbon-shaped crystals orientated perpendicular to the air-flow resulted. Therefore gas-flow technique shows sharply different behaviors under similar conditions, which makes this a not well-investigated method to growth crystals.

In this research, a first attempt to grow morphologically controlled TIPS-pentacene crystals was made using this method, further enhanced by heating substrate at an optimized temperature. Home-made equipment shown in Figure 2.4 has been built to blow a controlled air-flow inside a small polystyrene chamber where the substrate is located. To prevent a too fast solvent evaporation rate the polystyrene box was closed with its lid and sealed with few parafilm layers.

This attempt was quit due to several issues: equipment build-up turned out to be too complicated and affected by too many uncontrolled factors, above all air-flow's homogeneity. Air enters the chamber by a flat-shaped aluminum pipe, that assures a more homogeneous flow profile than a rounded

shape pipe, but at the ends of the profile, unavoidable vortexes disturb this regularity. Furthermore, air-flow homogeneity decreases increasing distance from the pipe end; it assumes a whirling behaviour in a too short distance not enough to ensure identical conditions on the whole substrate. An increased homogeneity can be reached increasing the air flow rate; but in this way also solvent evaporation rate increases leading to too fast solvent evaporation. Even if it is an interesting method to fabricate crystals, a precise equipment set up was required to control all the parameters involved accurately; since it was not possible to achieve, a different crystal growth method was chosen.

2.1.4 Thermal Gradient Assisted

Thermal gradient assisted growth has been revealed as the most effective drop-casting based method to grow organic crystals having enhanced morphological and electrical properties. This simple technology consists of applying different temperatures at the two ends of the substrate, and after that, drop the solution on the substrate. The thermal gradient creates a driving force for solvent evaporation and thus a preferred crystal growth direction.

Equipment set up is effortless and since the only external force to guide solvent evaporation is the thermal gradient, it is a static apparatus, thus errors related to uncontrollable factors, *e.g.* in growth assisted by gas-flow, are avoided. Equipment is made by a heater (kept at T_h) and support (T_l or assumed at room temperature, T_r), through which the substrate takes place, it can be placed inside a container, such as a petri dish, to control solvent evaporation. Therefore this method is suitable for both inorganic (rigid) and polymeric (flexible) substrates, the latter ones are even preferable due their low thermal conductivity that allows keeping a more uniform thermal gradient also during long time crystallization processes [49].

If temperature range is reduced, crystal nucleation and growth are controlled by supersaturation: it is known that solubility increases with temperature, thus when at T_h , afterward a part of the solvent has been evaporated, solute reaches solubility limit. At the same time at T_l solution is supersaturated; therefore, crystal growth will occur from the substrate edge at low temperature. In order to ensure a high morphologically controlled crystal growth a high nucleation density at T_l is required; it occurs when a balance between nucleation rate and growth rate is achieved [3]. As thermal gradient increases, also supersaturation increases, which means a gain in both nucleation and growth rate, but since growth rate increases more quickly than the nucleation rate, at small thermal gradients, few and bigger crystals are obtained. Afterward, when the competition between the two phenomena increases, more and smaller crystals are yielded. It is worth to be mentioned that an increasing temperature at the heated side leads to faster solvent evaporation, which hinders a large crystal growth. Thus, if T_h increases over a critical value, crystal growth is not controlled by supersaturation anymore but rather by solvent evaporation [42].

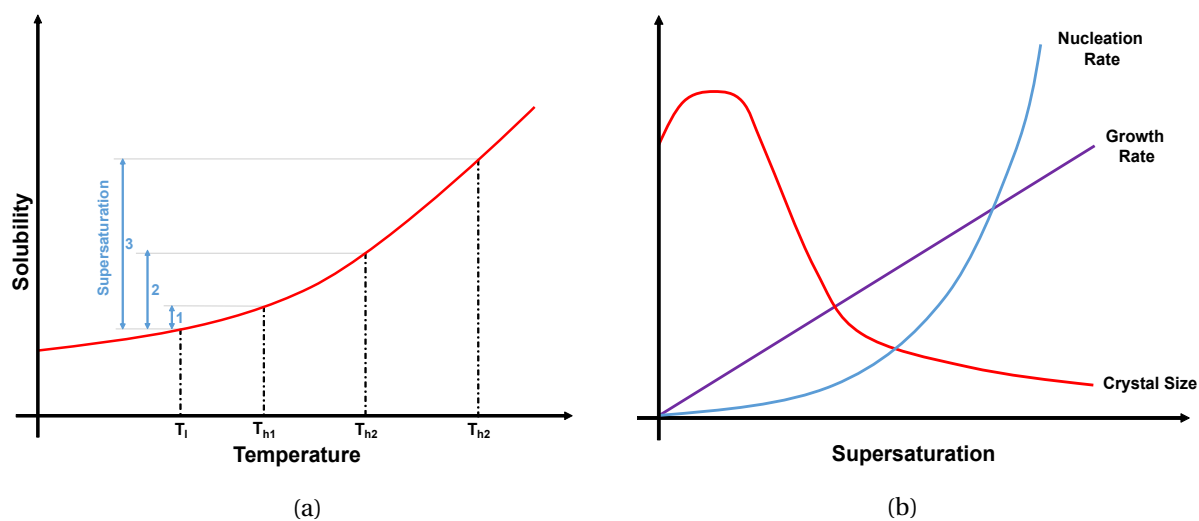


FIGURE 2.5: Schematic theoretical diagrams showing (a) effects of increasing of high temperature ($T_{h1} < T_{h2} < T_{h3}$) on supersaturation difference between substrate areas kept at different temperatures (T_l and T_h); and (b) dependence of supersaturation on nucleation rate, crystal growth rate and crystal size.

2.2 Additive Methods

Although much research has been conducted on external methods as innovative techniques to reduce crystal misalignment and mobility variation in optoelectronic devices; they show some critical issues. In particular, the fact that generally they can be applied only on localized and small substrate areas makes their application in large-scale production difficult. They require complex experimental setup and precise control of individual parameters; moreover, arrays of aligned crystals are generally attained, these enhance the mobility due to their orientation but do not help to overcome the issue of defects located at grain boundaries [50].

Therefore novel techniques have been studied for soluble small molecules semiconductors crystals fabrication: a suitable material can be added to semiconductor material-solvent system; it can be liquid (the so-called dual solvent technique) or solid, in this case, both small molecules and polymers have been used.

2.2.1 Dual Solvent

During a crystal growth in liquid-phase, it is essential to study the intermolecular interactions to predict the properties of the resulting film; generally, they are classified in forces between (i) solute-solute, (ii) solvent-solvent and (iii) solute-solvent [51]. Good solute-solvent interaction is required to dissolve the material in liquid and obtain a homogeneous solution. At the same time, a too strong interaction between solute and solvent is undesirable during crystal formation. A solvation shell of solvent molecules surrounds a solute molecule; thus, the solute-solute interaction is weaker than the

solute-solvent one. It leads to a repulsive force between two solute molecules that means a difficult crystallization process and an increasing disorder in the final result.

According to Hansen's solubility theory, the solvent affinity can be evaluated by observing dispersive, polar and hydrogen bonding component of the intermolecular forces. The basic principle of the dual solvent technique is mixing two solvents showing the lowest affinity possible: one should be a good solvent for the solute and the other a bad one [52]. In this way, globally solute-solvent interactions during crystallization result weaker, and thus, improved solute-solute interactions are possible. Bharti et Tiwari [51] studied various solvent combinations to dissolve TIPS-pentacene, toluene-hexane combination results to be the best one to obtain a higher degree of molecular aggregation and high crystallinity.

2.2.2 Small-Molecule Blends

One more approach consists of add small molecules directly in the solution to obtain similar results in properties optimization without impacting on process costs. Blending organic semiconductors with small molecules, surface roughness decreases and crystal size increases, reducing the number and extension of grain boundaries. It means fewer trap defects that affect charge carrier mobility. The same enhancement in electrical property is also caused by the impact of small molecules on film crystallinity and crystal orientation. Moreover certain small molecules act as nucleation agents able to tune the wettability of the organic semiconductor solution on the substrate: if it increases, the droplet once deposited can easily spread on all the substrate, forming a continuous film; thus, a more extensive areal coverage can be obtained. Furthermore, small molecules having similar molecular structure but different side group length can be used to adjust the vertical phase segregation of the active layer. Crystallization is modified by these additive molecules, which help the formation of an interfacial layer on the charge transport interface. Finally, it is reported that some small molecules, repelling water molecules from the environment, can enhance the operational stability of the OFETs [50].

2.2.3 Polymer Blends

Besides adding a second solvent or small molecules to the original solution, in recent years molecules semiconductors in blend with polymers have been widely studied to increase both morphological and electrical properties of organic semiconductor films. Films resulted by solution-processed small molecules semiconductor deposition are affected by non-uniform thickness, non homogeneous crystal alignment, and coating problems caused by dewetting. On the other hand, polymers show excellent film coverage properties but low electrical properties; therefore blends between these two classes of materials have been developed to combine their advantages [53].

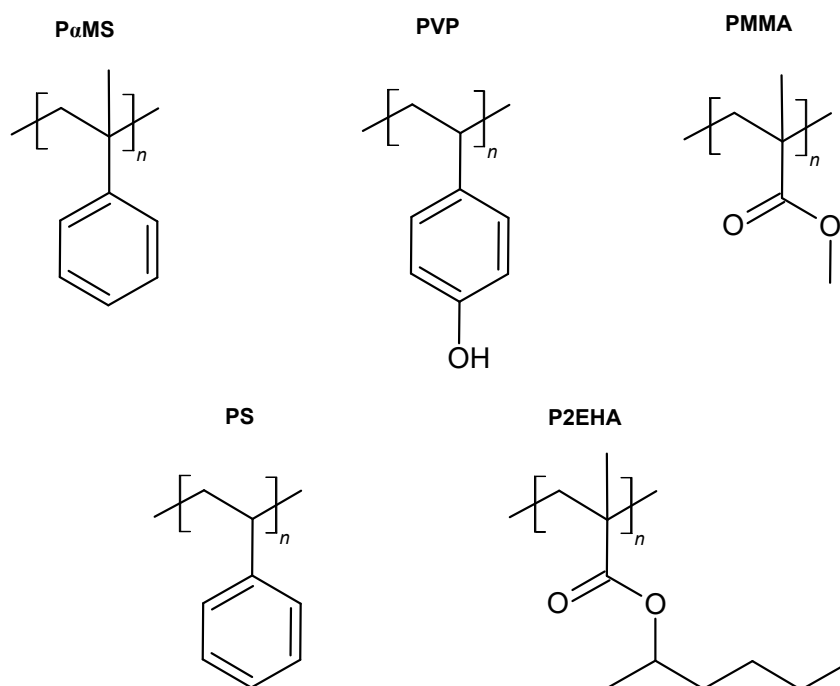


FIGURE 2.6: Structural formula of common polymers used in blend with small-molecules semiconductor

Several polymers have been studied in blend with TIPS-pentacene, includes poly(α -methyl styrene) (P α MS) [54, 55], poly-4-vinylphenol (PVP) [3], poly(methyl methacrylate) (PMMA) [32, 56], polystyrene (PS) [41, 46] and poly(2-ethylhexyl acrylate) (P2EHA) [57, 58]. Deposition of small-molecule semiconductor/polymer blend results in several advantages if compared with the deposition of pristine semiconductor: morphologically speaking more uniform film thickness, larger uniaxially orientated crystals have been observed; moreover, an enhanced crystallinity is proved through X-ray diffraction analysis. It results in notable optimized electrical properties, not only the absolute value of single properties such as mobility or $I_{on/off}$; but also performances consistency (defined as ratio between a magnitude and its standard deviation) after several tests [46] or after environmental exposure[59].

An electrical properties enhancement is possible only if an adequate pathway for charge carriers is formed between electrodes, it is proved that happens only in the case that a particular microstructure results after solvent evaporation: a vertical phase separation between small-molecule semiconductor and polymer layers. Therefore a careful theoretical analysis of this complex phenomenon is required; it depends on molecular parameters (miscibility of two polymers, concentration and solvent), thermodynamic parameters (composition, temperature, and pressure) and processing parameters (film deposition method) [33]. A solution is one mixed-phase system and during solvent evaporation, phase separation occurs leading to two individual phases. This process is thermodynamically controlled and dependent on the Gibbs free energy (G); in particular, at high temperature

(and thus high entropy) one mixed phase is favored, while two individual phases are preferred by enthalpic interaction when temperature decreases [59].

During solvent evaporation, phase separation can occur in two distinct modes: through spinodal decomposition or nucleation and growth; according to the different separation mode, a vertical or a lateral phase separation occurs. The properties of each system component control it:

- Solute: composition, solubility, molecular weight, concentration, and, above all, miscibility, measured through Flory-Huggins interaction parameter (χ).
- Solvent: boiling point and vapor tension control its evaporation rate, while wettability its interaction with the substrate surface.
- Substrate: surface energy and roughness govern the formation of the transient wetting layer during solvent evaporation.
- Processing conditions: fast crystallization processes gives too short time to phase separation kinetic.

In particular, thermodynamic approach of Flory-Huggins (if solute and solvent show remarkable structural differences), state Gibbs free energy of mixing a two-component binary system (solute-solvent) is given by [60]:

$$\frac{\Delta G}{RT} = \sum_{i=1}^2 n_i \ln \phi_i + n_1 \phi_2 \chi \quad (2.1)$$

where ΔG is the Gibbs free energy of mixing, n_i is the molar number for each component, ϕ_i is the fraction parameter of volume and χ is the Flory-Huggins interaction parameter. The term $\sum_{i=1}^2 n_i \ln \phi_i$ is the combinatorial entropy change, and $n_1 \phi_2 \chi$ is indicative of the contact dissimilarity.

The same equation for a three-component system is given by:

$$\frac{\Delta G}{RT} = \sum_{i=1}^3 n_i \ln \phi_i + \Gamma(T, \phi, N) \quad (2.2)$$

$$\Gamma(T, \phi, N) = n_1 \phi_2 g_{12} + n_1 \phi_3 g_{13} + n_2 \phi_3 g_{23} + n_1 \phi_2 \phi_3 g_{123} \quad (2.3)$$

where $\sum_{i=1}^3 n_i \ln \phi_i$ in Eq.2.2 stands for the combinational entropy; $\Gamma(T, \phi, N)$ accounts for the non-combinatorial entropy and enthalpy changes; g_{12} , g_{13} and g_{23} represent the interaction parameter between each component, g_{123} defines the interaction parameter among all three components. Finally, Γ is a function of Temperature (T), fraction parameter of volume (ϕ) and degree of polymerization (N) if in the ternary system a polymer is included.

It is proved that even for moderate molecular weight polymers, the entropic contribute to Gibbs free energy is negligible, while the enthalpic one (given by the interaction between polymer chains) is dominating. On the other hand, in small-molecule/polymer or small-molecule/small-molecule systems, entropic effects are more evident; so it is more difficult to observe a clear phase separation.

However, it can still occur in the form of crystalline molecular entities embedded in an amorphous or semi-crystalline matrix [61].

Since so many internal and external factors affect phase separation, different microstructure can be observed according to different TIPS-pentacene blends, *e.g.* trilayer structure TIPS-pentacene-polymer-TIPS-pentacene has been proved with PS [46] or P2EHA [57]; while in TIPS-pentacene/P α MS blend, a bilayer structure with semiconductive layer at Si/SiO₂ substrate surface and polymer at air interface is observed [3]. Finally, using a poly(3-hexylthiophene)/PMMA blend Qiu et al. obtained a bilayer structure; using a hydrophobic substrate PMMA layer lays above the active layer, while using a hydrophilic substrate the opposite result is reached [62].

Vertical phase separation strongly affects film properties and devices performances, so several studies have been conducted to provide a clear view of this phenomenon. He et al. reported a method to predict the switch between lateral and vertical phase separations in TIPS-pentacene based polymer blend films by simply varying the alkyl chain length of the polyacrylate polymer component [57]. Differences in alkyl chain length mean differences in hydrophobic forces acting between polymer and semiconductor molecules, thus during solvent evaporation these forces can modify the film morphology. Using poly(2-ethylhexyl acrylate) (P2EHA), a polymer characterized by eight carbon atom in the side group, in blend with TIPS-pentacene a vertical phase separation is observed; while TIPS-pentacene/ poly(ethyl acrylate) (PEA) blend film is characterized by a monolayer structure. It is thought that a long alkyl side chain has more influence on combinatorial entropy ($\sum_{i=1}^3 n_i \ln \phi_i$ in Eq.2.2) compared to less bulky groups. Besides, polymers with long-chain substituents, characterized by significant hydrophobicity, leads to a strong decreasing in enthalpic contribute ($\Gamma(T, \phi, N)$ in Eq.2.2), and thus, phase separation is favored. Therefore TIPS-pentacene/P2EHA film, with a confirmed vertical trilayer structure, provides excellent 2D confinement for TIPS-pentacene crystal growth, and hence, the best OFET performances; at the contrary TIPS-pentacene/PEA film, having a dominating lateral phase separation, shows a limited crystal growth confinement without any effect on the electrical properties.

Chapter 3

Materials and Methods

In this chapter details on experimental procedures will be provided; in the first section crystal fabrication process is presented, it includes materials preparation, equipment set up and deposition settings; in the latter section, all the analyses carried out are listed and briefly explained.

3.1 Crystal Fabrication

As outlined in Section 1.4, the present research is based on the fabrication and analysis of organic crystals yielded by two different methods and subsequently try to combine these two technologies to achieve the best results possible to implement these crystals as active layer in electronic devices. All these processes have the basic principle to employ a simple drop-casting technique to deposit a TIPS-pentacene based solution on Si/SiO₂ substrate to provide a not-expensive and easily reproducible method to yield morphologically optimized organic crystals.

3.1.1 Materials Preparation

Since solutions and substrates are prepared in an analogous way for each deposition technique, their preparation is explained only one time, in the following section.

TIPS-pentacene (purity >99%) was purchased from Ossilia and dissolved without any further purification in toluene, purchased from FUJIFILM Wako Pure Chemical Corporation, at two different concentrations: 8.5 mg/ml and 5.0 mg/ml. Separately polystyrene (PS, average M.W. 280,000), purchased from Aldrich Chemical Company, has been dissolved in toluene at a concentration of 5 mg/ml. All these solutions were electromagnetically stirred for over 1 hour to ensure a complete solute dissolution. Afterward TIPS-pentacene/toluene solution at 8.5 mg/ml was ready to be deposited; while the others were blended with polystyrene at different ratios to obtain the mixture of small-molecule organic semiconductor and polymer. Three different blend solutions were prepared: 1:1, 2:1 and 3:1 TIPS-pentacene/Polystyrene ratio in volume; the yielded solution have been ultrasonically agitated for over one hour to ensure the complete mixing; after that also the TIPS-pentacene/PS blend solutions were ready to be deposited.

Substrates were obtained cutting *n-type* doped silicon wafers, with a 100 nm layer of SiO₂ thermally grown, using a diamond pen in a rectangular shape of 15 mm by 10 mm. Cut Si/SiO₂ substrates were cleaned in acetone, 2-propanol, ethanol, and distilled water sequentially with an ultrasonic cleaner for 10 min; each solvent was renewed after 5 minutes of sonification. After that substrates were dried with a N₂ flow and then for 15 min in an oven at 120 °C. Finally, UV/O₃ treatment was conducted for 12 minutes to make the Si/SiO₂ substrate surface hydrophilic and ensure a complete spreading of the solution during the drop-casting.

3.1.2 Thermal Gradient Assisted Growth of Crystals from a Pristine TIPS-pentacene Solution

Figure 3.1 present the equipment set up: two metal blocks have been used to maintain the thermal gradient, one of them merely acts as a support and therefore at a lower temperature (T_l) if compared to the second metal block that is heated at a high temperature (T_h) controlled by a thermocouple. Once the heated block has reached the fixed temperature (~ 1 hour), a petri dish was placed to bridge this block and the support. A complete contact between the petri dish and metal blocks and, above all, absence of every slope in any direction have to be assured because it is required that the only driving force for the solvent evaporation is the difference in temperature between the both substrate ends. Before placing the substrate inside the petri dish it is needed that a homogeneous thermal gradient is reached through the petri dish itself; it takes approximately one hour. When this period of time has elapsed, Si/SiO₂ substrate is placed between the blocks so that its ends correspond to the edges of the blocks. In this way, the distance between support (at T_l) and heat source (T_h) is minimized, and therefore the thermal gradient obtained is the most homogeneous possible. Waiting half an hour more, a homogeneous thermal gradient through the Si/SiO₂ substrate is reached; hence the drop-cast can be carried out. Two different elements are involved in reducing the solvent evaporation rate: solvent annealing and petri dish sealing. In the former case, a small amount of toluene is left inside the petri dish to create a solvent-rich environment, while in the latter one some layers of parafilm are interposed between the petri dish and lid.

To investigate the effects of thermal gradient on solvent evaporation rate, the heated block has been heated at five different temperatures: from 40 °C to 60 °C according to 5 °C steps. Due to experimental equipment constrictions (such as the reduced distance between the blocks) the support, ideally maintained at room temperature, increases its temperature to 23 °C-27 °C depending on T_h value. In the case of pristine TIPS-pentacene solution deposition, 70 μ l of TIPS-pentacene/toluene solution at a concentration of 8.5 mg/ml were dropped, and 140 μ l of toluene were used as solvent annealing. Evaporation occurs in 45-150 minutes, depending on the different temperatures.

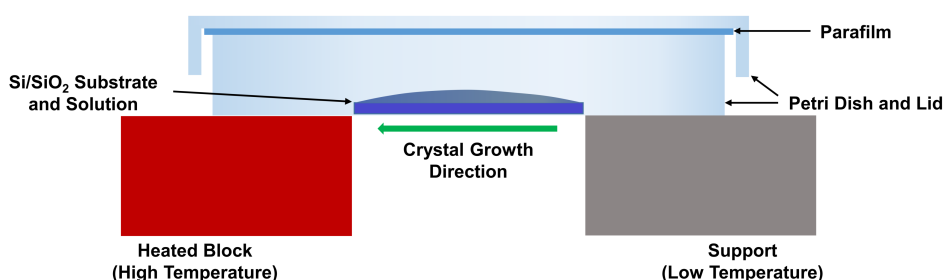


FIGURE 3.1: Schematic representation of experimental setup to grow crystals with thermal gradient assistance. Different temperatures at opposite substrate ends cause differences in solution supersaturation, this leads to a preferred crystal growth direction identified by the green arrow.

3.1.3 Crystals Growth from Drop-Casting of TIPS-pentacene/Polystyrene Blend Solution

In the case of TIPS-pentacene/polymer blend deposition the procedure is very simple and no particular equipment is required: Si/SiO₂ substrate, cleaned as explained in Subsection 3.1.1, was placed inside a petri dish located on a surface tilted by a small angle (5°) to provide a preferred crystal growth direction. In this case, no solvent annealing was requested because all the procedure was conducted at room temperature and therefore the solvent evaporation was slow enough to ensure the crystal formation. Similarly to the previous experiment some parafilm layers were placed between dish and lid.

A volume of 70 μl of TIPS-pentacene/PS blend was deposited on the substrate; solvent evaporation lasts between 3 and 4 hours.

3.1.4 Thermal Gradient Assisted Growth of Crystals from a TIPS-pentacene/Polystyrene Blend Solution

The final study consists of combining the two procedures previously explained: instead of depositing a pristine TIPS-pentacene/toluene solution, a toluene solution of TIPS-pentacene/PS blend has been drop-casted on a Si/SiO₂ substrate. How to set up the thermal gradient through the petri dish and substrate is totally analogous to the one presented in Subsection 3.1.2. In this case, three Si/SiO₂ substrates were placed in a single petri dish to ensure the same solvent evaporation conditions to all the samples. These three samples differ from the TIPS-pentacene/PS volume ratio (1:1, 2:1, 3:1) of the deposited solution.

Moreover to ensure vertical-phase separation between small-molecule semiconductor and polymer, a slow crystallization speed is required. Therefore, besides sealing the petri dish and lid with some parafilm layer as in previous experiments, a larger amount of solvent is required to use as solvent annealing. While in case of pristine TIPS-pentacene (Subsection 3.1.2) 140 μl was enough, in this

situation 1 ml of toluene was deposited inside the petri dish.

A volume of 70 μl of solution was deposited on each substrate, and solvent evaporation occurs in approximately 2-3 hours.

3.2 Characterization

In the following section, all the tools and techniques used to investigate and analyze organic crystals are summarized and briefly explained.

3.2.1 Morphology

A polarized light optical microscope is the tool used in the first stage to analyze samples; it can work both under bright field and polarized light. In the former case, samples are investigated through visible light and optical images give only information about the morphology of the sample. In the latter case, the optical anisotropic behavior of samples can be observed interposing a polarizer between light source and sample and an analyzer between sample and camera. Light from the source is forced to vibrate only along one single plane direction by the polarizer. Thus, after the interaction with the sample, the resulting wave components of the light are combined by the analyzer to produce the high contrast final image. According to the nature of the specimen, different wave components are obtained, in case of birefringent samples (optically anisotropic along with two directions), ordinary and extra-ordinary rays are generated. They are at right angle each other, and they have different velocities which vary with the propagation direction through the specimen. The analyzer recombines these wave components through constructive and destructive interference. Polarizer and analyzer can rotate in their locations, but are generally used one perpendicular to the other, in the so-called "cross nicols position"; thus, if no samples or optically isotropic specimens are interposed, light polarized by the polarizer can not pass through the analyzer, and it results in a completely dark image. On the contrary, when an anisotropic specimen is analyzed and then rotated through 360° , it will sequentially appear bright and dark (extinct), depending upon the rotation position. If the specimen long axis is oriented at a 45° angle to the polarizer vibration axis, the maximum degree of brightness will be achieved; in contrast the greatest degree of extinction will occur when the two axes coincide. Therefore during rotation over a complete range of 360° , specimen visibility will oscillate between bright and dark four times, in 90° increments. This phenomenon is because when polarized light impacts the birefringent specimen with a vibration direction parallel to the optical axis, the illumination vibrations will coincide with the principal axis of the specimen and it will appear isotropic (dark or extinct). If the specimen orientation is altered by 45° , incident light rays will be resolved by the specimen into ordinary and extraordinary components, which are then combined by the analyzer to yield interference patterns [63].

Thus polarized light analysis allows distinguishing between crystals and amorphous regions (both bare substrate or not crystallized material); and in second place, to identify different crystal orientations. Micrographs of crystals were taken using a Nikon COOLPIX 900 digital camera attached to a Nikon ECLIPSE LV100POL polarizing microscope under both bright field and polarized light in crossed nicols position.

Crystal Alignment

It is clear how film morphology has a significant influence on OFETs electrical properties, and in particular, since a lot of organic semiconductors show a remarkable charge carrier anisotropy, crystal orientation plays a key role in preventing undesirable variability in working conditions.

In order to evaluate TIPS-pentacene crystals orientation, misalignment angle between the long axis of each crystal and a fixed direction has been evaluated. In both cases of growth enhanced by thermal gradient application the direction assumed as the baseline is the thermal gradient direction (Figure 3.2.a). In case of growth of TIPS-pentacene/polystyrene crystals, since the method has not as the main goal to align crystals along a particular direction, the long axis of an arbitrarily chosen crystal is picked as the baseline (Figure 3.2.b). Furthermore, a reduced area of 75 mm by 50 mm of the substrate has been analyzed; this choice has been made to avoid measurements along substrate edges. In this edge part of the samples pinning effect at boundaries has a strong influence on crystal growth direction; therefore, the alignment effect is not generated by the only thermal gradient but also to this undesirable and unavoidable effect.

Crystal Size

Crystal size is one more morphological aspect that affects final electrical properties; if it increases the total length of grain boundaries decreases and, according to that, also defects concentration. In this study, crystal size is defined as the length of the short axis of ribbon shaped crystals (Figure 3.2); for this reason, it is also called crystal width or grain width.

Micro-graphs were taken by optical microscope on a reduced substrate area, as explained in previous paragraph, and analyzed to evaluate both average and maximum crystal sizes.

Crystal Thickness

Crystal thickness and its homogeneity have to be evaluated to ensure a uniformity in electrical properties across a whole sample. Furthermore, film thickness analysis is necessary before any deposition process above the crystal layer, such as gold electrode evaporation, in order to form devices. If surface roughness shows high variability, a larger deposited film thickness is required to ensure a complete coverage, and to avoid disconnections, leading to a lack in electrical performances.

Crystal thickness was measured using a ULVAC DEKTAK- 3ST surface profiler.

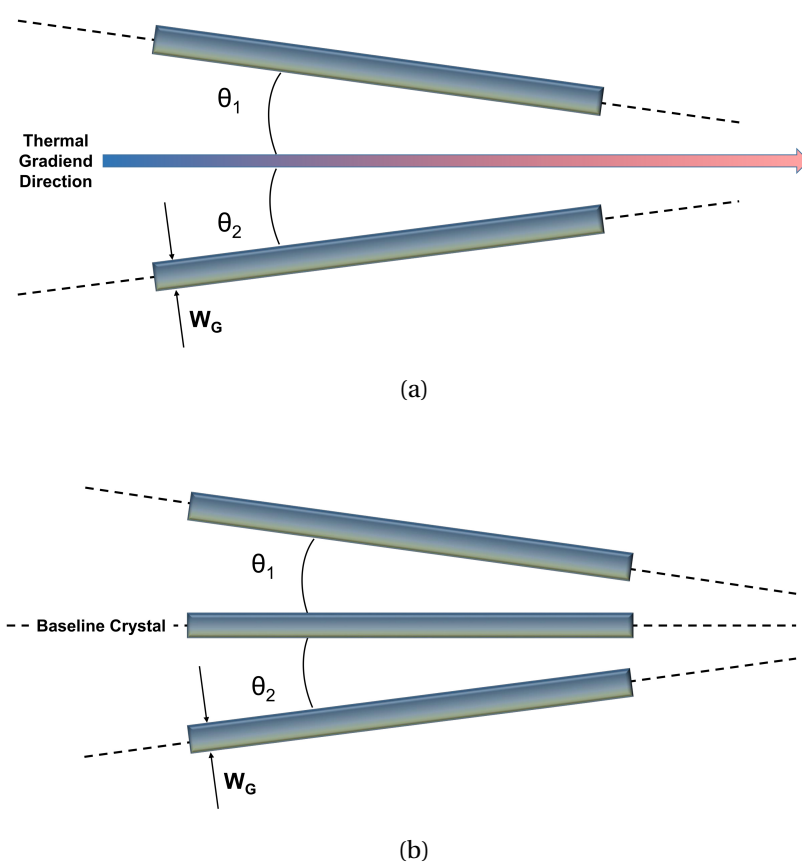


FIGURE 3.2: Organic crystal misalignment (θ) defined as (a) the angle between a crystal long axis and thermal gradient direction in case of growth assisted by thermal gradient or (b) the angle between long axis of a crystal and long axis of another one chosen as a baseline in case of growth not assisted by thermal gradient. Crystal size (W_G) is uniquely defined as crystal width measured along crystal short axis.

Areal Coverage

One of the main issues that affects pristine TIPS-pentacene deposition is the lack of film coverage, it can strongly hinder a correct and consistent device work. In this study, areal coverage is defined as the ratio of the area covered by crystals to the total substrate area. To estimate it, several scanning lines were acquired by ULVAC DEKTAK- 3ST surface profiler, in both parallel and perpendicular directions to the crystal long axis. After an analysis overall the scanning lines, a critical thickness value of 200 nm has been chosen to discriminate if a crystal was present or not; in this way ratio between scanning line length showing a thickness greater than the critical value and total scanning lines length, represents an evaluation of areal coverage of the substrate.

3.2.2 Microstructure

A microstructural analysis is required to confirm and evaluate phase separation in the case of crystals yielded by TIPS-pentacene and polymer blend solution. A substrate cross-section is needed to evaluate crystal morphology correctly. Since it is required to destroy the samples, after devices characterization they are cut in a perpendicular way to electrodes and analyzed by Scanning Electron Microscope (SEM).

SEM is a tool that allows us to carry out non-destructive analysis evaluating complex interaction between a focused electron beam and the sample. When electrons hit sample surface, interactions and emissions happen in a teardrop-shaped volume of material. Analysis of backscattered electrons (BSE), secondary electrons (SE), and characteristic X-rays are the most used by researchers. BSE counting, influenced by the atomic number of each element in the analyzed volume, gives information about chemical composition. Instead SE, generated by interaction of electron beam with shallow atoms (few nm in depth), give a topological evaluation of the surface. Finally, characteristic X-rays provide a compositional analysis of the sample up to some μm in depth [64].

For the aim of this research, images were taken using SE, and an Energy Dispersion X-ray Diffraction (EDS or EDXS) was carried out to distinguish which elements were present in each layer identified in SE images. Samples analyzed shown a layer structure including silicon (Si) as gate electrode, silicon dioxide (SiO_2) as gate insulator, polystyrene ($(\text{C}_8\text{H}_8)_n$), TIPS-pentacene ($\text{C}_{44}\text{H}_{54}\text{Si}_2$) as active layer and gold (Au) as electrode. Therefore hydrogen (H), carbon (C), oxygen (O), silicon (Si) and gold (Au) are the elements in the sample analyzed. The only way to differentiate each layer is to individuate an element that is not shared by adjacent layers. It is possible to distinguish substrate from active layer because the latter is a carbon-rich layer; polystyrene and TIPS-pentacene layers can be distinguished due to the presence of two silicon atoms in TIPS-pentacene molecule. In this case, it is needed to observe that both polystyrene and TIPS-pentacene are carbon-based molecules, while they differ by only silicon content. Therefore carbon signal is pretty much the same, while silicon signal is null in the polystyrene layer and very weak in the TIPS-pentacene layer; the signal separation is not so clear and has to be very carefully investigated tuning contrast and brightness in output signals.

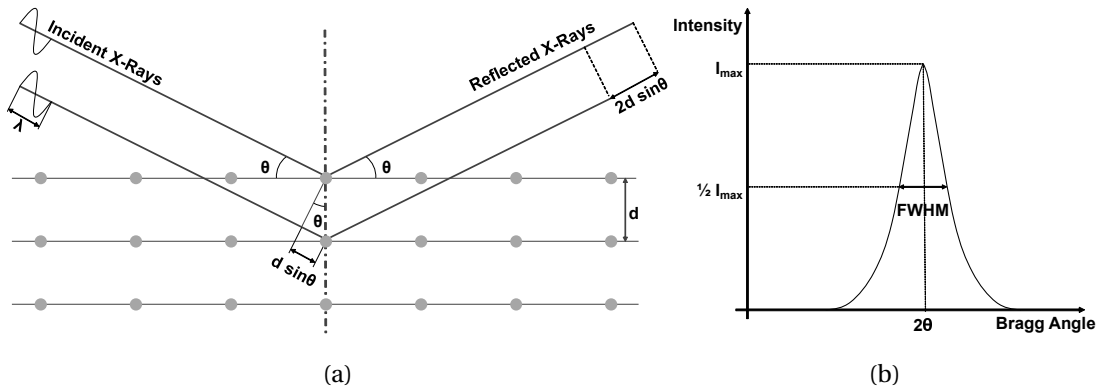


FIGURE 3.3: (a) Schematic representation of Bragg geometry showing two parallel X-rays incident on a crystalline sample with a θ angle and reflected out of phase by a length of $2d \sin \theta$. (b) Schematic representation of diffraction peak showing peak intensity (I_{max}), peak position (2θ) and peak width (FWHM).

Microscopic film morphology was observed using a JEOL JIB-4600F field-effect scanning electron microscope equipped with an energy dispersive fluorescent X-ray analyzer.

3.2.3 Crystallinity

Molecular structure and film crystallinity, as theoretically explained in Chapter 1, are two parameters that strongly affect charge carrier transport and in general devices performances. X-Ray Diffraction (XRD) is a simple and non-destructive analysis widely used in various research fields to get information about crystalline phases distribution, crystals morphology, and orientation [65].

X-rays, generated by a cathode ray tube, hit the sample placed on the stage and scatter in different directions and with different intensities according to the crystalline features. The detector registers reflected rays only if they produce constructive interference with incident X-rays. It occurs when the difference of traveled distance by two different rays is equal to an integer multiple of the X-Ray wavelength (Figure 3.3.a), namely, if Bragg law is satisfied:

$$n\lambda = 2d_{hkl}\sin\theta \quad (3.1)$$

where n is an integer number defining diffraction order, λ is X-rays wavelength, d distance between two adjacent atomic planes (or interlayer spacing or d-spacing), hkl are Miller indices and θ is X-ray incident angle. During the test, incident angle θ varies from 1.5° (ideally 0°) to 45° and while the detector record constructive interactions according to 2θ angle (an interval from 3° to 90°). Different instrumental geometries are available according to different positions and rotations of X-ray tube, sample and detector. In the so-called Bragg-Brentano geometry, the sample stage is kept in a fixed position while the X-Ray source and detector move independently around it, assuring that source and detector angles are always θ and 2θ , respectively [66].

XRD spectra is a diagram that reports peaks having different intensity at different 2θ angles. Knowing incident X-rays wavelength (λ) and peaks positions (2θ), referring to Bragg Law (Eq. 3.1), it is possible to get interlayer spacing between crystalline planes which originated scattering. Thus, comparing with documented values in literature, the nature of crystalline phases is determined. By fitting with a Gaussian function each peak, it is possible to estimate the film crystallinity: peak width at half of the maximum intensity (known as Full Width at Half Maximum, FWHM, Figure 3.3.b) is inversely proportional to crystallite size and in a more general outlook to degree of crystallization. Finally, peaks intensity due to dependence on instrumental features and experimental conditions - including areal coverage and film thickness - is not reliable for accurate analysis; only sometimes the relative intensity (each intensity divided by the maximum one) is used for a rough evaluation of crystalline properties.

Out-of-plane XRD analysis has been carried out by Rigaku MiniFlex 600 diffractometer equipped with HyPix-400 2D HPAD detector at scan speed of $20^\circ/\text{min}$ with an accuracy of 0.2° .

3.2.4 OFET Characterization

In order to evaluate the electrical performances of organic film yielded, both bottom-gate/bottom-contact (BG/BC, or BC) and bottom-gate/top-contact (BG/TC, or TC) devices have been produced.

BG/BC devices were prepared by depositing solutions on cleaned Si/SiO₂ substrate pre-patterned with comb-shaped electrodes; this device configuration has been used only for TIPS-pentacene/polymer blends.

On the other hand, top contact devices have been produced using Si/SiO₂ substrate without any pre-patterned metal layer; silicon substrate was used as gate electrode and silicon dioxide layer grown on it as insulator layer. After organic layer deposition, Au electrodes (1 mm x 4 mm) were deposited using a combination of PET sheet and tungsten (W) wire (50 μm in diameter) as a shadow mask. Au electrodes (140 nm or 200 nm in thickness) were thermally deposited at a rate of $0.17 \sim 0.23 \text{ nm/s}$ using VPC-260F vacuum evaporator ($< 10^{-3} \text{ Pa}$).

In Table 3.1 specifics of devices yielded are summarized. Note that in BG/TC configuration the variability in channel length is due to experimental conditions (W wire is not an high accurate shadow mask), while variability in channel width is due to difficulties in cutting PET sheet so precisely.

Devices characterization was carried out placing the substrate on a metal plate; then three metal probes were used to connect the Au electrodes (source and drain) and the metal plate (gate) with the analyzer. Some Indium-Gallium was placed at each probe-electrode contact in order to ensure a stable connection between the two parts. Current-voltage (I - V) characteristics were measured in a vacuum chamber ($\sim 10^{-3} \text{ Pa}$) using a Keithley Series 2400 SourceMeter[®]. Gate voltage (V_{GS}) and drain voltage (V_{DS}) were applied through the respective electrodes, while source electrode was grounded. Drain current (I_{D}) was measured by varying gate voltage in step mode (from +10 V to -40 V in -5 V

TABLE 3.1: Specifics of devices used to measure electrical properties of organic films.

Device Configuration	Insulator Layer Thickness (<i>nm</i>)	Channel	
		Length (μm)	Width (μm)
BG/BC	300	10	74000
BG/BC	300	30	38000
BG/BC	300	50	38000
BG/TC	100	48 ~ 51	680 ~ 1500

steps) and drain voltage in sweep mode (from +10 V to -40 V in -2 V steps). From output and transfer characteristics analysis electrical properties were estimated as explained in Section 1.3.

Chapter 4

Results and Discussion

In this chapter, the results obtained are summarized in three different sections (one for each method of growth). At the same time, both expected and unexpected results are discussed and, if possible, justified referring to theoretical sources.

4.1 Thermal Gradient Assisted Growth of Crystals from a Pristine TIPS-pentacene Solution

4.1.1 Morphology

Optical micrographs, taken both under bright field (Figure 4.1-1 column) and polarized light (Figure 4.1-2 column and -3 column for diagonal or extinction position), show representative portion of crystal films yielded applying a thermal gradient through the substrate. Different crystals colors in micrographs highlight different film thicknesses (in both cases of bright field and polarized light), or different crystal orientation (in case of polarized light). Thermal gradient direction is set from the left side (T_h) to the right side (T_l) of each micrograph in -1 and -2 column, while in -3 column samples are rotated by 45° . In order to quickly show misalignment between each crystal and thermal gradient direction, micrographs in -1 and -2 column are presented with the thermal gradient aligned along a horizontal line. Although the thermal gradient helps crystals align along one direction, it can be observed that this alignment is not unique; it causes that in Figure 4.1.b and 4.1.f extinction position occurs in case of rotating sample, while in Figure 4.1.c, 4.1.d and 4.1.e, the maximum brightness occurs with a rotating sample.

Although micrographs in Figure 4.1 have the only purpose of providing an example of typical films yielded, differences between images in 4.1.a and the others are remarkable. In figure 4.1.a are shown micrographs of pristine TIPS-pentacene crystals produced by simple drop-casting: random orientations, irregular shapes and thicknesses (high variation in crystal color), and poor areal coverage are evident. Orange triangles in 4.1.a-1 show the points presenting bare Si/SiO₂ substrate. On the

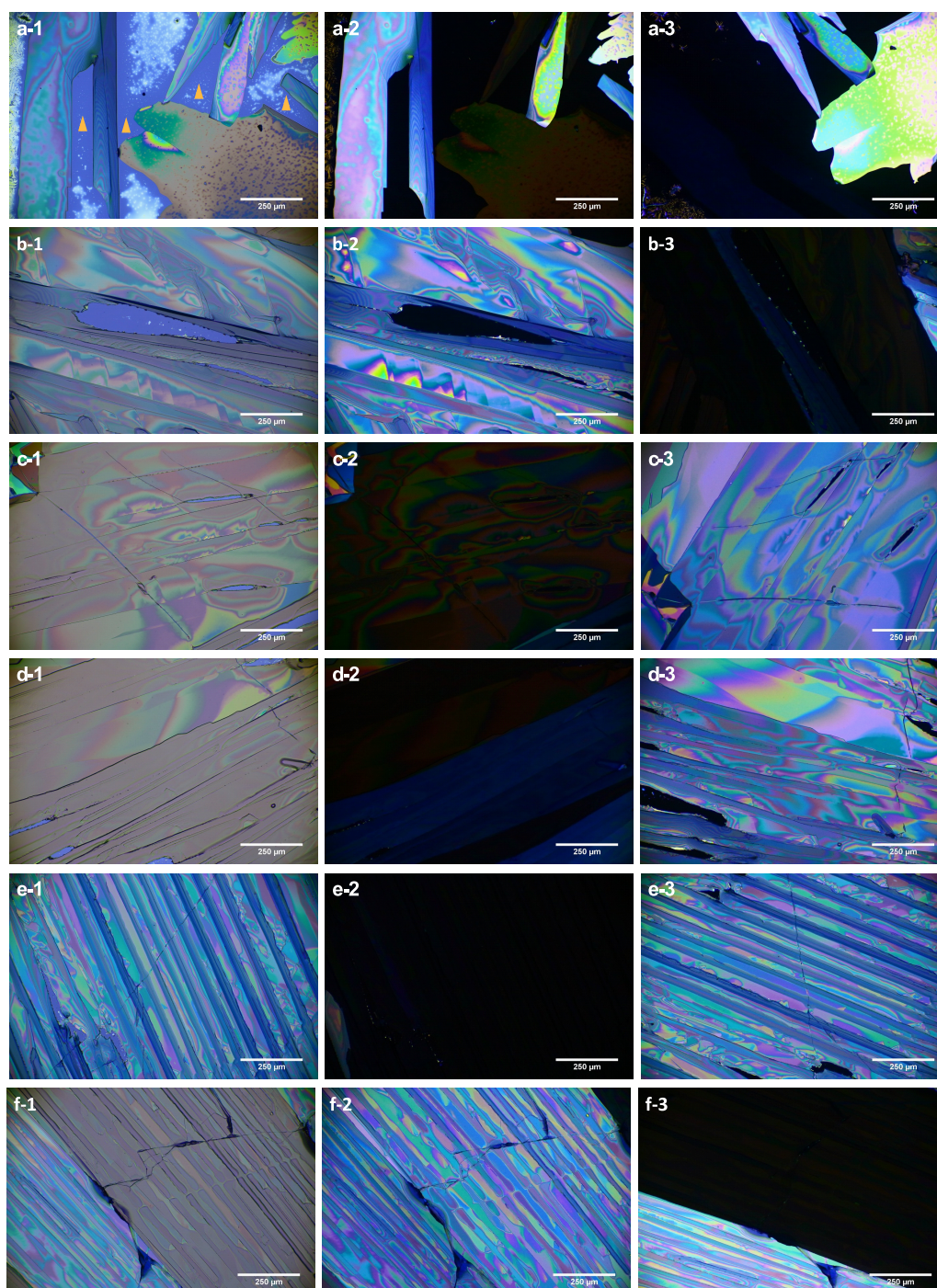


FIGURE 4.1: Optical micrographs under bright field (-1 column) and polarized light (-2 and -3 column in diagonal or extinction position) of pristine TIPS-pentacene crystals. Samples are obtained (a) by simple-drop casting, and (b-f) by drop-casting with thermal gradient application. Hot block temperature (T_h) are (b) 40 °C, (c) 45 °C, (d) 50 °C, (e) 55 °C, and (f) 60 °C. Thermal gradient is applied from the left (T_h) to the right (T_l) of each micrograph.

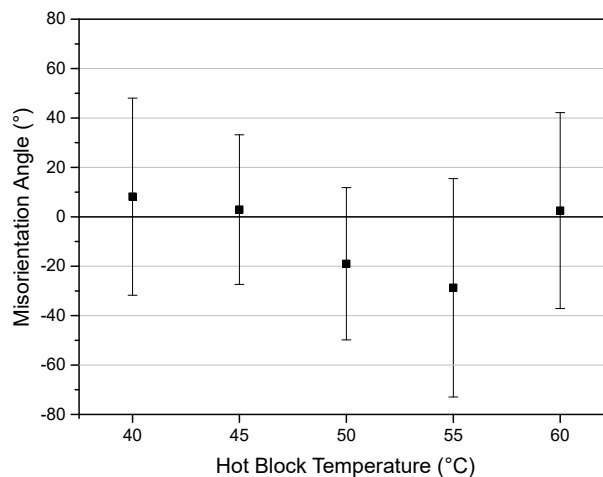


FIGURE 4.2: Average misorientation angle between crystals and thermal gradient direction for different T_h .

contrary, in Figure 4.1b-f, despite differences in morphology are notable, crystals produced by drop-casting assisted by thermal gradient show more homogeneity in crystal orientation, thickness, and shape; besides a dramatically enhanced areal coverage.

In particular, crystal orientation is a crucial parameter to control to attain films suitable for device applications. It is proved how the use of thermal gradient gives a preferable crystal growth direction (from T_l to T_h as theoretically explained in 2.1.4), thus, in this research, varying the the hot block temperature it is expected to provide an improved global crystal orientation. In Figure 4.2, an estimation of the misalignment angle between each crystal and thermal gradient direction is shown. Applying a high temperature of 45 °C and 60 °C the smallest values of misorientation angles are obtained: $2.93 \pm 30.26^\circ$ and $2.52 \pm 39.65^\circ$, respectively. Although results are very similar, the standard deviation of the population, expressed as error bar in Figure 4.2, is bigger than almost 10 degrees in case of $T_h = 60^\circ\text{C}$. It means that even if the average value of the misorientation angle is quite small, it is given by several angles very different each other in the case of $T_h = 60^\circ\text{C}$, The $T_h = 45^\circ\text{C}$ case shows the smallest value of standard deviation among all the samples. This result is directly connected to the number of crystalline domains observed; namely the array of crystals showing the same orientation. Domains number increases with temperature due to the dramatic rise in supersaturation which leads to increased values of nucleation rates (Figure 2.5.b). An increase in nucleation rate affects equilibrium between nucleation and growth rate, therefore at higher supersaturation levels (and thus at higher values of T_h), a larger number of smaller crystals will be yielded. On the other hand, at lower supersaturation levels (lower values of T_h), a smaller number but bigger crystals will be attained. It is hence clear how it is possible that in samples produced applying a higher hot block temperature, a larger variability in crystal orientation can be observed.

As explained at the end of the previous paragraph, an increase in supersaturation also affects crystal size. As shown in Figure 2.5.b, a trade-off between nucleation rate and growth rate determines a

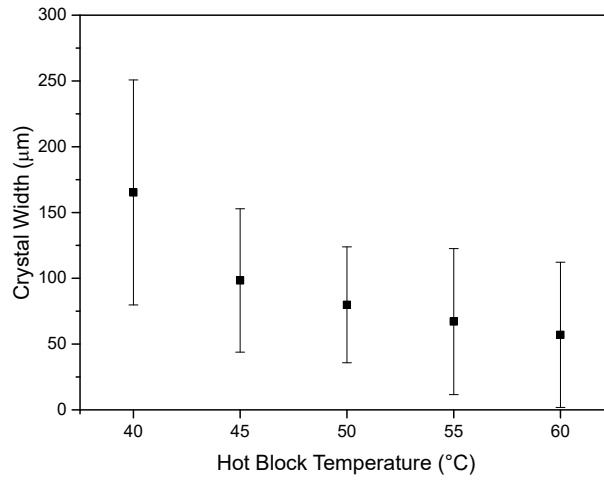


FIGURE 4.3: Crystal size for different T_h .

slightly increasing crystal size and, after a plateau, a sharp decrease until it reaches a quasi constant value. Theoretical behavior is partially confirmed by the results of morphological analysis summarized in Figure 4.3. The diagram only shows crystal size drop, without the slight rise at low values of supersaturation, one possible reason could be that even the smallest temperature used as T_h (40 °C) is still too high to produce the supersaturation level that leads to an increase in crystal size. Thus, experimental results confirm only the theoretical decreasing, a more comprehensive analysis including lower values of T_h should be carried out to confirm the hypothetical curve. Therefore, average crystal size shows a monotonically decreasing behavior from 170 μm attained at T_h of 40 °C to 60 μm at 60 °C. Despite average crystal sizes are generally smaller than 200 μm , giant crystals having a width of 1208 μm and 1016 μm are observed for value of T_h of 50 °C and 60 °C, respectively.

In order to investigate the thermal gradient effect on both crystal topology and areal coverage, analysis using Dektak profiler are carried out. Figure 4.4 shows benefits on crystal thickness: maximum values decrease by applying a thermal gradient through the substrate and also the roughness is more homogeneous. Furthermore, increasing thickness homogeneity, also the uncovered areas of the substrate are dramatically reduced. It is suggested by Figure 4.4 observing the continuous blue line corresponding to T_h of 55 °C, crystal thickness is globally approximately 1 μm and only in sporadic cases crystal profile reaches the baseline (substrate surface level). On the other hand, crystals yielded by simple drop-casting (dotted black line) are approximately 6 μm thick and show large empty spaces between each crystal.

The gain in thickness homogeneity has a primary consequence a sharp increase in areal coverage, namely the ratio of substrate area covered to crystals and total area. Figure 4.5 shows areal coverage percentages for samples produced without and with thermal gradient application. A monotonical increasing behavior is easily depicted; in particular, for samples yielded without enhancements given by thermal gradient, substrate coverage is 59.2%, while for values of hot temperature higher than 45

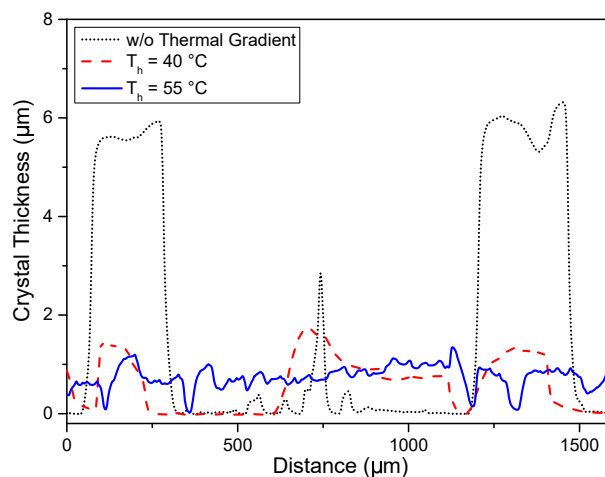


FIGURE 4.4: Surface topology comparison of crystals yielded with simple drop-casting, with hot block heated at $T_h = 40\text{ }^\circ\text{C}$ and at $T_h = 55\text{ }^\circ\text{C}$

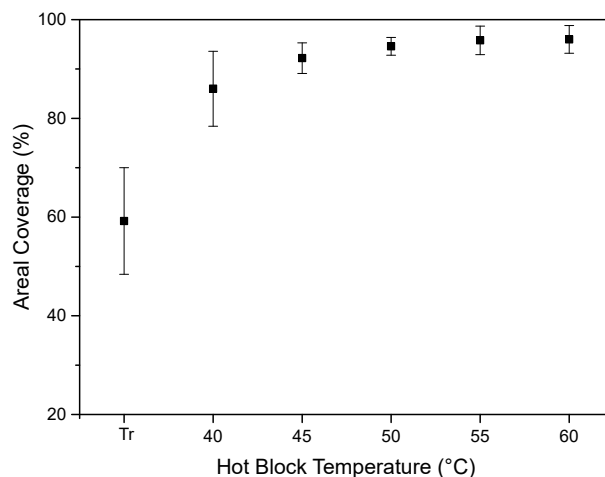


FIGURE 4.5: Areal coverage for different T_h .

$^\circ\text{C}$, the substrate is covered for more than the 90%, the maximum value of 96.0% of substrate coverage is attained for $T_h = 60\text{ }^\circ\text{C}$.

4.1.2 Crystallinity

Figure 4.6 shows out-of-plane XRD spectra resulting from samples yielded from simple drop-casting and applying different values of thermal gradient; each spectrum is vertically shifted in order to enable visual differentiation.

For all values of T_h peaks are placed at 5.8° , 11.1° , 16.5° and 27.3° for (001), (002), (003) and (005) planes of TIPS-pentacene crystal, respectively. XRD spectra show only sharp (00 l)-type reflections. This indicates that TIPS-pentacene molecules are highly ordered and oriented with the silyl group on the substrate surface and the aromatic backbone parallel to that [67, 68]. Peak positions are slightly

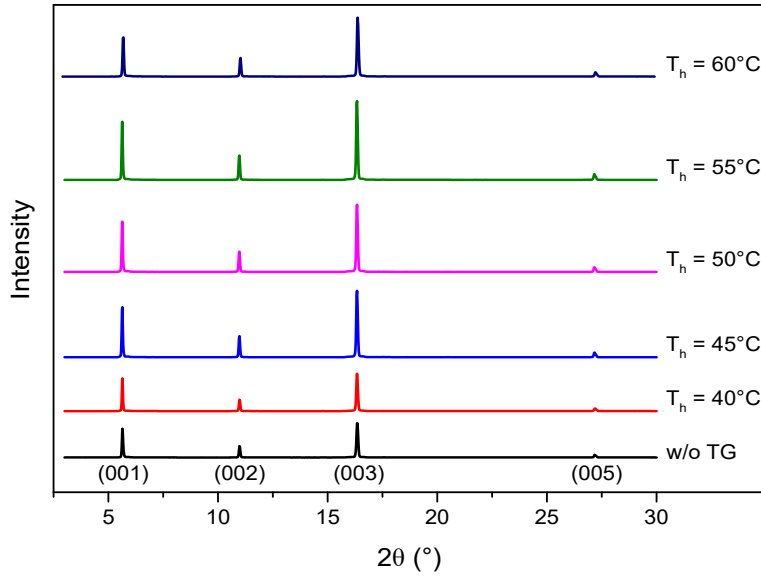


FIGURE 4.6: X-Ray diffraction spectra for different T_h and FWHM values correspondent to (001) peak of each T_h .

TABLE 4.1

Hot block Temperature (°C)	FWHM ₍₀₀₁₎
T_r	0.0668
40	0.0615
45	0.0630
50	0.0612
55	0.0610
60	0.0621

right shifted if compared with values reported in previous studies, 0.5° for (001) planes [69, 70]; since such shift is observed for all samples, it is assumed to be related to a systematic error during the measurement, *e.g.* misalignment, tilting of the sample on the sample holder, or mistake in equipment setup. For the same reason also distances between crystalline planes, calculated through the Bragg law (Equation 3.1), will be affected by errors if compared to results in the literature. The plane distance d_{001} for (001) plane was calculated to be 15.3 \AA along the c -direction, which is different from values of $16.6 \text{ \AA} \sim 16.8 \text{ \AA}$ generally reported for TIPS-pentacene crystals [71]. Since all samples show an error of 0.5° in (001) peak position, assuming that it is related to a systematic error, d -spacing has been calculated using the experimental value shifted to left by 0.5° and it results that $d_{001} = 16.7 \text{ \AA}$, perfectly fitting with reported data. Furthermore, d_{001} is constant for all samples, so it does not depend on different thermal gradient values, thus molecular stacking along this direction is not affected by temperatures used in this research.

Moreover, FWHM is calculated through a Gaussian curve fitting carried out on each peak. Because it is a parameter slightly affected by instrumental variation (*e.g.* if the instrument includes a low-resolution monochromator, it tends to be wider), FWHM can be used to determine film crystallinity. In Table 4.1 average FWHM values for (001) planes are reported for different values of T_h applied, it can be noticed that all values are between 0.0610° and 0.0630° except for the film yielded without any enhancements that is 0.0668° . These results show how the application of high temperature at one substrate end leads to a slight gain in crystallinity that is, at the same time, not affected by different values of thermal gradient, as previously reported [3].

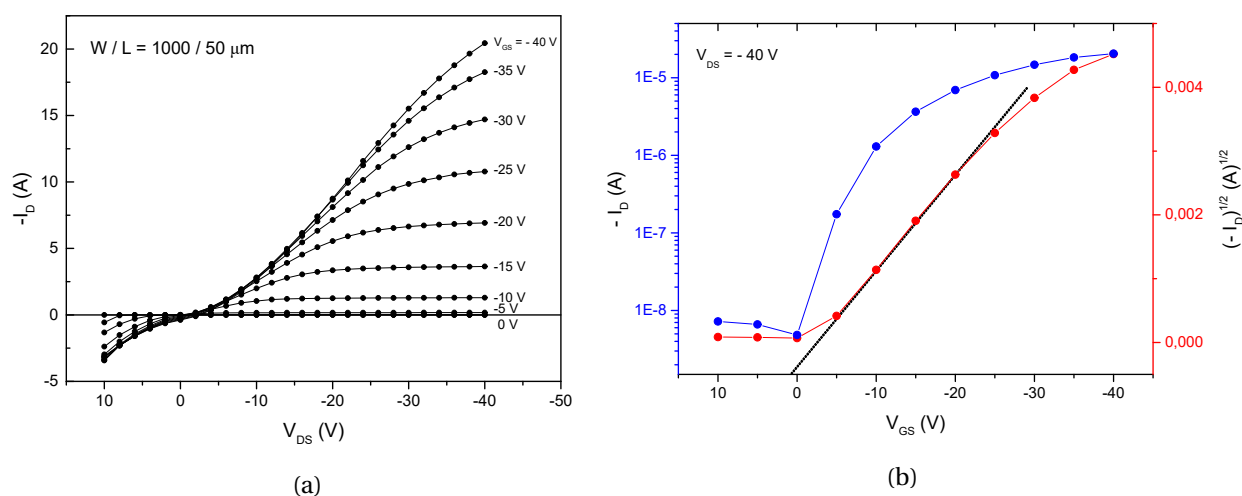


FIGURE 4.7: Typical (a) output and (b) transfer characteristic of organic field effect transistors having a TIPS-pentacene film as active layer grown with thermal gradient assistance. Dotted line in (b) represents the linear fitting used to determine mobility and threshold voltage.

4.1.3 OFET Characterization

Top contact devices were produced depositing source and drain electrodes (140 nm in thickness) on the active layer and afterward measured in vacuum ($\sim 10^{-3}$ Pa) and dark. Figure 4.7 presents (a) a typical output characteristic obtained from electrical measurements and (b) transfer characteristics in saturation region; the dotted line in (b) represents the fitting one used to determine mobility in saturation regime (line slope) and threshold voltage (intercept with V_{GS} axis). Transfer characteristics show the dependence of both drain current (I_D in logarithmic scale, blue line) and the square root of drain current ($\sqrt{I_D}$, red line) on gate voltage (V_{GS}) at one defined value of drain voltage (in this case $V_{DS} = -40V$). Highest mobility of $4.1 \times 10^{-2} \text{ cm}^2/\text{V s}$ was measured for sample yielded with a thermal gradient generated by a T_h of 50°C ; the device also shows a threshold voltage of 1.36 V and an optimal subthreshold slope of 3.02 V/dec. Mobility attained is almost twice as high as value resulted for samples yielded from simple drop-casting ($2.2 \times 10^{-2} \text{ cm}^2/\text{V s}$). Enhancements given by the gain in areal coverage and crystal orientation are also reflected in better results of threshold voltage and subthreshold slope, which are 4.25 V and 4.10 V/dec, respectively for samples produced from simple drop-casting. Finally, on/off current ratio is not so strongly affected by thermal gradient application: in both of cases it is bigger than 10^3 .

Figure 4.8 shows overall results of (a) mobility, calculated in saturation region, (b) threshold voltage, (c) subthreshold slope, and (d) on/off current ratio for different T_h . Globally, the mean values of properties for high temperature lead to better performances than those for $T_h = 40^\circ\text{C}$ and $T_h = 60^\circ\text{C}$. This is because these temperatures lead to organic films affected by morphological issues. As matter of fact, low values of thermal gradient TIPS-pentacene film show remarkable lacks in areal

coverage and bad global crystal alignment; on the other hand for high values of thermal gradient, despite the active layer almost completely covers Si/SiO₂ substrate, the fast solvent evaporation leads to smaller crystal domains and thus a sharp increase in the number of grain boundaries which affects electrical properties. Besides this, at higher temperature both Si/SiO₂ substrate and organic film are exposed to higher thermal stresses and the differences in thermal expansion coefficients frequently produces cracks originated by high temperature as observed in TIPS-pentacene films shown in Figure 4.9. These images are relative to samples produced with T_h of (a) 55 °C and (b) 60 °C, and increase in areal coverage and drop in crystal size, namely two of the main morphological enhancements given by thermal gradient application, are also evident.

Mainly saturation mobility and subthreshold slope reflect enhancements given by mean value of thermal gradient, while it is not so evident in threshold voltage and on/off current ratio trend. Anyway, all average threshold values are between -1V and +3V, representing a small range of variability. On the other hand, average values of on/off current ratio show a peak of 2100 for $T_h = 45$ °C, that is more than doubled than 920, the value attained at $T_h = 40$ °C; average values decrease for $T_h = 50$ °C and $T_h = 55$ °C to 1420, while a slight rise to 1700 is measured for $T_h = 60$ °C. This variability in electrical properties observed at high value of thermal gradient can be related first to the large number of crystal domains, which gives a large number of crystal orientations and grain boundaries, and secondly to the presence of thermal cracks.

Figure 4.7.a shows a representative output characteristic attained for devices having as active layer a TIPS-pentacene crystal film grown with thermal gradient application. Although this representative and usual curve (a similar one is also reported in Figure 4.10.a) was measured for a large part of devices, in some cases an anomalous output characteristic, shown in Figure 4.10.b, was measured. In regular characteristics, all I_D curves referring to different V_{GS} pass through the origin, then increase linearly in the ohmic region and finally become voltage-independent in the saturation region. In anomalous ones, each curve crosses x axis at different V_{GS} values. This unusual behavior of output characteristic curves can be related to surface morphology near to channel area. If crystals are aligned with the charge flow (so-called parallel configuration, Figure 4.10.c), current flows unhindered between electrodes, and thus potential decreases smoothly along with the crystal. On the contrary, if crystals are not optimally oriented (perpendicular configuration, Figure 4.10.d), charge flow is hindered by defects such as grain boundaries; thus, the profile potential between drain and source electrodes follows an irregular and sharp fall [24]. This poor film morphology is generally observed in areas close to substrate boundaries, where edge pinning effect contrasts thermal gradient effect, and thus, crystal orientation is not optimal. Due to this inconvenient behavior of output characteristics, the measurement of mobility in linear region is not reliable [4], therefore all mobility values reported in this section refer to mobility calculated in saturation region.

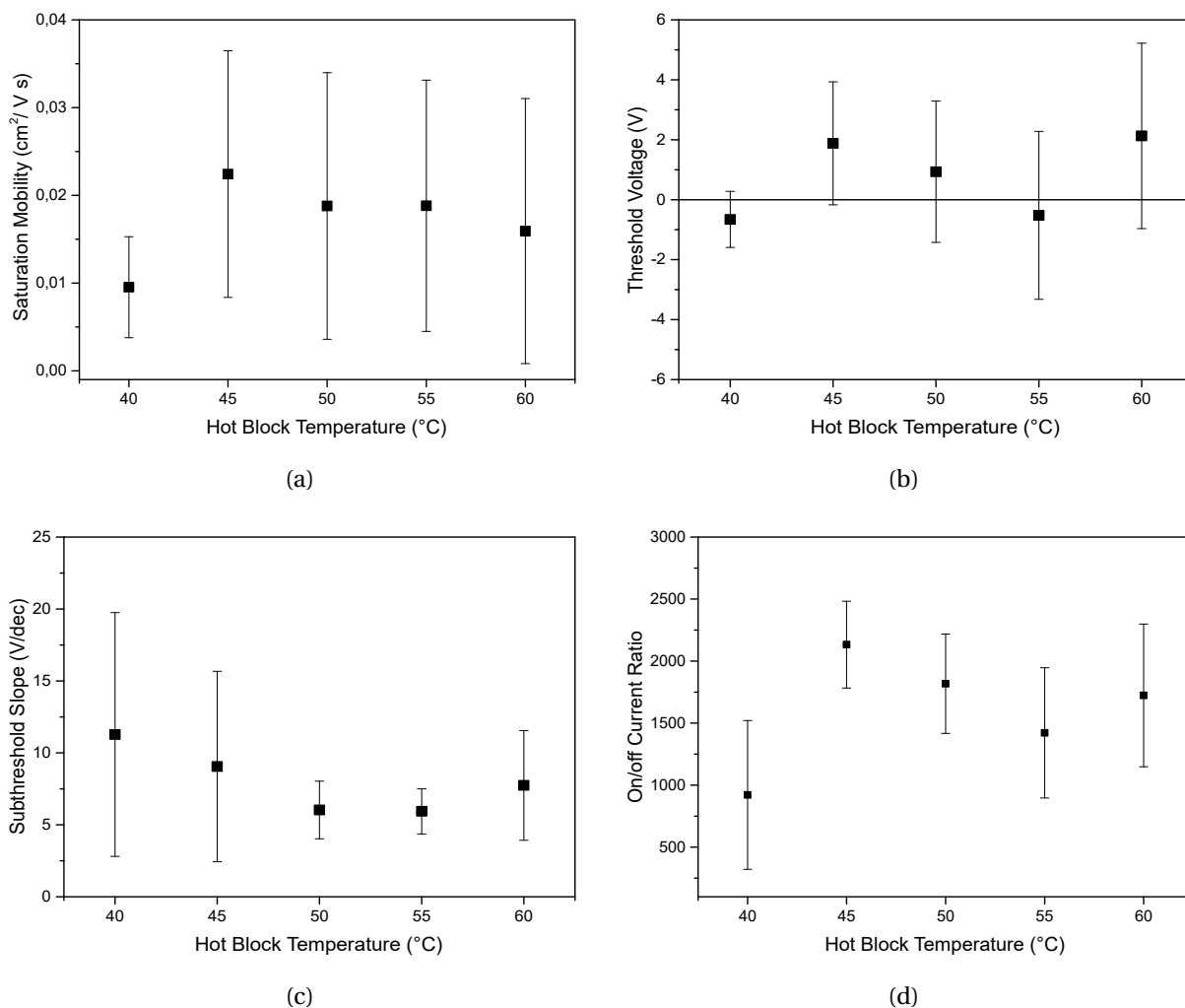


FIGURE 4.8: Average (a) saturation mobility and (b) threshold voltage, (c) subthreshold slope and (d) on/off current ratio for different T_h .

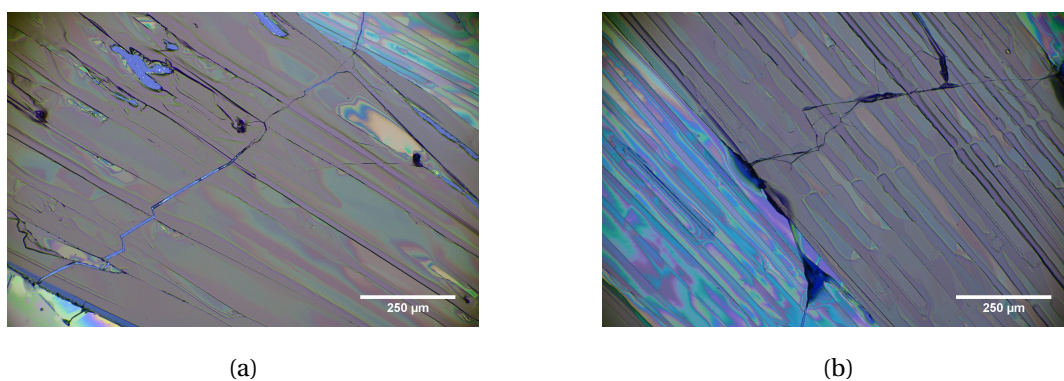


FIGURE 4.9: Thermal cracks originated in pristine TIPS-pentacene films grown with thermal gradient generated by T_h of (a) 55 $^{\circ}\text{C}$ and (b) 60 $^{\circ}\text{C}$.

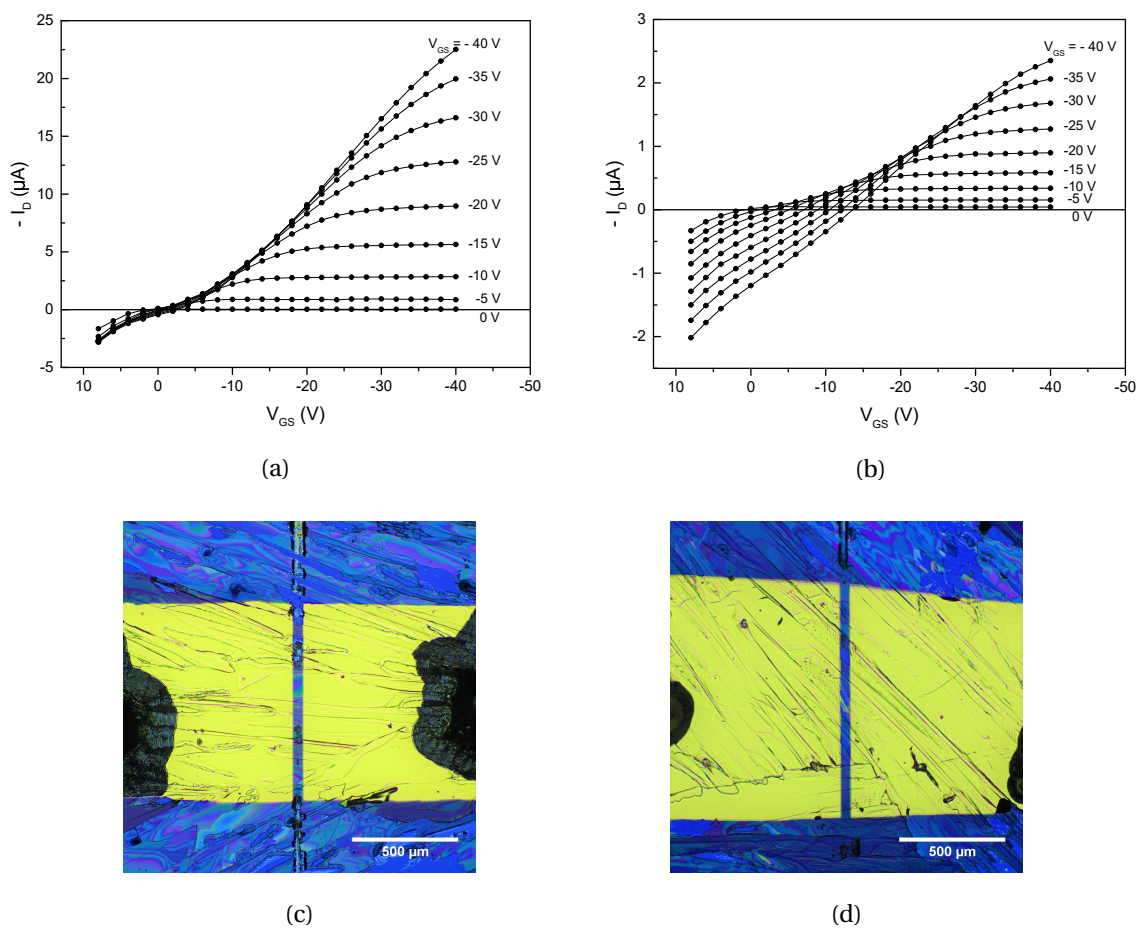


FIGURE 4.10: Output characteristics (a,b) and optical channel images (c,d) showing how good (a,c) or bad (b, d) crystals alignment through device channel influence OFET output characteristic.

4.2 Crystals Growth from Drop-Casting of TIPS-pentacene/PS Blend Solution

4.2.1 Morphology

Figure 4.11 shows optical micrographs of films grown from TIPS-pentacene/Polystyrene blend solution at different mixing ratios. These images are taken under both bright field (-1 column) and polarized light (-2 column and -3 column in diagonal and extinction position, respectively). Micrographs of pristine TIPS-pentacene solution are presented in Figure 4.11.a, while in 4.11.b-d the volume ratio of TIPS-pentacene and polystyrene are 1:1, 2:1, and 3:1, respectively. All samples are prepared by simple drop-cast on pre-cleaned Si/SiO₂ substrates placed into a petri dish on a inclined surface to give a preferred crystal growth direction. Slope direction goes from the left side (higher edge) to the right one (lower edge) in all images reported in Figure 4.11.

Differences between films obtained from pristine TIPS-pentacene solutions and blend solution are remarkable. First of all areal coverage is dramatically increased. In the former case bare substrate spots, pointed with orange triangles in Figure 4.11.a, can be easily identified; while in all cases of TIPS-pentacene/polystyrene blend, substrate can not be seen from micrographs. Dark spots are observed in micrographs taken under polarized light in diagonal position. These are due to amorphous regions between crystals. In many cases they are polystyrene films uncovered by organic layer. But sometimes it happens that some amorphous organic regions are present between ribbon-shaped crystals. Unlike in the case of pristine TIPS-pentacene, a systematic analysis to investigate areal coverage was not possible because surface profiler used for thickness measurements cannot distinguish polystyrene from TIPS-pentacene. Thus areas, where polymer uncovered by semiconductor layer is observed, would contribute to increase areal coverage even if there is no TIPS-pentacene film.

Besides areal coverage, also crystal shape and orientation results were notably enhanced. In pristine TIPS-pentacene sample crystals show irregular and different shapes and random orientation. On the other hand, blending small organic semiconductor with the polymer, regular ribbon-shaped crystals are obtained. These crystals show an almost perfect alignment in the same direction, but this direction often does not match with slope direction. Therefore misalignment angles (summarized in Figure 4.12) are not measured using slope direction as a baseline but the long axis of one chosen crystal. It can be justified by the fact that this growing method has not the main purpose of aligning crystals in one particular direction, but rather to improve crystal size, areal coverage, or crystallinity. Although one strict orientation along one particular direction is not obtained, the diagram in Figure 4.12 shows high crystal alignment along the chosen baseline. Both absolute value and error (standard deviation is used as error bar in the diagram) are reduced if compared to results obtained in the case of pristine TIPS-pentacene growth assisted by thermal gradient (Figure 4.2). Using the external driving force given by the application of thermal gradient quite small misorientation angles are attained, but those value are affected by high variability (the smallest value of standard deviation was

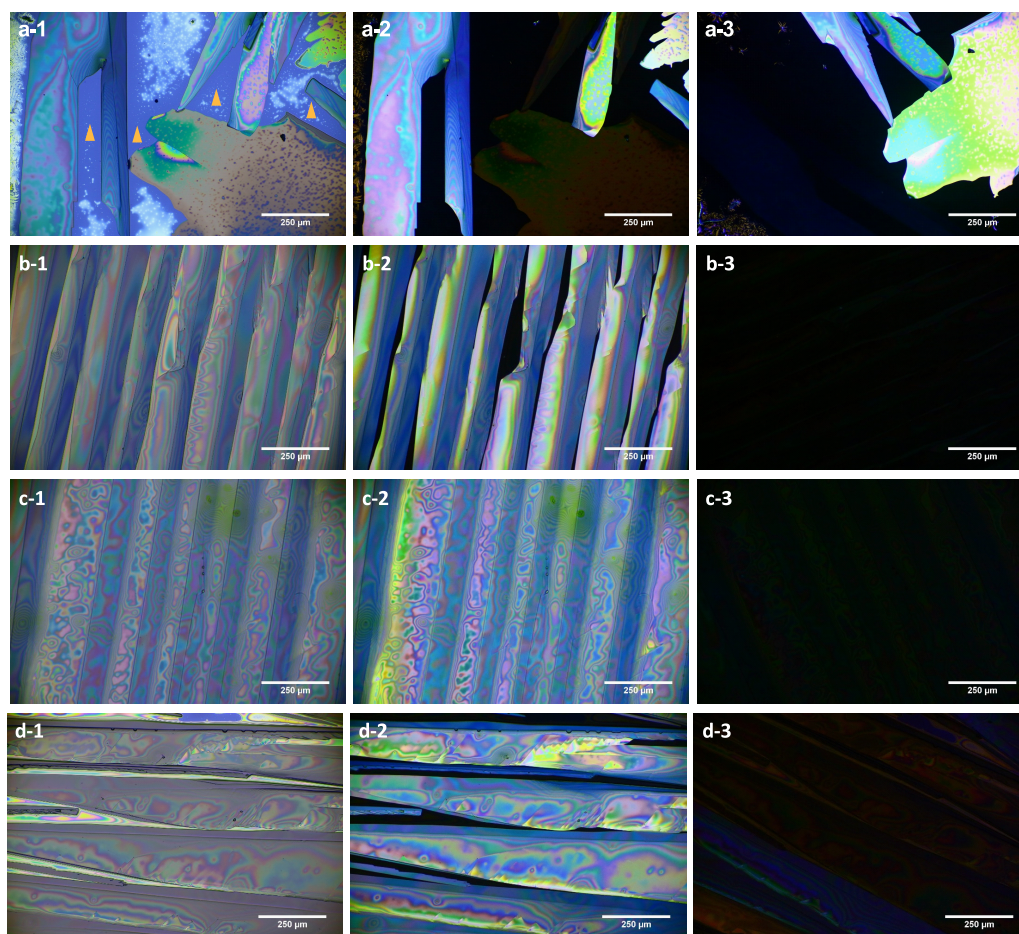


FIGURE 4.11: Optical micrographs under bright field (-1 column) and polarized light (-2 and -3 column in diagonal and extinction position) of crystals made from TIPS-pentacene/polystyrene blend solution. Samples are obtained by simple drop-casting on a tilted substrate of solutions at different volume: (a) pristine TIPS-pentacene, (b) 1:1, (c) 2:1, and (d) 3:1.

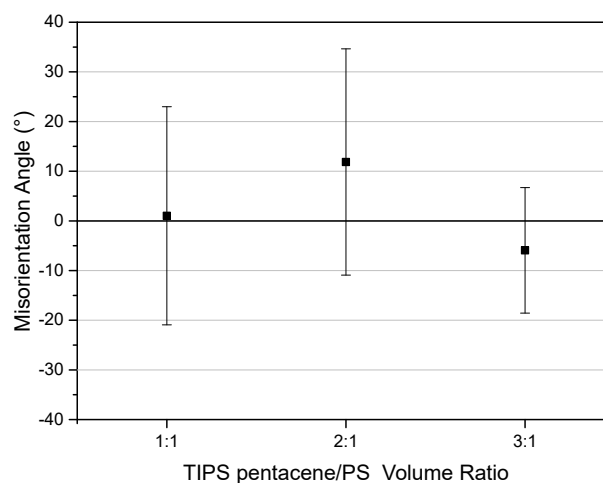


FIGURE 4.12: Average misorientation angle between crystals and long axis direction of a crystal chosen as a baseline for different volume mixing ratios.

30.2° for $T_h = 45$ °C), while in this case errors are 21.9°, 22.7° and 12.7° for mixing blend ratios of 1:1, 2:1 and 3:1, respectively.

One further morphological enhancement given by polystyrene blend is the increase in crystal size. For all ratios tested TIPS-pentacene crystals show an average size higher than 200 μm , which is bigger than sizes obtained for pristine TIPS-pentacene crystals. In addition to that, huge crystals having widths of 2236 μm and 2576 μm are observed in films grown from ratios of 1:1 and 2:1, respectively. In the case of mixing ratio of 3:1 both average and maximum crystal size results slightly reduced. It can be related to the fact that the amount of polymer is not enough to form a uniform film enable to give the same advantages observed for the other ratios.

4.2.2 Microstructure

Cross-sectional SEM images of samples produced from TIPS-pentacene/polystyrene blend are reported in Figure 4.13. Images are taken by analyzing secondary electrons, while EDS analysis has been used to investigate different layers composition.

vertical phase separation is observed for all samples produced from semiconductor/polymer blend: a thin polystyrene layer is laid on the Si/SiO₂ substrate, and above that, a TIPS-pentacene rich layer is formed. A vertical phase separation between polymer and semiconductor layers was previously reported [46], but in those cases one more thin TIPS-pentacene rich layer below the PS one has been observed. To understand layer formation, vertical phase separation process has to be investigated. It is originated by differences in solubility between semiconductor and polymer. Therefore, during solvent evaporation, the less soluble material (TIPS-pentacene) reaches first the supersaturation at the air-solvent interface, where it starts to crystallize [58]. Afterward also the second solute (polystyrene) reaches the supersaturation threshold, and therefore it starts to solidify below the first

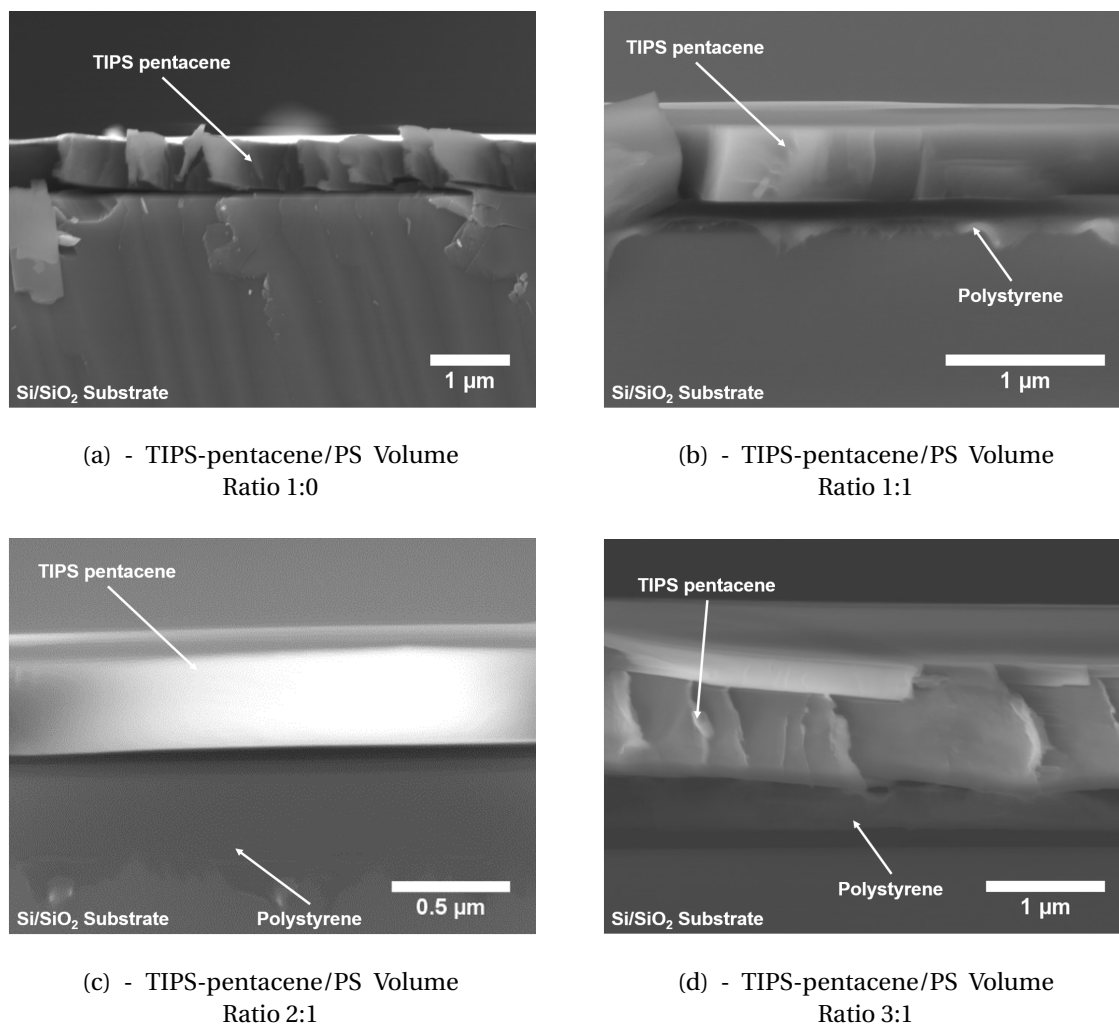


FIGURE 4.13: SEM images of cross-section of samples yielded from a mixture of TIPS-pentacene and polystyrene at different blend ratios.

layer. If the solvent evaporation is a stable and long enough process, a complete separation between TIPS-pentacene and polystyrene is reached and a bilayer structure is attained. On the contrary, if the process is not optimal, a certain amount of TIPS-pentacene may remain in solution during PS layer formation, and it crystallizes below the polymer layer forming a trilayer structure.

4.2.3 Crystallinity

Figure 4.14 shows out-of-line XRD spectra of samples produced from TIPS-pentacene/ polystyrene blend at room temperature. Each spectrum, related to a different volume ratio, is vertically shifted in order to enable visual differentiation.

Peak positions have been identified at 5.6° , 11.0° , 16.3° and 27.2° for (001), (002), (003) and (005) planes, respectively, being left-shifted by an amount of $0.1\sim 0.2^\circ$ from the peak positions measured

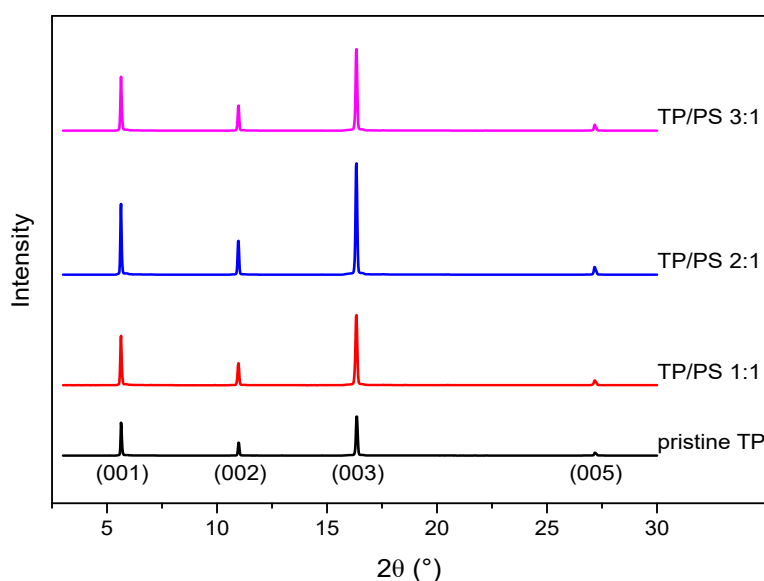


TABLE 4.2

TP / PS Volume Ratio	FWHM ₍₀₀₁₎
pristine TP	0.0668
1:1	0.0756
2:1	0.0630
3:1	0.0732

FIGURE 4.14: X-Ray diffraction spectra for different TIPS-pentacene/polystyrene volume ratio and FWHM values correspondent to (001) plane of each volume ratio.

for pristine TIPS-pentacene films (Subsection 4.1.2). As a consequence of this shift, the d-spacing along the c -direction between two adjacent molecular layers will increase according with the Bragg law by blending TIPS-pentacene with an insulator polymer at any blend ratio. Assuming the same correction explained in Subsection 4.6, for (001) plane a d-spacing increase from 16.7 Å to 17.3 Å is calculated. It can be related to some polymer molecules stuck in the TIPS-pentacene rich layer when it has solidified, and thus a close molecular packaging is prevented. Although increasing in intermolecular distance along the c -direction does not directly affect orbitals overlapping (see Figure 1.7), possible PS molecules trapped in TIPS-pentacene lattice suggest that the presence of polymer molecules is not only limited between (00l)-type planes. Indeed, polystyrene long chain can be stuck between TIPS-pentacene molecules along the a and b -directions affecting orbitals overlapping and thus electrical properties.

Furthermore, polystyrene addition to organic semiconductor has a bad consequence on crystallinity, indeed, as reported in Table 4.2. FWHM values show that crystallinity is slightly increased for 2:1 volume ratio, while a smooth lost is observed for 1:1 and 3:1 ratios. This result is unexpected because some studies have reported strong FWHM drops (87% [41] and 42% [72]) given by blending TIPS-pentacene and PS (volume ratio of 1:1). In those cases HfO₂ coated substrates have been used as support, while in studies where Si/SiO₂ have been involved a less evident fall has been observed (13% [73]). In my research a gain of 13% in FWHM is observed for the same volume ratio, this opposite behavior can be also related to an undesirable presence of polymer molecules in semiconductor layer which induce some deformation in the original TIPS-pentacene lattice. Although in SEM images (Figure 4.13) TIPS-pentacene rich layer above a PS rich layer have been observed, EDS analysis was not able to show if and how much foreigner molecules are stuck in the other layer.

4.2.4 OFET Characterization

Electrical properties have been measured both in bottom contact and top contact (Au electrodes thickness 200 nm) configuration; devices specifics have been previously summarized in Table 3.1. It is worth to mention that the main advantage given by blending TIPS-pentacene and polystyrene is to allow to obtain organic films easily testable after electrodes deposition. Despite several devices have been produced using pristine TIPS-pentacene as active layer, only 20% of those have been correctly tested without undergo in breakdown; on the contrary 95% of OFETs produced with blend solutions showed correct working conditions. Therefore electrical properties summarized in Figure 4.15 for pristine TIPS-pentacene (mixing blend ratio 1:0) refer to only few devices. The fact that these tested devices were the ones that showed the best morphological properties (crystal size and thickness) dramatically reduces the reliability of these measurements.

Referring to Figure 4.15, mobility (calculated in saturation region) and on/off current ratio show to be stronger influenced by the blending ratio. In particular, both of them show a fall for high content of polystyrene in the solution (mixing ratio of 1:1), while they result gradually enhanced for increasing contents of organic semiconductor. A mixing ratio of 3:1 the best properties have been measured. Using blending ratio of 3:1, the highest value of mobility in top contact configuration was measured: $5.14 \times 10^{-2} \text{cm}^2/\text{V s}$ (twice mobility attained for pristine TIPS-pentacene); the same devices also showed the highest ratio between on and off current (3600), a threshold voltage of 0.39 V and a subthreshold slope of 5.49 V/dec.

If mobility and on/off current ratio show a strong correlation with the mixing ratio, threshold voltage and subthreshold slope show lower variance. The average values of V_{Th} are between 1.67 V and 2.88 V (bottom contact devices) for all blending ratios, highlighting a great enhancement if compared to the threshold voltage measured for pristine TIPS-pentacene (6.22 V). On the other hand, subthreshold slope values are between 4.00 V/dec and 6.27 V/dec for all top and bottom contact configuration samples.

Devices analysis was carried out both in bottom and top contact configuration to investigate the influence of phase separation on OFET performances, in particular if the insulator layer would have affected in some way electrical properties. Mobility, threshold voltage and subthreshold slope show comparable values hence they do not seem to be affected by different electrodes position. Furthermore, mobility shows the same trend in top contact and bottom contact configuration, validating one more time results reliability. Values of mobility measured for TC devices are slightly higher than those attained for BC devices. This can be related not only to the microstructure (in BC, polystyrene layer is placed between electrodes and the active layer) but also to the intrinsic better performances given by a TC configuration. As a matter of fact, lack in coverage, high metal-semiconductor contact resistance, and lower contact area generally affect bottom contact devices; and thus, lower electrical performances have been reported [3]. Even if mobility results higher in TC devices than BC, it is not so dramatically increased as observed by Gupta et al [36] who attained a two order of magnitude

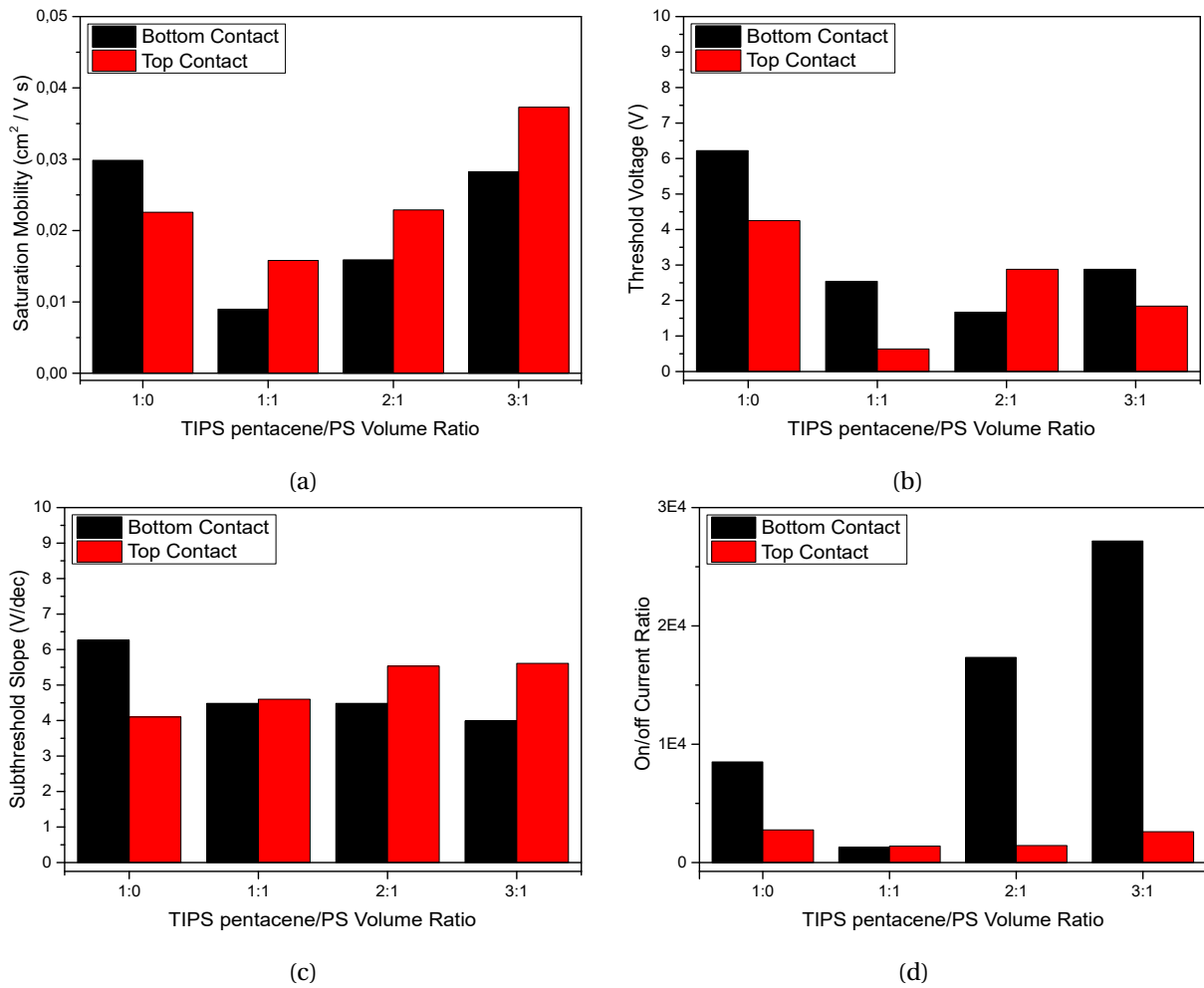


FIGURE 4.15: Average (a) saturation mobility, (b) threshold voltage, (c) subthreshold slope, and (d) on/off current ratio for different mixing blending ratio. Electrical properties are summarized for both bottom contact (black bars) and top contact (red bars) device configurations.

gain. Smaller differences between TC and BT performances and extremely low ratio between on and off current in TC OFETs (one order of magnitude less than TC devices); could be caused by a bad Au deposition. If film roughness is not homogeneous some disconnections through the electrode occur, which causes a remarkable reduction of contact area available for charge carrier injection and transport.

The gain in mobility consistency represents one more confirmation of the effectiveness of mixing TIPS-pentacene and polystyrene. Consistency is defined as the ratio between average mobility and the error (standard deviation) associated, thus it gives an idea of results variability. In Figure 4.16 values of this magnitude are presented for different blend mixing ratios. It is clear how devices produced using solution at 3:1 ratio show better performance repeatability (for TC devices 3.58 vs 1.09 for 1:1 blend ratio). This is related to film morphology, at the beginning of this section optical micrographs

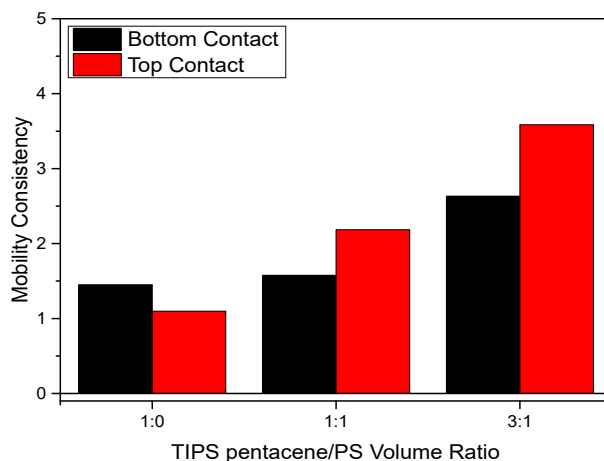


FIGURE 4.16: Mobility consistency at different TIPS-pentacene/polystyrene blend ratios.

of crystals have been shown (Figure 4.11), it is clear how blends of TIPS-pentacene and polystyrene give more homogeneous films across all the substrate. Therefore, it is easy to understand how devices produced using these films are less affected by device-to-device variability.

It is worth to be noticed that a further gain in charge carriers mobility, and in general in all electrical performances, can be obtained by enhance the phase separation between TIPS-pentacene and polystyrene. Indeed, some polymer molecules are probably trapped in the active layer, as shown by XRD results, causing increased d-spacing and drop in crystallinity. As a consequence, a weaker orbitals overlapping and a smaller integral orbital are attained, justifying in this way a lack of carriers mobility.

4.3 Thermal Gradient Assisted Growth of Crystals from a TIPS-pentacene/PS Blend Solution

4.3.1 Morphology

Before the presentation and discussion of the results, an explanation about the temperature used to determine the thermal gradient is needed. The heated block was kept at (40 °C) and despite not excellent morphological and electrical properties of pristine TIPS-pentacene films that were yielded at this value of temperature, it turned out to be the best one for blend solutions. Many factors have to be considered to decide which temperature the block has to be heated to obtain optimal crystals. In pristine TIPS-pentacene case a trade off between crystal size (decreases with increase in temperature), crystal orientation, and areal coverage (increase increase in temperature) has to be achieved. However, using a blend solution, a novel factor has great impact on morphological and electrical properties: the phase separation between organic semiconductor and insulator polymer. In order to achieve advantages assured by using a blend solution, a vertical phase separation is required;

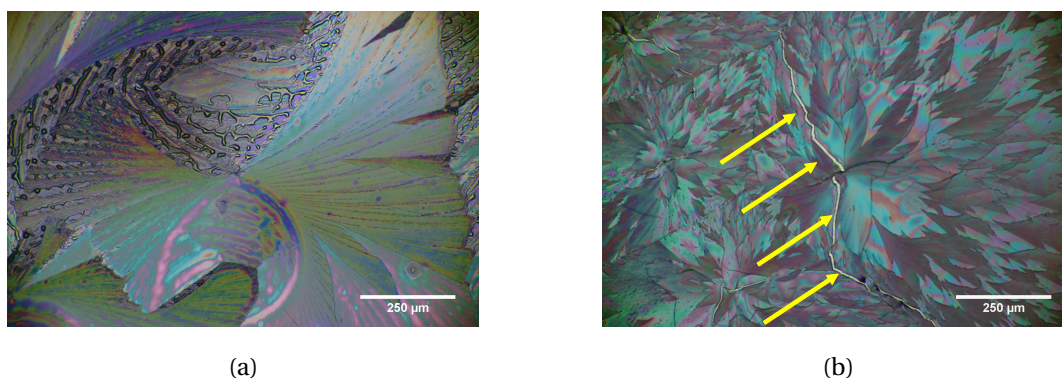


FIGURE 4.17: Optical micrographs under bright field of samples obtained by thermal assisted growth of mixture of TIPS-pentacene and polystyrene at 1:1 mixing ratio. High temperature of (a) 50 °C and (b) 60 °C are applied on the left side of each image. Yellow arrows in (b) indicate a thermal crack.

it is aided by a low solution temperature (thermodynamical point of view) and a long crystallization time (kinetical point of view). Therefore both thermodynamic and kinetic require a reduced temperature and a large amount of toluene as solvent annealing. Besides these theoretical reasons, temperatures higher than 40 °C have been asserted to be not suitable also due to morphological reasons. Figure 4.17 shows optical micrographs taken under bright field of samples yielded from TIPS-pentacene/polystyrene blend solution at mixing ratio of 1:1 with a thermal gradient applied. Organic film yielded using T_h of 50 °C (4.17.a), shows a large area covered by needle-shaped crystals, and even where larger crystals are produced, an excess of polymer can be widely observed above TIPS-pentacene layer. In the case of T_h of 60 °C (Figure 4.17.b), the situation is even worse: needle-shaped crystals disposed of in a circular way cover almost all the substrate. Moreover, the temperature is too high for polystyrene layer to be able to avoid thermal cracks formation (pointed by yellow arrows in Figure 4.17b). Finally, the high temperature of 40 °C has been chosen because a lower temperature would not be effective to give a significant crystal orientation. It is also the lowest temperature used to grow pristine TIPS-pentacene crystals, so benchmark results without polystyrene blend are available.

Figure 4.18 shows optical micrographs of films grown from TIPS-pentacene/polystyrene blend solution at different mixing ratios with a thermal gradient applied through the substrate. Images are taken under both bright field (-1 column) and polarized light (-2 column and -3 column in diagonal and extinction position, respectively). Crystals were yielded from pristine TIPS-pentacene solution (Figure 4.18.a) and TIPS-pentacene/PS blend solution at mixing ratios of 1:1, 2:1 and 3:1 (Figure 4.17.b-d, respectively) with thermal gradient application ($T_h = 40$ °C).

Micrographs show remarkable differences in morphology between different blend ratios if compared to the case of TIPS-pentacene/polystyrene blend solution crystallized without thermal gradient application (Figure 4.12). Also in this situation, accurate analysis of areal coverage is not possible for the

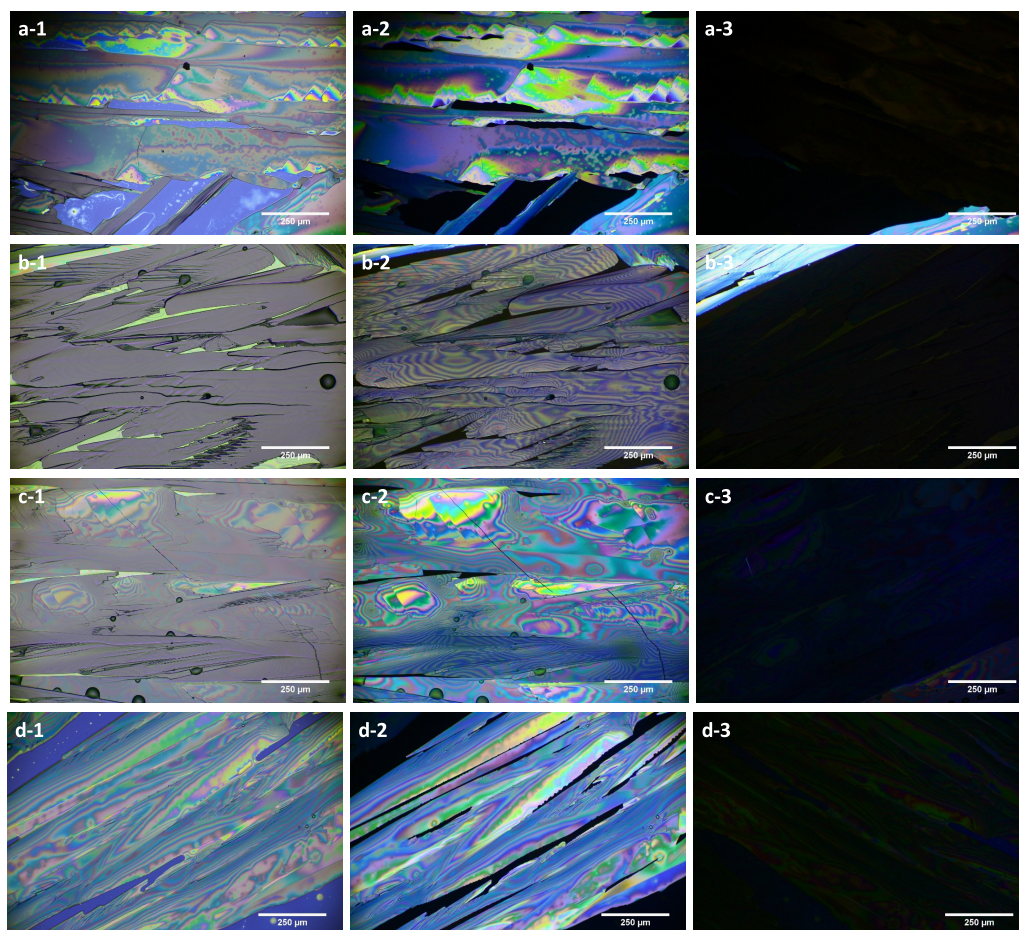


FIGURE 4.18: Optical micrographs under bright field (-1 column) and polarized light (-2 and -3 column in diagonal and extinction position) of crystals made from TIPS-pentacene/polystyrene blend solution and grown with thermal gradient assistance. Samples are obtained from solutions at different volume ratios: (a) pristine TIPS-pentacene, (b) 1:1, (c) 2:1, and (d) 3:1. Thermal gradient is applied from the left (T_h) to the right (T_l) of each micrograph, heated block is kept at 40 °C.

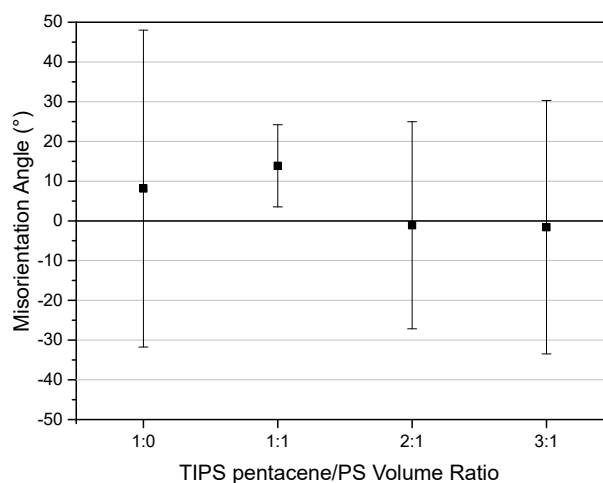


FIGURE 4.19: Average misorientation angle between crystals and thermal gradient direction at different blend ratios.

same reasons mentioned in Section 4.2. An estimation can be given observing optical images: both pristine TIPS-pentacene and 3:1 ratio show notable gaps in the organic film, and so Si/SiO₂ spots can be observed. On the contrary, 1:1 and 2:1 blend ratios show almost the total coverage of the substrate covered, even if some polystyrene layer spots can be observed, mainly in 1:1 case. Increasing the relative amount of TIPS-pentacene in solution, as an obvious consequence, the relative amount of polystyrene decreases; therefore forming a continuous polymer film on the substrate, that helps a homogeneous TIPS-pentacene growth, is more difficult due to lower amount of polymer. Although a similar lack in substrate coverage is rarely observed also in some samples yielded without thermal gradient application, it is definitely more common if the thermal gradient is applied. A higher substrate temperature means a faster solvent evaporation, which if not properly balanced by an adequate solvent annealing, reduces crystallization time and prevents the formation of an homogeneous polymer film on the substrate. Hence, in areas where TIPS-pentacene is in contact with bare Si/SiO₂ substrate, there are areal coverage issues similar to ones observed with pristine TIPS-pentacene solutions.

One of the main targets of the thermal gradient application is to give a preferred crystal orientation along the thermal gradient direction. Despite good morphological properties, blend solutions yield crystalline domains not orientated along a fixed direction leading to high batch-to-batch variation in crystal orientation. Thus the same kind of solutions has been deposited with thermal gradient application. Figure 4.19 reports average misorientation angles and errors (standard deviations) for solutions at different mixing ratios deposited on substrate with a thermal gradient ($T_h = 40$ °C). Although crystals produced from TIPS-pentacene/PS 1:1 solution show bigger average misorientation angle ($13.9 \pm 10.3^\circ$) than ones yielded from pristine TIPS-pentacene solution ($8.1 \pm 39.9^\circ$), it is impressive the decrease in angles variability represented by standard deviation (4-fold decreased). For other mixing ratios, optimal average values close to zero are attained, but an increase in standard

deviation suggests a higher orientation variability than 1:1 case.

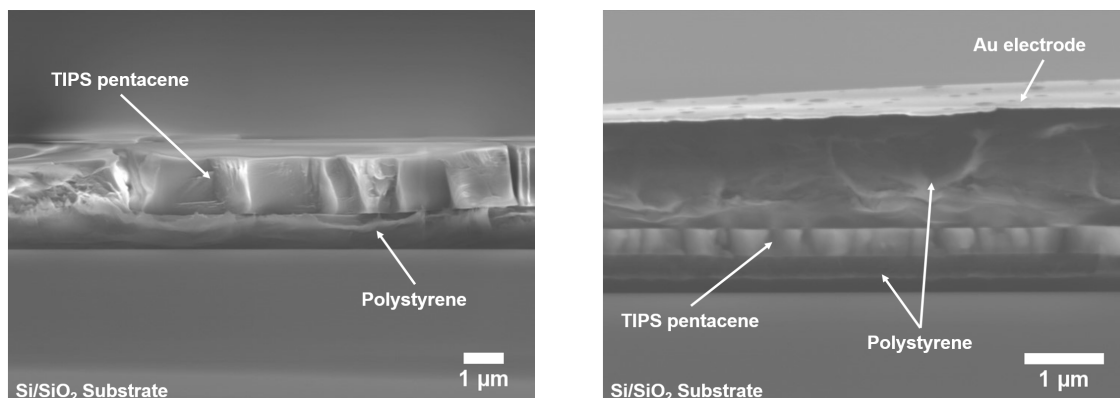
Despite differences in morphology and irregularity in crystal shapes, average crystal size is almost independent on blending ratio: 190.7 μm , 181.9 μm and 195.6 μm have been measured for ratios of 1:1, 2:1 and 3:1, respectively. It represents a slight improvement if compared to 165.2 μm of average crystal size obtained for pristine TIPS-pentacene, while not remarkable differences in average size are produced by applying a thermal gradient on blend solutions. Notable differences are instead produced on maximum crystal size by using mixture of TIPS-pentacene and polystyrene: in pristine case crystals not bigger than 815 μm were yielded, while using mixture at mixing ratio of 1:1 this value reaches 2490 μm .

4.3.2 Microstructure

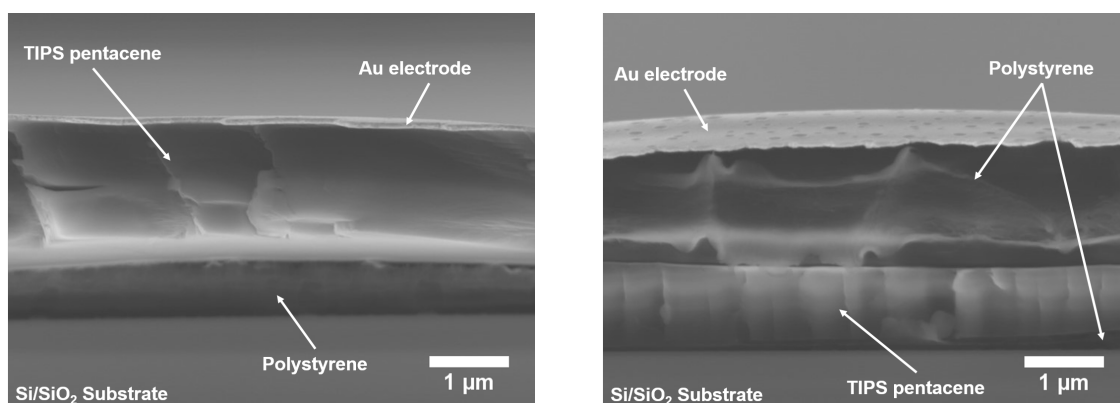
Cross-sectional SEM images of samples produced from TIPS-pentacene/polystyrene blend with thermal gradient application ($T_h = 40\text{ }^\circ\text{C}$) are reported in Figure 4.20. Two pictures of each volume ratio are shown. On the left column, the optimal bilayer configuration is observed, while on the right undesirable microstructure is reported.

The optimal bilayer configuration has already been observed in samples yielded without thermal gradient assistance (Subsection 4.2.2). It was explained how the kinetic and thermodynamic of solution evaporation strongly affects the vertical phase separation. Unlike the previous case, heating one of the substrate ends leads to a slight increase in solution temperature once it is dropped on the substrate, and it has some consequences on crystal formation. First of all the solvent evaporation occurs faster at high temperatures, despite solvent annealing has been involved to avoid a too fast evaporation rate. Secondly, high temperature has a strong influence on TIPS-pentacene and polystyrene solubility in toluene, causing some differences in phase separation process if compared to the case carried out at room temperature.

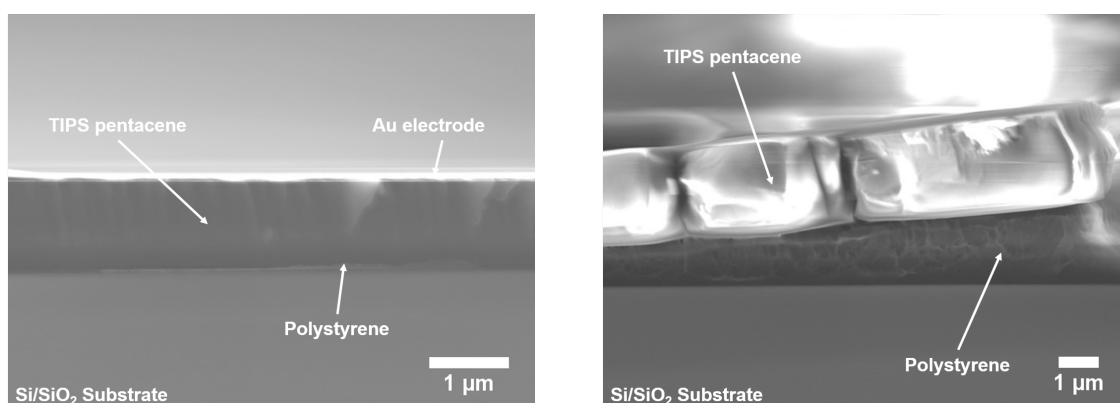
Bad effect of thermal gradient application can be observed in images on the right column in Figure 4.20. In the case of volume ratio 1:1 and 2:1 an extremely thick polystyrene layer is formed above the semiconductor one, while in the case of 3:1, a structure similar to the optimal one is observed, but polymer layer is thicker (up to 3 μm). It is worth mentioning that optimal and bad microstructures are seen at analogous location in all the samples: substrate areas near the edges show the ideal configuration, and the central area shows the undesirable microstructure. This can be related to the solvent evaporation process too; near substrate boundaries solution-air interface is more extensive than at the center, therefore solvent evaporation is enhanced, and crystallization starts from these areas. As a consequence, an optimal configuration (thick TIPS-pentacene rich layer above a thin PS layer) is attained, while the remain solution has a higher PS concentration due to PS higher solubility. So, in the central area, the last one to reach complete solvent evaporation, an excess of polymer is observed that results in an extremely thick PS layer.



(a, b) - TIPS-pentacene/PS Volume Ratio 1:1



(c, d) - TIPS-pentacene/PS Volume Ratio 2:1



(e, f) - TIPS-pentacene/PS Volume Ratio 3:1

FIGURE 4.20: SEM images of cross section of samples yielded from a mixture of TIPS-pentacene and polystyrene at different blend ratios with thermal gradient application ($T_h = 40\text{ }^\circ\text{C}$). Images on the left column (a, c, e) report optimal vertical phase separation, while images on the right one (b, d, f) undesirable microstructure.

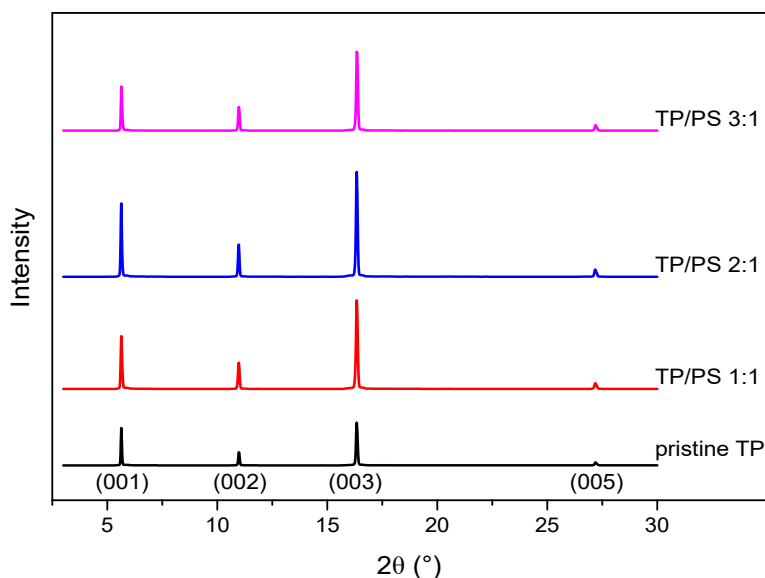


FIGURE 4.21: X-Ray diffraction spectra for different TIPS-pentacene/polystyrene volume ratios, and FWHM values correspondent to (001) peak of each volume ratio. Samples are yielded with thermal gradient assistance ($T_h = 40^\circ\text{C}$).

TABLE 4.3

TP / PS Volume Ratio	FWHM ₍₀₀₁₎
pristine TP	0.0615
1:1	0.0743
2:1	0.0640
3:1	0.0693

4.3.3 Crystallinity

Figure 4.21 shows out-of-plane XRD spectra of samples produced from TIPS-pentacene/ polystyrene blend applying a thermal gradient ($T_h = 40^\circ\text{C}$). Each spectrum, related to a different volume ratio, is vertically shifted in order to enable visual differentiation.

In Subsection 4.1.2 and 4.2.3 peaks positions of XRD spectra have been reported and it has shown how they are not affected by thermal gradient but instead, they are by mixing TIPS-pentacene with an insulator polymer. It is further confirmed by peak position evaluation for the combined method: they are located at 5.6° , 11.0° , 16.3° and 27.2° for (001), (002), (003) and (005) planes, respectively. As already reported for blend solutions without thermal gradient application, it involves a gain in d-spacing along with c -direction, possibly related to trapped polystyrene chain in TIPS-pentacene rich layer. This suggestion is furthermore supported by the fact that the gain in interlayer distance (0.5 \AA , from 16.7 \AA to 17.3 \AA , calculated using a correction on raw data as explained in Subsection 4.6) is the same for both situation, with and without high temperature involved. Therefore polystyrene is not able to produce a strong phase separation if blended with TIPS-pentacene and simply drop-casted, independently by substrate temperature.

In Table 4.3 FWHM values for each volume ratio are reported, referring to values reported for TIPS-pentacene/polystyrene without thermal gradient (Table 4.2). It is clear that thermal gradient not only does not affect peak positions but either degree of crystallinity. Indeed, FWHM values for samples yielded without and with applying thermal gradient differs by only 1.7%, 1.6%, and 5.3% for volume ratio of 1:1, 2:1, and 3:1, respectively.

4.3.4 OFET Characterization

Electrical properties have been measured after Au electrodes (200 nm in thickness) have been deposited, to investigate differences in microstructure between central and peripheral areas of the substrate at least 4 devices have been formed on the same substrate.

In figure 4.22, average values of (a) saturation mobility, (b) threshold voltage, (c) subthreshold slope and (d) on/off current ration are reported for devices produced from solution at different volume ratios. All these properties show strong differences varying the amount of polymer in solution. In particular at high polystyrene content bad performances are attained, but reducing the amount of polymer down to 3:1 in volume ratio the best performances are observed, even better than pristine TIPS-pentacene. Comparing the film with a blending ratio of 3:1 with that of 1:0, threshold voltage decreases from 6.30 V to 0.19 V, and subthreshold slope decreases from 11.28 V/dec to 6.25 V/dec. Instead, mobility is only slightly enhanced (from $9.5 \times 10^{-3} \text{ cm}^2/\text{V s}$ to $1.1 \times 10^{-2} \text{ cm}^2/\text{V s}$) and on/off current ratio shows a drop from 920 to 800. Globally, similar behavior to one observed for samples produced without thermal gradient (Subsection 4.2.4) is reported: a sharp decline in properties for blending ratio of 1:1 and remarkable performances for ratio of 3:1. Similarly to the previous case, also in this situation, a further enhancement in charge carrier mobility is prevented by unsharp phase separation between semiconductor and polymer, as can be deduced by XRD results.

OFET performances are affected by high device-to-device variability: mobility values vary from $2.41 \times 10^{-4} \text{ cm}^2/\text{V s}$ to $1.65 \times 10^{-2} \text{ cm}^2/\text{V s}$ and from $7.81 \times 10^{-4} \text{ cm}^2/\text{V s}$ to $2.16 \times 10^{-2} \text{ cm}^2/\text{V s}$ for 2:1 and 3:1 volume ratio, respectively. This high variability is a consequence of differences in microstructure highlighted by SEM observations (Subsection 4.2.0). A thick polymer layer (up to 2-3 μm) hinders charge carrier injection and transport if it is located between electrode and semiconductor film (Figure 4.20b and c). Otherwise, if placed between gate electrode and active layer it can act as an extra gate insulator layer and thus considerably increase (at least one order of magnitude) substrate capacitance. As a consequence, according to Equation 1.4, also saturation mobility will increase by the same magnitude.

On the contrary, other electrical properties (threshold voltage and subthreshold slope) show a significant gain in mean values besides variability, as demonstrated by shorter error bars in diagrams in Figure 4.22.

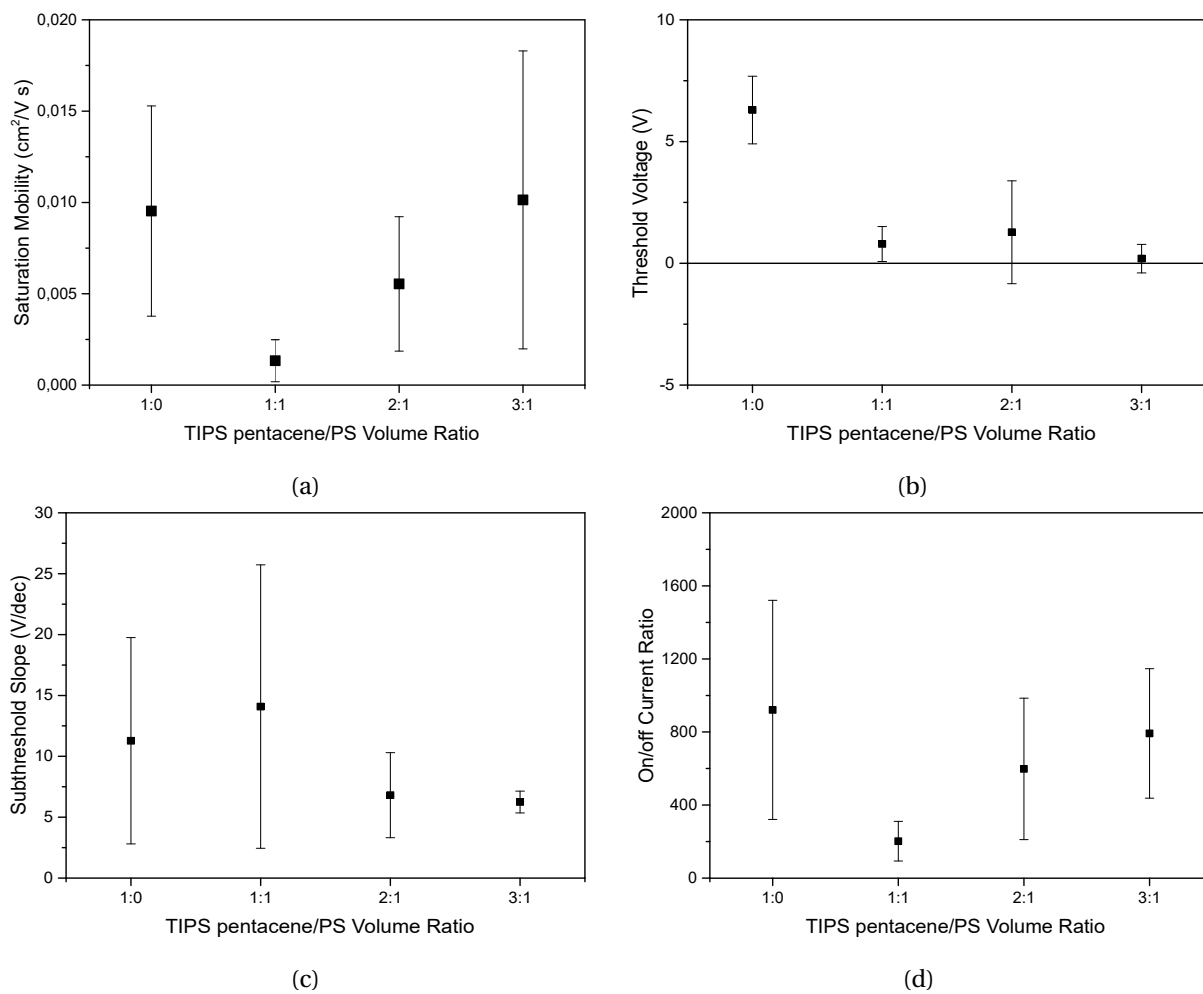


FIGURE 4.22: Average (a) saturation mobility, (b) threshold voltage, (c) subthreshold slope, and (d) on/off current ratio for different blend ratios. Samples are produced by drop-casting blend solution on substrate with thermal gradient application ($T_h = 40$ °C).

Chapter 5

Conclusions

In this research, a novel method of organic crystal growth from a solution has been studied to attain film with controlled morphology and enhanced electrical properties. TIPS-pentacene has been used as a semiconductor material and dissolved in toluene. Two approaches have been investigated: an external one, consisting of applying to the solution an external driving force able to control crystal growth direction, and an additive one consisting of blending the semiconductor material with a third one to attain enhancements in devices performances. In the former case, a thermal gradient has been used as external force, while in the latter one an insulator polymer, polystyrene, has been added to the TIPS-pentacene/toluene solution at different volume ratios. After having singularly investigated each one of these technologies to get benchmarks results, these have been used together, in order to try to combine advantages given by each one of them.

Chapter 1 contains a brief overview of theoretical principles of conductivity in organic materials and an explanation of advantages given by using a soluble processable small molecule semiconductor material such as TIPS-pentacene. The theoretical principle of OFET working conditions and data processing are also provided at the end of the chapter.

In Chapter 2 the state of art of the most common technologies to produce organic crystal is provided, distinguishing between external and additive methods. Moreover, the techniques further employed in this study have been more deeply explained also with theoretical references.

The first part of Chapter 3 contains information about materials used and experimental parameters needed to set up the experiment. In the second section, tools used to carry out quantitative and qualitative analysis have been listed, and their operational principle briefly exposed.

Chapter 4 is divided into three sections, each one containing results attained from the analysis of samples and devices yielded by each different methods. These results are then summarized in this final chapter.

Thermal gradient application has been proved to be effective in controlling crystal morphology: all samples produced with this method show similar film topology with crystal aligned along with thermal gradient direction. Average values of thermal gradient applied (hot block temperature of 45 °C

and 50 °C) lead to a trade-off between crystal alignment, crystal size (decreases with temperature increase), crystal thickness homogeneity, and areal coverage (increases with temperature increase). These enhancements in morphology and the conservation of degree of crystallinity lead to better electrical performances for mean values of thermal gradient. Furthermore, applying a reduced temperature, a limited number of thermal cracks is observed, preventing drops in electrical properties and their consistency.

Secondly, blending TIPS-pentacene with polystyrene, remarkable gain in areal coverage and crystal misorientation between crystals belonging to the same domain are attained; however an alignment along a fixed direction was more difficult to control. Furthermore, as shown in SEM images, a vertical phase separation between polymer and semiconductor layer has been seen with a thin layer of polystyrene laid on Si/SiO₂ substrate and the TIPS-pentacene layer above that. However, XRD analysis of films yielded from blend shows a gain in d-spacing between molecular layers and a drop in crystallinity if compared to pristine case, it is probably related to undesirable polystyrene molecules trapped in TIPS-pentacene rich layer. Despite it, enhanced electrical properties have been obtained for TIPS-pentacene/polystyrene blend ratio of 3:1 in volume; it takes advantages from polymer ability to easily form films and thus enhance morphological properties without being affected by lack in OFET performances due to a too thick insulator layer. Furthermore, mobility consistency, namely the ratio between mobility and its standard deviation, shows higher values for devices produced from blend solution than those produced from pristine TIPS-pentacene. Therefore high measurement repeatably and low device-to-device variance is attained.

Finally, the thermal gradient was applied through substrates before the drop-casting of a blend solution to produce morphologically controlled crystals having optimal electrical properties. Well-oriented crystals along thermal gradient direction are actually attained, but sufficient coverage and regular shapes are not observed too. Furthermore, SEM images highlight differences in vertical phase separation between different areas of the same substrate leading to a high and undesirable device-to-device performance variation. Moreover XRD analysis confirms the same issues for molecular packaging and crystallinity which have been observed for blend films produced by simple drop-casting. Therefore, despite crystals attained with the "combined method" show better electrical properties than pristine TIPS-pentacene films, these are lower than the ones attained from crystal produced without thermal gradient application. Hence, temperature used as an external force is effective on pristine TIPS-pentacene solution, but in case of blend solution, it excessively disturbs the weak equilibrium that rules the phase separation. Thus, advantages given by blending semiconductor and polymer are partially lost.

In conclusion, an external method to grow organic crystals, such as thermal gradient application, was proved to be effective only with pristine semiconductor solution, while some issues, including undesirable microstructure given by uncontrolled solvent evaporation, occur if a blend solution is deposited. In this case, thermal gradient application was effective only on crystal morphology but

not on electrical properties. Although some issues related to unsharp phase separation between small-molecule semiconductor and polymer, growing crystals from a mixture of TIPS-pentacene and polystyrene was the most effective method to enhance electrical properties and their consistency. Therefore this method is a good starting point for further studies that should focus on two main topics: enhancing the crystal alignment along with a fixed direction and optimizing the phase separation between blend components.

Bibliography

- [1] S. C. Wang, W. Hu, C. Wang, H. Dong, “Organic semiconductor crystals”, *Royal Society of Chemistry* **2018**, *47*, 422–500.
- [2] Z. F. Yao, J. Y. Wang, J. Pei, “Control of π - π Stacking via Crystal Engineering in Organic Conjugated Small Molecule Crystals”, *Crystal Growth and Design* **2018**, *18*, 7–15.
- [3] K. Asare-Yeboah, PhD thesis, Graduate School of The University of Alabama, **2015**.
- [4] Y. Inada, M. Koda, Y. Urabe, T. Katagiri, T. Yamao, Y. Yoshida, S. Hotta, “Microcrystalline array structures induced by heat treatment of friction-transferred organic semiconductor films”, *Scientific Reports* **2019**, *9*, 1–11.
- [5] H. Shirakawa, E. J. Louis, A. G. MacDiarmid, C. K. Chiang, A. J. Heeger, “Synthesis of electrically conducting organic polymers: halogen derivatives of polyacetylene, (CH)”, *J. Chem. Soc., Chem. Commun.* **1977**, 578–580.
- [6] F. Li, A. Nathan, Y. Wu, B. S. Ong, *Organic Thin Film Transistor Integration : A Hybrid Approach*, John Wiley and Sons, Incorporated, Weinheim, Germany, **2011**.
- [7] T. Yamao, K. Juri, A. Kamoi, S. Hotta, “Field-effect transistors based on organic single crystals grown by an improved vapor phase method”, *Organic Electronics* **2009**, *10*, 1241–1247.
- [8] Y. Fukaya, A. Inoue, Y. Fukunishi, S. Hotta, T. Yamao, “Organic-crystal field-effect transistors based on terminal-substituted sexithiophenes”, *Japanese Journal of Applied Physics* **2013**, *52*, 5–10.
- [9] T. Yamao, S. Ota, T. Miki, S. Hotta, R. Azumi, “Improved sublimation growth of single crystals of thiophene/phenylene co-oligomers”, *Thin Solid Films* **2008**, *516*, 2527–2531.
- [10] K. Sugahara, T. Nakagawa, R. Hirase, T. Katagiri, Y. Inada, T. Yamao, S. Hotta, “Growth of alkylmonosubstituted thiophene/phenylene co-oligomer crystals and their device application”, *Japanese Journal of Applied Physics* **2018**, *57*, 1–8.
- [11] Y. Inada, T. Yamao, M. Inada, T. Itami, S. Hotta, “Giant organic single-crystals of a thiophene/phenylene co-oligomer toward device applications”, *Synthetic Metals* **2011**, *161*, 1869–1877.
- [12] T. Yamao, T. Miki, H. Akagami, Y. Nishimoto, S. Ota, S. Hotta, “Direct formation of thin single crystals of organic semiconductors onto a substrate”, *Chemistry of Materials* **2007**, *19*, 3748–3753.
- [13] Z. Lin, X. Guo, L. Zhou, C. Zhang, J. Chang, J. Wu, J. Zhang, “Solution-processed high performance organic thin film transistors enabled by roll-to-roll slot die coating technique”, *Organic Electronics* **2018**, *54*, 80–88.

- [14] X. Wang, M. Yuan, X. Xiong, M. Chen, M. Qin, L. Qiu, H. Lu, G. Zhang, G. Lv, A. H. W. Choi, "Process optimization for inkjet printing of triisopropylsilylethynyl pentacene with single-solvent solutions", *Thin Solid Films* **2015**, 578, 11–19.
- [15] T. Yamao, K. Juriy, T. Sakaguchiz, Y. Sakurai, H. Kurikix, A. Kamoi, S. Hotta, "Melt molding of uniaxially-oriented crystal domains onto a substrate", *Japanese Journal of Applied Physics* **2010**, 49, 8–11.
- [16] A. Boudrioua, M. Chakaroun, A. Fischer in *Organic Lasers*, (Eds.: A. Boudrioua, M. Chakaroun, A. Fischer), Elsevier, **2017**, pp. 1–47.
- [17] F. Caravelle, Università di Bologna, **2015**.
- [18] L. Pauling, *General Chemistry*, Dover Publications, Reading, Massachusetts, **1970**.
- [19] A. N. Sokolov, T. Frišćić, L. R. MacGillivray, "Enforced Face-to-Face Stacking of Organic Semiconductor Building Blocks within Hydrogen-Bonded Molecular Cocrystals", *Journal of the American Chemical Society* **2006**, 128, 2806–2807.
- [20] H. Dong, X. Fu, J. Liu, Z. Wang, W. Hu, "Key Points for High-Mobility Organic Field-Effect Transistors", *Advanced Materials* **2013**, 25, 6158–6183.
- [21] Y. Takeyama, S. Ono, Y. Matsumoto, "Organic single crystal transistor characteristics of single-crystal phase pentacene grown by ionic liquid-assisted vacuum deposition", *Applied Physics Letters* **2012**, 101.
- [22] V. Coropceanu, J. Cornil, D. A. da Silva Filho, Y. Olivier, R. Silbey, J.-L. Brédas, "Charge Transport in Organic Semiconductors", *Chemical Reviews* **2007**, 107, 926–952.
- [23] Z. He, J. Chen, D. Li, "Review Article: Crystal alignment for high performance organic electronics devices", *Journal of Vacuum Science & Technology A* **2019**, 37, 040801.
- [24] M. Kucinska, M. Z. Szymanski, I. Frac, F. Chandezon, J. Ulanski, "Correlation between surface morphology and potential profile in OFETs with zone-cast TIPS-Pentacene as seen by scanning Kelvin probe microscopy", *Materials Science- Poland* **2019**, 37, 249–256.
- [25] S. K. Park, T. N. Jackson, J. E. Anthony, D. A. Mourey, "High mobility solution processed 6,13-bis(triisopropyl-silylethynyl) pentacene organic thin film transistors", *Applied Physics Letters* **2007**, 91, 6–9.
- [26] J. Mi, Y. Diao, A. L. Appleton, L. Fang, Z. Bao, "Integrated Materials Design of Organic Semiconductors for Field-Effect Transistors", *Journal of the American Chemical Society* **2013**, 135, 6724–6746.
- [27] O. D. Jurchescu, M. Popinciuc, B. J. Van Wees, T. T. Palstra, "Interface-controlled, high-mobility organic transistors", *Advanced Materials* **2007**, 19, 688–692.
- [28] W. H. Lee, D. H. Kim, Y. Jang, J. H. Cho, M. Hwang, Y. D. Park, Y. H. Kim, J. I. Han, K. Cho, "Solution-processable pentacene microcrystal arrays for high performance organic field-effect transistors", *Applied Physics Letters* **2007**, 90.
- [29] J. E. Anthony, J. S. Brooks, D. L. Eaton, S. R. Parkin, "Functionalized Pentacene: Improved Electronic Properties from Control of Solid-State Order", *Journal of the American Chemical Society* **2001**, 123, 9482–9483.

- [30] J. Chen, D. C. Martin, J. E. Anthony, "Morphology and molecular orientation of thin-film bis (triisopropylsilylethynyl) pentacene", *Journal of Materials Research* **2007**, *22*, 1701–1709.
- [31] Z. He, J. Chen, Z. Sun, G. Szulczewski, D. Li, "Air-flow navigated crystal growth for TIPS pentacene-based organic thin-film transistors", *Organic Electronics* **2012**, *13*, 1819–1826.
- [32] J. H. Park, K. H. Lee, S. J. Mun, G. Ko, S. J. Heo, J. H. Kim, E. Kim, S. Im, "Self-assembly of organic channel/polymer dielectric layer in solution process for low-voltage thin-film transistors", *Organic Electronics* **2010**, *11*, 1688–1692.
- [33] W. H. Lee, Y. D. Park, "Organic semiconductor/insulator polymer blends for high performance organic transistors", *Polymers* **2014**, *6*, 1057–1073.
- [34] Y. Diao, B. C. Tee, G. Giri, J. Xu, D. H. Kim, H. A. Becerril, R. M. Stoltenberg, T. H. Lee, G. Xue, S. C. Mannsfeld, Z. Bao, "Solution coating of large-area organic semiconductor thin films with aligned single-crystalline domains", *Nature Materials* **2013**, *12*, 665–671.
- [35] H. Koezuka, A. Tsumura, T. Ando, "Field Effect Transistor with Polythiophene Thin Film", *Journal of Chemical Information and Modeling* **1987**, *18*, 699–704.
- [36] D. Gupta, M. Katiyar, D. Gupta, "An analysis of the difference in behavior of top and bottom contact organic thin film transistors using device simulation", *Organic Electronics* **2009**, *10*, 775–784.
- [37] S. Saxena, B. Kumar, B. K. Kaushik, Y. S. Negi, "Effect of contact thickness on electrical properties of Organic Thin Film Transistors", *2013 International Conference on Signal Processing and Communication ICSC 2013* **2013**, 387–391.
- [38] I. Kaur, W. Jia, R. P. Kopreski, S. Selarasah, M. R. Dokmeci, C. Pramanik, N. E. McGruer, G. P. Miller, "Substituent Effects in Pentacenes: Gaining Control over HOMO LUMO Gaps and Photooxidative Resistances", *Journal of the American Chemical Society* **2008**, *130*, 16274–16286.
- [39] M. T. Lloyd, J. E. Anthony, G. G. Malliaras, "Photovoltaics from soluble small molecules Solution-processable small molecules have attractive features for", *Materials Today* **2007**, *10*, 34–41.
- [40] C.-M. Keum, J.-H. Bae, W.-H. Kim, M.-H. Kim, J. Park, S.-D. Lee, "Effect of Thermo-gradient-assisted Solvent Evaporation on the Enhancement of the Electrical Properties of 6,13- bis (triisopropylsilylethynyl)-Pentacene Thin-film Transistors", *Journal of the Korean Physical Society* **2011**, *58*, 1479–1482.
- [41] V. Raghuvanshi, D. Bharti, A. K. Mahato, I. Varun, S. P. Tiwari, "Semiconductor:polymer blend ratio dependent performance and stability in low voltage flexible organic field-effect transistors", *Synthetic Metals* **2018**, *236*, 54–60.
- [42] C. M. Keum, J. H. Kwon, S. D. Lee, J. H. Bae, "Control of the molecular order and cracks of the 6,13- bis(triisopropylsilylethynyl)-pentacene on a polymeric insulator by anisotropic solvent drying", *Solid-State Electronics* **2013**, *89*, 189–193.
- [43] R. D. Deegan, O. Bakajin, T. F. Dupont, "Capillaryflowasthecause of ring stains fromdried liquid drops Robert", *Nature* **1997**, *389*, 827–829.

- [44] Y. Yuan, G. Giri, A. L. Ayzner, A. P. Zoombelt, S. C. Mannsfeld, J. Chen, D. Nordlund, M. F. Toney, J. Huang, Z. Bao, "Ultra-high mobility transparent organic thin film transistors grown by an off-centre spin-coating method", *Nature Communications* **2014**, 5, 1–9.
- [45] H. Li, B. C. Tee, J. J. Cha, Y. Cui, J. W. Chung, S. Y. Lee, Z. Bao, "High-mobility field-effect transistors from large-area solution-grown aligned C 60 single crystals", *Journal of the American Chemical Society* **2012**, 134, 2760–2765.
- [46] D. Bharti, S. P. Tiwari, "Phase separation induced high mobility and electrical stability in organic field-effect transistors", *Synthetic Metals* **2016**, 221, 186–191.
- [47] Z. T. Huang, G. B. Xue, J. K. Wu, S. Liu, H. B. Li, Y. H. Yang, F. Yan, P. K. Chan, H. Z. Chen, H. Y. Li, "Electron transport in solution-grown TIPS-pentacene single crystals: Effects of gate dielectrics and polar impurities", *Chinese Chemical Letters* **2016**, 27, 1781–1787.
- [48] J. Tong, A. Doumbia, A. Alieva, M. L. Turner, C. Casiraghi, "Gas Blow Coating : A Deposition Technique To Control the Crystal Morphology in Thin Films of Organic Semiconductors", *American Chemistry Society* **2019**, 4, 11657–11662.
- [49] G. Grau, R. Kitsomboonloha, H. Kang, V. Subramanian, "High performance printed organic transistors using a novel scanned thermal annealing technology", *Organic Electronics* **2015**, 20, 150–157.
- [50] Z. He, Z. Zhang, S. Bi, "Small-molecule additives for organic thin film transistors", *Journal of Materials Science: Materials in Electronics* **2019**, 30, 20899–20913.
- [51] D. Bharti, S. P. Tiwari, "Crystallinity and performance improvement in solution processed organic field-effect transistors due to structural dissimilarity of the additive solvent", *Synthetic Metals* **2016**, 215, 1–6.
- [52] M. Lada, M. J. Starink, M. Carrasco, L. Chen, P. Miskiewicz, P. Brookes, M. Obarowska, D. C. Smith, "Morphology control via dual solvent crystallization for high-mobility functionalized pentacene-blend thin film transistors", *J. Mater. Chem.* **2011**, 21, 11232–11238.
- [53] J. Kang, N. Shin, D. Y. Jang, V. M. Prabhu, D. Y. Yoon, "Structure and Properties of Small Molecule-Polymer Blend Semiconductors", *Journal of the American Chemical Society* **2008**, 130, 12273–12275.
- [54] T. Ohe, M. Kuribayashi, R. Yasuda, A. Tsuboi, K. Nomoto, K. Satori, M. Itabashi, J. Kasahara, "Solution-processed organic thin-film transistors with vertical nanophase separation", *Applied Physics Letters* **2008**, 93, 053303.
- [55] Z. He, Z. Zhang, K. Asare-Yeboah, S. Bi, "Poly(α -methylstyrene) polymer and small-molecule semiconductor blend with reduced crystal misorientation for organic thin film transistors", *Journal of Materials Science: Materials in Electronics* **2019**, 30, 14335–14343.
- [56] N. Onojima, K. Hara, A. Nakamura, "Vertical phase separation of 6,13-bis (triisopropylsilyl)ethynyl pentacene / poly (methyl methacrylate) blends prepared by electrostatic spray deposition for organic field-effect transistors modification poly (methyl methacrylate) blends prepared", *Japanese Journal of Applied Physics* **2017**, 56, 05WB03–1 –05WB03–4.

- [57] Z. He, D. Li, D. K. Hensley, A. J. Rondinone, J. Chen, "Switching phase separation mode by varying the hydrophobicity of polymer additives in solution-processed semiconducting small-molecule/polymer blends", *Applied Physics Letters* **2013**, *103*, 1–5.
- [58] Z. He, S. Bi, K. Asare-Yeboah, Z. Zhang, "Phase segregation effect on TIPS pentacene crystallization and morphology for organic thin film transistors", *Journal of Materials Science: Materials in Electronics* **2020**, *31*, 4503–4510.
- [59] A. C. Arias, "Vertically segregated polymer blends: Their use in organic electronics", *Polymer Reviews* **2006**, *46*, 103–125.
- [60] Z. He, Z. Zhang, S. Bi, "Polyacrylate polymer assisted crystallization: Improved charge transport and performance consistency for solution-processable small-molecule semiconductor based organic thin film transistors", *Journal of Science: Advanced Materials and Devices* **2019**, *4*, 467–472.
- [61] J. Smith, R. Hamilton, I. McCulloch, N. Stingelin-Stutzmann, M. Heeney, D. D. Bradley, T. D. Anthopoulos, "Solution-processed organic transistors based on semiconducting blends", *Journal of Materials Chemistry* **2010**, *20*, 2562–2574.
- [62] L. Qiu, J. A. Lim, X. Wang, W. H. Lee, M. Hwang, K. Cho, "Versatile Use of Vertical-Phase-Separation-Induced Bilayer Structures in Organic Thin-Film Transistors", *Advanced Materials* **2008**, *20*, 1141–1145.
- [63] T. J. Fellers, M. W. Davidson, Anatomy of the MIC-D Digital Microscope - Polarized Illumination, <https://www.olympus-lifescience.com/en/microscope-resource/micd/anatomy/micdpolarized/>, (accessed: 17.06.2020).
- [64] J. I. Goldstein, D. E. Newbury, J. R. Michael, N. W. M. Ritchie, J. H. J. Scott, D. C. Joy, *Scanning Electron Microscopy and X-Ray Microanalysis*, 4th edition, (Ed.: Springer), Springer Nature, New York, **2018**.
- [65] E. J. Mittemeijer, P. Scardi, *Diffraction Analysis of the Microstructure of Materials*, First Edit, (Eds.: R. Rull, R. M. J. Osgood, J. Parisi, H. Warlimont), Springer, New York, **2004**.
- [66] Y. University, XRD Principle, <https://ywcmatsci.yale.edu/principle-0>, (accessed: 31.07.2020).
- [67] J. A. Lim, W. H. Lee, D. Kwak, K. Cho, "Evaporation-Induced Self-Organization of Inkjet-Printed Organic Semiconductors on Surface-Modified Dielectrics for High-Performance Organic Transistors", *Langmuir* **2009**, *25*, 5404–5410.
- [68] H. Zhao, Z. Wang, G. Dong, L. Duan, "Fabrication of highly oriented large-scale TIPS pentacene crystals and transistors by the Marangoni effect-controlled growth method", *Physical Chemistry Chemical Physics* **2015**, *17*, 6274–6279.
- [69] D. K. Hwang, C. Fuentes-Hernandez, J. D. Berrigan, Y. Fang, J. Kim, W. J. Potscavage, H. Cheun, K. H. Sandhage, B. Kippelen, "Solvent and polymer matrix effects on TIPS pentacene polymer blend organic field-effect transistors", *J. Mater. Chem.* **2012**, *22*, 5531–5537.

-
- [70] Y. Nicolas, F. Castet, M. Devynck, P. Tardy, L. Hirsch, C. Labrugère, H. Allouchi, T. Toupance, “TIPS-triphenodioxazine versus TIPS-pentacene: Enhanced electron mobility for n-type organic field-effect transistors”, *Organic Electronics* **2012**, *13*, 1392–1400.
- [71] X. Li, B. K. Kjellander, J. E. Anthony, C. W. Bastiaansen, D. J. Broer, G. H. Gelinck, “Azeotropic binary solvent mixtures for preparation of organic single crystals”, *Advanced Functional Materials* **2009**, *19*, 3610–3617.
- [72] V. Raghuwanshi, D. Bharti, I. Varun, A. K. Mahato, S. P. Tiwari, “Performance enhancement in mechanically stable flexible organic-field effect transistors with TIPS-pentacene polymer blend”, *Organic Electronics* **2016**, *34*, 284–288.
- [73] A. K. Mahato, V. Raghuwanshi, D. Bharti, I. Varun, S. P. Tiwari, “Effect of polymer blend on electrical performance and photo-response of TIPS-Pentacene OFETs”, *2019 IEEE 14th Nanotechnology Materials and Devices Conference NMDC 2019* **2019**.